THIOL-BASED REDOX MODULATION OF TRANSCRIPTIONAL REGULATORS; CprK AND Rev-erbβ

By

Nirupama Gupta

A dissertation submitted in partial fulfillment
of the requirements for the degree of
Doctor of Philosophy
(Biological Chemistry)
in the University of Michigan
2011

Doctoral Committee:

Professor Stephen W. Ragsdale, Chair
Professor Ruma V. Banerjee
Associate Professor Jeffrey R. Martens
Assistant Professor Patrick J. O'Brien
Research Assistant Professor Jeanne Stuckey

ACKNOWLEDGEMENTS

No project can be described as a one-man show. It needs the close co-operation of friends, colleagues and the guidance of experts in the field, to achieve something worthwhile and substantial. In this context, I am privileged to have an opportunity to acknowledge the people who have provided enormous support throughout my graduate school in the last six and half years. I would like to extend my gratitude towards my mentor, my thesis committee, lab members, department administration, and my family. Without their support and encouragement, this dissertation would have not been possible.

First and foremost, I would like to express my sincere thanks and gratitude to my advisor, Prof. Stephen Ragsdale, who has been a great mentor for both my professional and personal development. He was my mentor during my master's program at the University of Nebraska-Lincoln and also my Ph.D program at the University of Michigan-Ann Arbor. The knowledge and experience I have acquired under his mentorship throughout these years is invaluable. His enthusiasm, encouragement and dedication towards science are unavoidable and kept me constantly motivated. His quest for science, endless patience and easily approachable qualities always welcomed an open discussion. He not only gave his precious guidance throughout my graduate studies, but always promoted my ideas and encouraged its pursuit. And this has resulted in my thesis; all of this work would not have been possible without his incredible mentorship and his faith in me. It was an honor for me to be his student.I have been fortunate to have Prof. Ruma Banerjee as one of my

committee members during my Master's studies at the University of Nebraska-Lincoln and Ph.D program at the University of Michigan-Ann Arbor. Her strong understanding and love for science is contagious and motivates others. Her faith and passion for science is a great inspiration for me. She never accepted less than my best efforts. Many of her brilliant ideas helped me moving forward smoothly in my research. I would also like to acknowledge and extend my heartfelt gratitude to other committee members, Dr. Jeffrey Martens, Dr. Patrick O'Brien and Dr. Jeanne Stuckey, who provided their support and insightful suggestions during yearly committee meetings or during individual meetings. I greatly appreciate the tremendous help, guidance and encouragement they have provided me over the years. I also would like to take this opportunity to thank Dr. Daniel Bochar who was initially a committee member but is no longer on my committee due to change in his job. He made available his support in a number of ways; He not only shared his expertise in mammalian cell culture but also provided me plasmids, instruments and other tools required to execute the experiments.

I would like to thank the past and present members of Dr. Ragsdale's laboratory, who provided a very friendly environment in the lab to work. Especially I am indebted to many of my colleagues for their selfless support, particularly, Li Yi, Elizabeth Pierce, Dr. Gunesh Bender, Dr. Yuzhen Zhou, Dr. Darek Sliwa, Andrea Morris, Dr. Joseph Darthy, Dr. Xianghui Li, Dr. Ireena Bagai, and Ali Bogart. Their endless support, understanding, cooperation and friendliness are truly appreciated. I would also like to show my gratitude to members of Dr. Banerjee's lab, who helped me periodically especially Dr. Dominique Padovani, Dr. Carmen Gherasim, and Valentin Cracan.

I would also like to thank the staff in the Department of Biological Chemistry, especially Beth, Julie and Prasanna. They are not only helpful with administrative work but have always provided their warm friendliness, which is priceless. Many thanks to the faculty members and the students in the Department of Biological Chemistry for providing me such a stimulating research environment.

Last but not least, I would like to express my deepest gratitude to my family. Words can not express what I owe them. Their encouragement and patient love has enabled me to complete this dissertation. I dedicate my thesis to my mom who passed away during my Ph.D, but has left behind her love and blessings with me eternally. I would also like to dedicate my thesis to my son Aaryen who came into my family last year. He fills my life with love and joy everyday. Moreover, I am grateful to my father for his everlasting love and unconditional support since the beginning of my career. My acknowledgement would be incomplete without mentioning the unconditional love and unlimited support of my husband, Sanjay Garg. He not only has provided me great companionship at home but also guided and helped me in my research. Finally, I would like to thank each and everyone who has supported me directly or indirectly during my studies and whose best wishes have always seen me through ordeals.

PREFACE

Oxidative stress has been associated with a number of notorious diseases including Parkinson's disease, cancer, and it exerts its effect on cellular machineries primarily via thiols which are very sensitive to oxidation due to their chemical nature. Thiol-based redox modulation of cellular functions is an emerging field of study and there are numerous examples of proteins whose activity has been shown to be under the control of cellular redox status. Transcriptional regulators are key targets of reactive oxygen species (ROS) under oxidative stress conditions due to the capability of transcription regulators to control the expression of various genes involved in redox processes. The last decade has witnessed the identification of many transcriptional regulators whose activity is controlled by ROS.

The aim of this research was to gain knowledge on redox-modulation of two transcriptional regulators; CprK (Section I) and Rev-erbβ (Section II). Recognition of the molecular mechanism underlying the redox regulation and function of these transcriptional regulators is the main focus of this thesis. We focused primarily on the following three issues: 1) The identification of the redox-active cysteines, 2) determination of the type of modifications of the redox-sensitive cysteines upon oxidation and, 3) unraveling the downstream effects of oxidation of redox-active cysteines on the cellular function of these proteins. This thesis is composed of 7 chapters. The general introduction (chapter 1) describes our current understanding of thiol based

redox modulation of transcriptional regulators. Chapter 2 provides an introduction and prior knowledge about a bacterial transcriptional activator, CprK. Chapter 3 is a copy of the publication by Gupta N et al (Gupta N and Ragsdale SW. Dual roles of an essential cysteine residue in activity of a redox-regulated bacterial transcriptional activator. J Biol Chem. 2008 Oct 17;283(42):28721-8). In this chapter, Steve Ragsdale and I designed the experiments, interpreted the results and wrote the manuscript, and I performed the experiments. Chapter 4 is an introduction to the eukaryotic transcription regulator, Rev-erb, which is emerging as a key controller of many cellular functions. The contents of chapter 5 were published in the following paper: Gupta, N., and Ragsdale, SW. 2011. Thiol-disulfide redox dependence of heme binding and heme ligand switching in the nuclear hormone receptor, Rev-erbβ. J. Biol. Chem. 286(6):4392-403. Epub 2010 Dec 1. In this chapter, both authors contributed to the research design, data analysis and writing. I performed the experiments.Chapter 6 reports on the analysis of redox-dependent gas binding to Rev-erbβ. Chapter 7 describes ongoing work and potential future directions for the project.

TABLE OF CONTENTS

LIST OF FIGURES

LIST OF TABLES

LIST OF ABBREVIATIONS

CD; Circular dichroism

CHPA; 3-chloro-4-hydroxyphenylacetate

Cpr ; Chlorophenol reduction

Cys; Cysteine

DA; diamide

DMSO ; Dimethyl sulfoxide

DBD; DNA binding domain

DTT; dithiothreitol

DTH; Sodium dithionite

DTNB; 5, 5'-Dithiobis(2-nitrobenzoic acid)

EMSA; Electrophoretic mobility shift assays

EPR; Electron paramagnetic resonance

HRM; Heme regulatory motif

ICAT; Isotope coded affinity tag

IPTG; Isopropyl-β-D-thiogalactopyranoside

LBD; Ligand binding domain

ONPG; O-nitrophenyl-β-D-galactoside

Ox; Oxidized

Red; Reduced

RT ; Room temperature

SDS-PAGE; Sodium dodecyl sulfate-polyacrylamide gel electrophoresis

TCEP; Tris(2-carboxyethyl)phosphine

ABSTRACT

THIOL-BASED REDOX MODULATION OF TRANSCRIPTIONAL REGULATORS; CprK AND Rev-erbβ

By

Nirupama Gupta

Chair: Stephen W Ragsdale

Thiol-based redox regulation of both prokaryotic and eukaryotic systems plays an important role in modulating cellular functions such as gene expression. Transcriptional factors play an important role in these modulations and exert redox-dependent activity through highly conserved cysteine residues in them. This thesis illustrates thiol-disulfide redox regulation of two such transcriptional regulators: CprK and Rev-erbβ.

CprK is a positive transcriptional regulator from a prokaryotic organism, *Desulfitobacterium dehalogenans*. CprK has been shown to contain a thiol/disulfide redox switch that undergoes reversible inactivation upon oxidation. We have demonstrated that a disulfide bond, formed between Cys11 and Cys200 *in vivo*, is responsible for oxidative inactivation of CprK. Moreover, we have shown that Cys11 is also required for binding DNA and that Cys11 mutants are unable to bind DNA due to a

change in their tertiary structures. Therefore, Cys11 plays dual roles in maintaining the normal activity of CprK and its redox inactivation.

Rev-erbβ is a human nuclear receptor and downregulates the expression of target genes in the presence of heme. Our studies with the ligand binding domain of Rev-erbβ (Rev-erbβ LBD) have revealed that its affinity for heme is controlled by a thiol-disulfide redox-switch, where the oxidized LBD exhibits 5-fold lower affinity for heme than the reduced LBD. Oxidation of the protein also triggers a ligand switch in which the reduced Rev-erbβ LBD binds heme via Cys 384/His568 while the oxidized protein coordinates heme primarily via His/neutral residue ligand pair.

Gas binding analyses with the heme-Rev-erbβ LBD complexes show a dependence of binding on the redox status of the heme and the protein. The binding constants for CO and H_2S are low and below their physiological concentrations. In contrast, NO shows very low binding affinities for heme-Rev-erbβ LBD complexes.

Currently, we are characterizing full-length hRev-erbβ and our preliminary results corroborate our earlier findings on the redox-regulation of heme binding and heme ligand switching in the isolated LBD. In addition, full-length hRev-erbβ shows redox regulation of DNA binding.

Overall, these findings indicate a potential role for the thiol-disulfide redox-switch in Rev-erbβ in responding to changes in redox poise in the cell under oxidative stress.

Chapter 1

GENERAL INTRODUCTION: TRANSCRIPTIONAL REGULATORS AND THEIR REDOX REGULATION

1.1 Transcriptional regulators

Transcription is the process of generating a complementary RNA copy of a DNA sequence, via RNA polymerase (12). The process of transcription is highly regulated to fulfil the dynamic demands of the cell for meeting its metabolic needs and in responding to its environment. Transcription is partly controlled by transcriptional regulators alone or in complex with other proteins that can either promote (as an activator) or block (as a repressor) the recruitment of RNA polymerase to promoters or enhancers of specific target genes (11, 16, 20).

Transcriptional regulators are essential for gene regulation and found in all living organisms (28). Transcription regulators may control gene expression by various mechanisms (7), including but not limited to the following ones that are pertinent to this dissertation. One mechanism is to stabilize or inhibit the binding of RNA polymerase to a promoter or enhancer DNA sequence. Another mode of action is to directly catalyze the acetylation or deacetylation of histones or recruit enzymes to perform the same actions. For example, histone acetylation occurs via histone acetyltransferase (HAT) activity.

Acetylation weakens the association of histones with DNA making the gene more accessible and thus upregulating expression. On the other hand, deacetylation of histones is caused by histone deacetylase (HDAC) activity, which enhances DNA-histone association, resulting in decreased accessibility of DNA and down-regulation of transcription (18). A third mechanism of regulation is via recruitment of co-activators or co-repressors to the site of transcription, adding another level of complexity to modulation of gene expression (31). Transcriptional regulators themselves are also subject to regulation at the transcriptional, translational and posttranslational levels. Examples include NF-κB and p53, key transcriptional regulators. NF-κB is inducible by serum, growth factors and cytokines at the transcriptional level and is regulated by association/dissociation of IκB at posttranslational level. p53 is regulated at the posttranslational level via phosphorylation/dephosphorylation. Additionally, at the posttranslational level, oxidation of cysteine(s) has also been shown to affect the function of many transcriptional regulators (19, 25, 27) and this thesis focuses on two such thiol-based redox-regulated transcriptional regulators.

1.2 Thiol-based redox modulation of transcriptional regulators

1.2.1 Thiol-based redox modulation

Oxygen is the terminal electron acceptor for all aerobic organisms; however, the incomplete reduction of oxygen results in generation of reactive oxygen species (ROS). ROS are continuously generated as a natural byproduct from the leakage of the respiratory chain in mitochondria and have important roles in cell signaling and homeostasis. However, under conditions of environmental stress (e.g. exposure to toxins, heavy metals, UV-radiation, heat shock) or during infection and inflammation, the levels

of ROS can increase dramatically and can cause deleterious effects (23, 24). When production of ROS supersedes the antioxidant capacity of the cell, it causes oxidative stress. The beneficial effects of ROS in host defense during microbial infection, in wound healing and in the redox signaling have been well documented (3, 10, 29). However, ROS are implicated in varieties of diseases including cancers, cardiovascular (heart attack, stroke), neurodegenerative (Alzheimer's and Parkinson's disease) and autoimmune diseases (1, 4, 16). Because ROS can damage cellular proteins, nucleic acids and lipids, cells have evolved various mechanisms to eliminate ROS. Cells have several antioxidant enzymatic systems such as superoxide dismutases, catalases, glutathione peroxidases or small molecule antioxidants such as ascorbic acid, tocopherol, uric acid and glutathione that play important role in detoxifying ROS. Superoxide dismutase ameliorates the damaging effects of superoxide by converting it into hydrogen peroxide. Catalase converts the hydrogen peroxide into oxygen and water (2). Glutathione peroxidase, a selenoprotein, also reduces hydrogen peroxide to water in a redox dependent manner. This process also involves glutathione (GSH), which upon reaction with ROS is converted to disulfide state (GSSG) (9).

ROS, as mentioned above, can damage vital molecules in cells including proteins, nucleic acids and lipids. The effect of ROS on nucleic acid damage and lipid oxidation is beyond the scope of this thesis and only protein modifications during oxidative stress are described here. In general, proteins carrying cysteine and methionine residues are targets of oxidants stress. Being electron rich and polarizable, sulfur, present in both cysteine and methionine, is sensitive to various oxidants. This thesis focuses only on cysteine (thiol) oxidation in proteins. The sulfhydryl group (-SH) in cysteine is sensitive to ROS and

(Figure 1) is oxidized to cysteine sulfenic acid (Cys-SOH) by a 2-electron oxidation. However, Cys-SOH is generally a short-lived, intermediate and can form intra- or inter-molecular disulfides. Sulfenic acid can also form a S-thiolated adduct with low molecular weight (LMW) thiols such as GSH or can form thiosulfinate (4) with other sulfenic acids. Overoxidation of cysteines may result in reversible cysteine modification forming sulfinic ($-SO_2H$) or irreversible cysteine modification forming sulfonic ($-SO_3H$) acids. Re-reduction of these thiols can occur either by LMW-thiols, by glutaredoxin (Grx), or by thioredoxin (Trx) (24).

Oxidation of cysteine residues in proteins can result in changes in their structure or in their cellular localization, or redox properties. These changes can affect the function of redox-sensitive cellular proteins. For example, thiol oxidation can change a protein's ligand binding affinity [e.g. glucocorticoid receptor (17)], modify the DNA binding affinity of a DNA binding protein [e.g. OhrR (21)] or alter the activity of an enzyme [e.g. GapDH (32)]. These functional changes following thiol modification by ROS allow proteins to act as redox-sensors. In most instances, these thiol modifications in the protein during redox sensing are reversible and contribute to thiol-based switches (1, 6). Thiol-based switches can be defined as proteins whose function can be reversibly modulated by the oxidation state of redox-active cysteine(s)

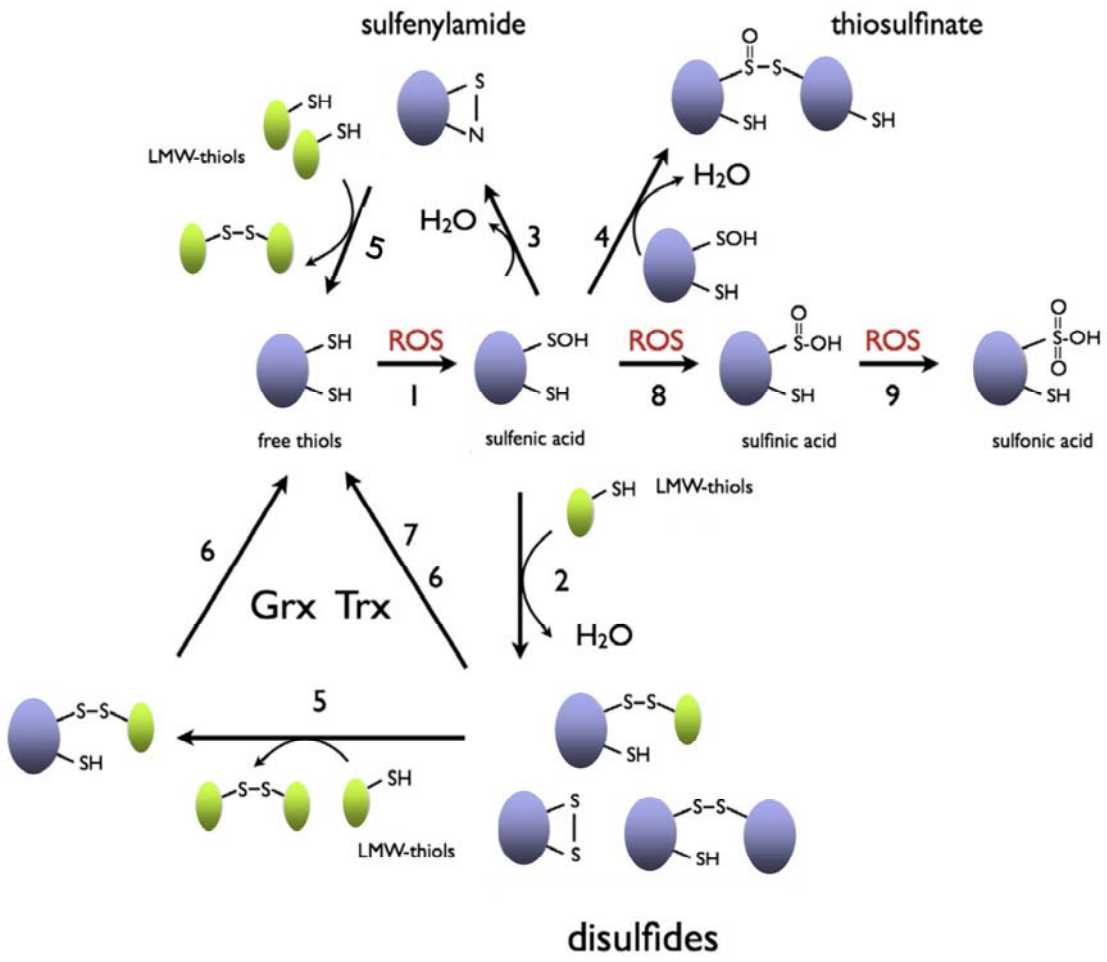

Figure 1.1: Cysteine modifications via ROS. Cysteines are reversibly oxidized by ROS from R-SH to R–SOH (sulfenic acid) (1). Sulfenic acid (1) is unstable and can form intra- or inter- molecular disulfides (2). Sulfenic acid can also make an s-thiolated adduct with low molecular weight thiols such as GSH (2). On the other side sulfenic acid can also be converted to a cyclic sulfenylamide (3) with a polypeptide backbone amide or thiosulfinate (4) with other sulfenic acid. Re-reduction of these thiols can occur either by low molecular weight (LMW)-thiols (5), or by glutaredoxin (Grx) (6), or by thioredoxin (Trx) (7). Overoxidation results in irreversible modification of cysteines forming sulfinic (8) and sulfonic (9) acids. This figure has been modified from Roos and Messeens, 2001, Free Radical Biology & Medicine (23).

1.2.2 Thiol-based redox switches

Thiol-based redox switches are present both in prokaryotes and eukaryotes. These switches play a protective role in the detoxification of ROS limiting the deleterious effects of oxidative stress. This regulation is often controlled by transcriptional regulators

via their redox-sensitive cysteines (1). These redox-sensitive transcriptional regulators have received a lot of attention in the last decade because of the growing interest in the area of free radicals and oxidative stress. Furthermore, it has been shown that the development and progression of many human diseases are linked to redox-sensitive transcriptional regulators (8). For example, redox-sensitive transcription factors such as NFκB and AP-1 are prime targets for chemoprevention with anti-inflammatory and antioxidative phytochemicals (26). OxyR was the first transcriptional regulator discovered to have the ability to sense ROS (2). Since then, many transcriptional regulators have been studied in prokaryotes (such as OxyR, OhrR, MerR and others) and in eukaryotes such as Yap1, Keap1/Nrf2 and others, which show thiol-based redox regulation. Some of these redox regulated transcription regulators are described below to facilitate a better understanding of thiol-based redox modulation of transcriptional regulators.

OxyR belongs to the LysR family of DNA binding proteins and positively regulates the expression of a large peroxide inducible-regulon. OxyR from *E. coli* gets activated in response to peroxide stress via an intramolecular disulfide bond between two conserved cysteines; Cys199 and Cys208. Cys199 first forms a sulfenic acid, which then undergoes reaction with Cys208, thus forming a disulfide. Then, the activated oxidized form of OxyR binds as a tetramer to promoters and activates the transcription of target genes (4, 13).

Another prokaryotic transcriptional regulator, OhrR, is a repressor that senses organic hydroperoxide and other ROS. Unlike OxyR, OhrR from *Xanthomonas campestris*

becomes inactivated upon oxidation, thus derepressing target genes. During oxidative stress, Cys22 is oxidized to sulfenic acid followed by formation of an intermolecular disulfide with Cys12. The disulfide interferes with DNA binding, thus allowing the transcription of target genes (21). OhrR from *Bacillus subtilis* also causes the derepression of target genes via oxidation of cysteine. However, the exact mechanism of oxidative inactivation in the *B. subtilis* OhrR is not known. A conserved cysteine, Cys15, is required for redox sensing and has been demonstrated to form the sulfenic acid *in vitro*. However, the sulfenic acid form of Ohr is still active and further modification is required for oxidative inactivation to occur, which has not been identified yet (15).

Yap1p is one of the best characterized eukaryotic thiol-based redox switches. Yap1 activates the expression of ~100 genes in response to ROS. The target genes include thioredoxin, GSH biosynthetic enzymes, glutathione reductase and others, which have conspicuous roles in thiol homeostasis (14). Yap1 has two cysteine rich domains (CRD) at the N-and C-termini that contain redox-sensitive cysteines. Under normal circumstances Yap1 is exported to the cytoplasm via a nuclear export receptor (Crm1), which binds to the CRD at the C-terminus. When peroxide stress occurs, Cys36 of glutathione peroxidase is oxidized and interacts with Cys598, one of the redox-sensitive cysteines in the C-terminal CRD. Further thiol-disulfide exchange reactions subsequently lead to disulfide formation between Cys303-Cys598 and Cys310-Cys629. These disulfides induce a conformational change in Yap1 that brings the N- and C-termini close together. This change in conformation restricts Crm1 binding to Yap1 and causes nuclear accumulation of Yap1, which leads to enhanced expression of target genes (1, 30).

Nrf2, another eukaryotic transcriptional regulator, plays a significant role in the activation of genes that contain an antioxidant response element (ARE), such as heme oxygenase-1, glutathione-S-transferase, catalase and others. The redox-sensitive Keap1 protein usually remains associated with Nrf2 and targets it for ubiquitin-dependent proteosomal degradation. Keap1 contains more than 25 Cys residues including redox-sensitive Cys151, Cys236 and Cys613. Keap1 also has Cys residues, such as Cys273 and Cys288, which coordinate Zn. Upon oxidation of Keap1, an intermolecular disulfide bond between two Cys151 residues and an intramolecular disulfide bond between Cys236 and Cys613 are formed. Upon oxidation of Cys273 and Cys288 Zn is released. Apparently a disulfide bond is not formed between Cys 273 and Cys 288 and their oxidation prodcuts are not known. Oxidation of these cysteines causes conformational changes in Keap1 and results in release of Nrf2 and its subsequent nuclear accumulation (22).

Cysteines, due to their facile redox-chemistry (5), play a key role in thiol-based redox switches, in responding to oxidative stress as described above (8). Redox-regulation of two similar systems is described in this thesis: (1) Section I describes, CprK, which is a prokaryotic transcriptional regulator, and (2) Rev-erbβ, a human transcriptional regulator has been described in Section II. CprK is a prokaryotic transcriptional regulator and is involved in the process of dehalorespiration. In the presence of ortho-haloaromatic compounds, which are recalcitrant to degrade in nature, CprK gets activated and induces expression of the genes involved in biodegradation of these compounds. We have identified the oxidative modification of redox-active cysteines in CprK and have characterized the dual role of one of the redox-active cysteines, Cys11 in the structure

and activity of CprK. Rev-erbβ, on the other hand, is a human transcriptional repressor and is implicated in different cellular processes such as circadian rhythm, metabolism, growth and inflammation. In this study, we have identified redox-active cysteines in Rev-erbβ and studied their oxidative modification. We have found that the function of Rev-erbβ is redox regulated and have elucidated the mechanism of redox modulation of Rev-erbβ *in vitro*. Discovery of Rev-erbβ as a redox-switch opens the doors to elucidating its role in several redox sensitive cellular processes.

1.3 References

1. Antelmann H, Helmann JD. 2011. Thiol-based redox switches and gene regulation. *Antioxid Redox Signal* 14: 1049-63

2. Aslund F, Zheng M, Beckwith J, Storz G. 1999. Regulation of the OxyR transcription factor by hydrogen peroxide and the cellular thiol-disulfide status. *Proc Natl Acad Sci U S A* 96: 6161-5

3. Cairns RA, Harris IS, Mak TW. Regulation of cancer cell metabolism. *Nat Rev Cancer* 11: 85-95

4. Choi H, Kim S, Mukhopadhyay P, Cho S, Woo J, et al. 2001. Structural basis of the redox switch in the OxyR transcription factor. *Cell* 105: 103-13

5. Fomenko DE, Marino SM, Gladyshev VN. 2008. Functional diversity of cysteine residues in proteins and unique features of catalytic redox-active cysteines in thiol oxidoreductases. *Mol Cells* 26: 228-35

6. Ghezzi P. 2005. Oxidoreduction of protein thiols in redox regulation. *Biochem Soc Trans* 33: 1378-81

7. Gill G. 2001. Regulation of the initiation of eukaryotic transcription. *Essays Biochem* 37: 33-43

8. Haddad J, J. 2002. Science review: Redox and oxygen-sensitive transcription factors in the regulation of oxidant-mediated lung injury: role for nuclear factor-κB. *Critical Care* 6: 481–90

9. Hayes JD, McLellan LI. 1999. Glutathione and glutathione-dependent enzymes represent a co-ordinately regulated defence against oxidative stress. *Free Radic Res* 31: 273-300

10. Jiang N, Tan NS, Ho B, Ding JL. 2007. Respiratory protein-generated reactive oxygen species as an antimicrobial strategy. *Nat Immunol* 8: 1114-22

11. Karin M. 1990. Too many transcription factors: positive and negative interactions. *New Biol* 2: 126-31

12. Latchman DS. 1997. Transcription factors: an overview. *Int J Biochem Cell Biol* 29: 1305-12

13. Lee C, Lee SM, Mukhopadhyay P, Kim SJ, Lee SC, et al. 2004. Redox regulation of OxyR requires specific disulfide bond formation involving a rapid kinetic reaction path. *Nat Struct Mol Biol* 11: 1179-85

14. Lee J, Godon C, Lagniel G, Spector D, Garin J, et al. 1999. Yap1 and Skn7 control two specialized oxidative stress response regulons in yeast. *J Biol Chem* 274: 16040-6

15. Lee JW, Soonsanga S, Helmann JD. 2007. A complex thiolate switch regulates the Bacillus subtilis organic peroxide sensor OhrR. *Proc Natl Acad Sci U S A* 104: 8743-8

16. Lee TI, Young RA. 2000. Transcription of eukaryotic protein-coding genes. *Annu Rev Genet* 34: 77-137

17. Makino Y, Okamoto K, Yoshikawa N, Aoshima M, Hirota K, et al. 1996. Thioredoxin: a redox-regulating cellular cofactor for glucocorticoid hormone action. Cross talk between endocrine control of stress response and cellular antioxidant defense system. *J Clin Invest* 98: 2469-77

18. Narlikar GJ, Fan HY, Kingston RE. 2002. Cooperation between complexes that regulate chromatin structure and transcription. *Cell* 108: 475-87

19. Nelson DE, Ihekwaba AE, Elliott M, Johnson JR, Gibney CA, et al. 2004. Oscillations in NF-kappaB signaling control the dynamics of gene expression. *Science* 306: 704-8

20. Nikolov DB, Burley SK. 1997. RNA polymerase II transcription initiation: a structural view. *Proc Natl Acad Sci U S A* 94: 15-22

21. Panmanee W, Vattanaviboon P, Poole LB, Mongkolsuk S. 2006. Novel organic hydroperoxide-sensing and responding mechanisms for OhrR, a major bacterial sensor and regulator of organic hydroperoxide stress. *J Bacteriol* 188: 1389-95

22. Paulsen CE, Carroll KS. 2010. Orchestrating redox signaling networks through regulatory cysteine switches. *ACS Chem Biol* 5: 47-62

23. Roos G, Messens J. 2011. Protein sulfenic acid formation: From cellular damage to redox regulation. *Free Radic Biol Med*

24. Storz G, Imlay JA. 1999. Oxidative stress. *Curr Opin Microbiol* 2: 188-94

25. Sun Y, Oberley LW. 1996. Redox regulation of transcriptional activators. *Free Radic Biol Med* 21: 335-48

26. Surh YJ, Kundu, J. K., Na, H. K., and Lee, J. S. 2005. Redox-Sensitive Transcription Factors as Prime Targets for Chemoprevention with Anti-Inflammatory and Antioxidative Phytochemicals. *The journal of nutrition* 135: 2993S-3001S

27. Tanaka H, Makino Y, Okamoto K, Iida T, Yoshikawa N, Miura T. 2000. Redox regulation of the nuclear receptor. *Oncology* 59 Suppl 1: 13-8

28. van Nimwegen E. 2003. Scaling laws in the functional content of genomes. *Trends Genet* 19: 479-84

29. Winterbourn CC, Hampton MB. 2008. Thiol chemistry and specificity in redox signaling. *Free Radic Biol Med* 45: 549-61

30. Wood MJ, Storz G, Tjandra N. 2004. Structural basis for redox regulation of Yap1 transcription factor localization. *Nature* 430: 917-21

31. Xu L, Glass CK, Rosenfeld MG. 1999. Coactivator and corepressor complexes in nuclear receptor function. *Curr Opin Genet Dev* 9: 140-7

32. Ziegler DM. 1985. Role of reversible oxidation-reduction of enzyme thiols-disulfides in metabolic regulation. *Annu Rev Biochem* 54: 305-29

SECTION I

Chapter 2

CprK, A TRANSCRIPTIONAL REGULATOR OF DEHALORESPIRATION

2.1 Halogenated organic compounds and their biodegradation

2.1.1 Halogenated organic compounds

One of the largest groups of xenobiotics, halogenated organic compounds, are continuously released in the atmosphere by plants, marine animals, bacteria, fungi, mammals and other natural processes (10). Natural production of these halogenated organic compounds has been a vital part of our ecosystem, but anthropogenic accumulation (industrial and agricultural) of these compounds, in the last century, has resulted in significant environmental contamination (22). These compounds are widely used in industrial applications because of their specific chemical and physical properties, such as excellent dielectric properties, stability to oxidation, flame resistance and relative inertness (14).

The halogenated organic compounds have hazardous effects on human health and have been implicated in different types of cancers, reproductive disorders in males and females, birth defects, infant mortality, cardiovascular problems, muscle dysfunction, liver damage and others (2). To safeguard human health and the environment from these

harmful chemicals that are persistent in the environment as persistent organic pollutants (POPs), the Stockholm Convention treaty was signed in 2001. POPs are toxic halogenated organic compounds and are comprised of three groups: (1) industrial chemical products such as PCBs, (2) combustion and by-products including dioxins, and (3) pesticides such as DDT. The list of POPs initially started with twelve halogenated organic compounds (the "dirty dozen"), but since May 2009, 9 more POPs which might have devastating effects on the environment and effect on human health such as cancer and diminished intelligence, have been added to the list. Interestingly, 16 of these POPs are chlorinated organic compounds (Stockholm Convention on POPs, United Nations Environment Program, 2001).

2.1.2. Remediation strategies and biodegradation

Halogenated organic compounds are present as pollutants in the air, soil, underground water and sediments. These compounds are persistent in nature and thus require aided degradation. There are various physiochemical treatments available for soil remediation, such as thermal cleaning or extraction of the contaminants by adsorption on activated carbon preceded by evaporation (33). Unfortunately, all these processes are not only costly and inadequate, but also cause damage to soil (23). Providentially, some microbes can remove the halogen groups from these compounds, otherwise a very difficult process, and make the compound easier to degrade further in the environment.In fact, bioremediation of soil is emerging as a viable alternate for soil-cleanup. Microorganisms can degrade halogenated organic compounds by the following mechanisms (9).

1. **Oxidative dehalogenation:** This process is catalyzed via mono-and di-oxygenases in co-metabolic or metabolic reactions. Halogenated organic compounds are used as a carbon/oxidizable electron source (9, 28).
2. **Dehydrohalogenation:** In the process of dehydrohalogenation, the halogen is removed in the form of the acid (e.g. HCl) from the halogenated organic compounds by dehydrohalogenases (9).
3. **Substitutive dehalogenation:** Dehalogenation of halogenated organic compounds is largely mediated by hydrolytic dehalogenases (halidohydrolases), but thiolytic dehalogenation is also possible with the help of glutathione-S-transferase. Additionally, dehalogenation via intramolecular substitution takes place via halohydrin halogen-halide lyases (9).
4. **Dehalogenation by methyl transfer:** Dehalogenation via this mechanism involves transfer of a methyl group from the substrate to tetrahydrofolate in some strictly anaerobic bacteria and is also called fermentative dehalogenation (9, 11).
5. **Reductive dehalogenation:** Reductive dehalogenation is an important process in the biodegradation of halogenated aliphatic and aromatic compounds and might occur in three different ways that are described in section 2.2 (9, 25, 34).

Halogenated organic compounds, especially halogenated aromatic compounds, such as polychlorinated biphenyls (PCBs), are relevant to section I of this thesis and are also known to be toxic for human health (35). Due to the presence of the halogen group in the benzene ring, the water solubility of these molecules is reduced and molecules are hydrophobic innature. Therefore, these halogenated aromatic compounds when released into the environment, eventually settle into sediments (humic acid) or form sludges (oil-

water mixtures) on the bottom of rivers, lakes and oceans (36). Mechanical disturbance by wind and rain help these compounds enter into the food chain. These compounds, being lipophilic in nature, eventually accumulate in the fatty tissue of living animals including human beings and are distributed at higher concentration at the top of the food chain (36).

Halogenated aromatic compounds, in general, are stable in the environment due to their long half lives (35). Their biodegradation mainly depends on the aerobic oxidative and anaerobic reductive dehalogenation. The aerobic oxidative dehalogenation of halogenated aromatic compounds has been extensively studied, though this mechanism is feasible only for lightly halogenated organic compounds.Heavily halogenated organic compounds are resistant to oxygen-aided degradation, because the electronegative nature of halogens inhibits oxygen attack on the carbon backbone (12, 38). Moreover, in many cases, only the top few millimeters of sediments are aerobic and the remaining sediments where halogenated aromatic compounds primarily reside are anaerobic. Therefore their degradation mostly depends on reductive dehalogenation via anaerobic bacterial flora that will be described in detail in section 2.2 (36).

2.2 Reductive dehalogenation

Microbial reductive dehalogenation, which is an anaerobic process in most instances, is a critical step in the metabolism of highly halogenated organic compounds including PCBs. The reductive dehalogenation mechanism involves removal of the halogen substituent with concurrent addition of electrons to the molecule. This process can take place either via replacement of a halogen with a hydrogen atom (hydrogenolysis) or via elimination

of two halogens from adjacent carbon atoms, leaving behind a double bond (vicinal reduction). Both processes require an electron donor and release the halogen atom as a halide ion (20). Overall, three different kinds of microbial reductive dehalogenation have been described in Nature (36).

1. **Co-metabolic reductive dehalogenation:** Abiotic or co-metabolic reductive dehalogenation has been proposed to be catalyzed mostly by metal ion-containing, heat-stable tetrapyrroles or enzymes using the same as cofactors (25). This process is common among methanogenic, acetogenic, sulfate reducing and iron-reducing bacteria with no benefit to the organism. Haloalkanes are the most common substrate for this kind of reductive dehalogenation reaction.
2. **Reductive dehalogenation linked to carbon metabolism:** Reductive dehalogenation is not confined to strictly anaerobic bacteria. For example, some phototropic bacteria, such as *Rhodospirillum rubrum,* a facultative anaerobe*,* grow phototropically on C2 and C3 halocarboxylic acids in the absence of oxygen. Reductive dehalogenation is followed by assimilation of the carboxylic acids.
3. **Metabolic dehaloganation/dehalorespiration:** The metabolic dehalogenation reaction is also known by other names such as halorepiration, dehalorespiration or halidogenesis. This process connects the reductive dehalogenation reaction to microbial growth by specific bio-catalysts (25). The reductive dehalogenation process is a two-electron transfer reaction that releases the halogen as a halogenide ion and replaces the halogen with hydrogen.

Among the three processes described above, dehalorespiration is most relevant to this chapter and will be discussed further. Dehalorespiration is mainly performed by

anaerobic bacteria that use halogenated organic compounds as electron acceptors. Halogenated organic compounds are excellent electron acceptors because the standard redox potential for most of the R-Cl/R-H couples falls between +250 and +600 mV (8). The high redox-potential of the R-Cl/R-H couples ensures that reductive dehalogenation is a thermodynamically favorable reaction ($\Delta G \approx$ -130 to -180 kJ/mol per chlorine removal), which in turn enables the microbes to couple reductive dehalogenation to their growth (25).

2.3 Microbial dehalorespiration

Isolation and characterization of *Desulfomonile tiedjei* pioneered the field of microbial dehalorespiration because this anaerobic bacterium was first demonstrated to couple the reductive dehalogenation of 3-chlorobenzoate to energy conservation (Figure 2.1) (7). In this process, the carbon-halogen bond is cleaved during reductive dehalogenation by a specific dehalogenase, which uses halogenated organic compounds as a substrate and transfers electrons to a respiratory chain for energy generation (Figure 2.1).

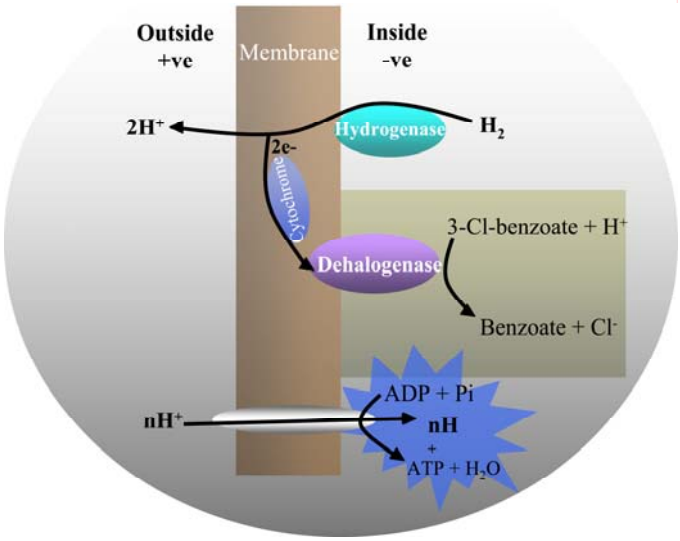

Figure 2.1: Hypothesis for coupling between reductive dehalogenation and energy generation in *D. tiedjei*. Hydrogen acts as an electron donor and 3-chlorobenzoate serves as an electron acceptor in the respiratory chain under anaerobic conditions and results in the generation of ATP. This figure is based on Fantroussi et al. 1998 (8).

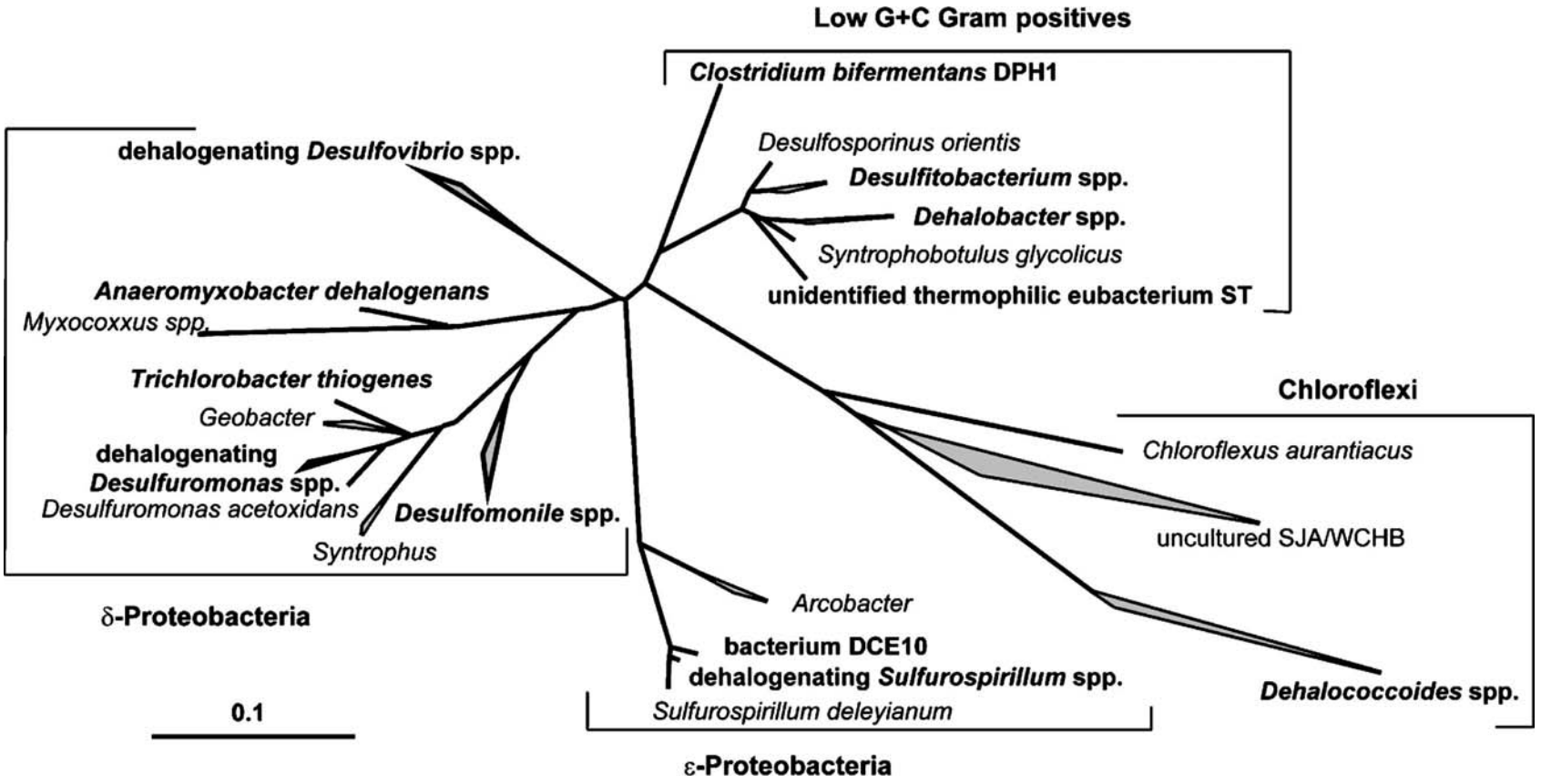

Figure 2.2: Phylogenetic tree of halorespirating bacteria based on bacterial small ribosomal subunit (SSU) rRNA sequences. The bacteria have been divided into four main branches, δ-Proteobacteria, ε-Proteobacteria, Low G+C Gram positives and Chloroflexi (from Hauke and Willem, 2004 (25)).

Since then, many dehalorespirating bacteria have been described, including *D. dehalogenans* (Figure 2.2). The CprK protein described in this thesis is from *D. dehalogenans*.

2.4 Dehalorespiration in *Desulfitobacterium dehalogenans*

Desulfitobacterium spp. is a species of anaerobic bacteria that belongs to the low G+C Gram positive branch of the dehalorespiring bacteria (Figure 2.2), which comprises a major group of isolates. Most of the *Desulfitobacterium* strains were initially collected from a site contaminated with anthropogenic halogenated aromatic compounds. Interestingly, the entire *Desulfitobacterium* genera can utilise a broad spectrum of substrates for dehalogenation (29).

2.4.1 *Desulfitobacterium dehalogenans*

Desulfitobacterium dehalogenans was first isolated from methanogenic lake sediments in North America and is the first characterized dehalorespirating desulfitobacterium. The organism was found to be resistant to microaerophilic conditions (30). *D. dehalogenans* can only use ortho-haloaromatic compounds (described in the earlier part of this chapter) as a substrate for dehalorespiration (Figure 2.3). A commonly studied substrate on which this bacterium can grow is 3-chloro-4-hydroxyphenylacetate (CHPA). The optimum pH for growth is 7.5, and the doubling time for the bacterium is around 3.5 hours at 37 °C. *D. dehalogenans* can grow utilizing pyruvate, lactate, formate or hydrogen as electron donors and CHPA as an electron acceptor. However, there is no electron transport coupled phosphorylation when the bacterium is grown on lactate+CHPA or pyruvate+CHPA. Nevertheless, formate and hydrogen, when used as electron donors for

dehalorespiration, establish a proton motive force that can be used for ATP generation. The bacterium can also use sulfite, thiosulfate, fumarate, nitrate and CO_2 as alternate electron acceptors (Figure 2.3) (30, 31).

Desulfitobacterium dehalogenans (JW/IU-DCI)

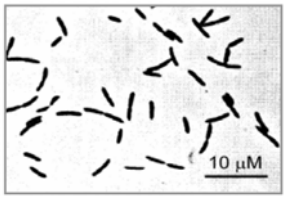

Phylum: *Firmicutes*, Class: *Clostridia*,

Order: *Clostridiales*, Family: *Peptococcaceae*.

Fermentative	Electron donars	Electron acceptors	
		Alternative	Halogenated
pyruvate	pyruvate, lactate, formate, hydrogen	Sulphite, thiosulphie, sulphur, nitrate, fumarate, CO_2, Fe^{III}, Se^{VI}, Mn^{VI}, AQDS	CHPA, 2,3,-DCP, 2,4-DCP, 2,6-DCP, 2,3,4-TCP, 2,3,6-TCP, 2,4,6-TCP, PCP, 2,3,4,5-TeCP, 2,3,4,6-TeCP, para-hydoxylated PCBs

Figure 2.3: Classification and growth properties of *D. dehalogenans*. CHPA, 3-chloro-4hydroxyphenylacetic acid; DCP, dichlorophenol; TCP, trichlorophenol; TeCP, tetrachlorophenol; PCP, petachlorophenol; PCBs, polychlorobiphenyls; AQDS, anthraquinone-2,6-disulfonate (humic acid analogue) (17, 21, 29, 30, 37).

The observation that *D. dehalogenans* can use CHPA in the presence of other energy-yielding terminal electron acceptors has strengthened the argument that chlorinated phenols can competitively serve as alternative electron acceptors for *D. dehalogenans* and that reductive dehalogenation of these compounds leads to energy release, apparently through electron transport coupled phosphorylation (18, 26).

D. dehalogenans can dehalogenate a variety of haloaromatic compounds, including pentachlorophenol, tetrachlorophenols, trichlorophenols, dichlorophenols, bromophenols at ortho position, hydroxyl-polychlorinated biphenyls, along with CHPA (Figure 2.3). It is unable to dehalogenate most fluorophenols and monochlorophenols with the exception

of CHPA in which the chlorine is present ortho to the hydroxyl group (19, 29, 30, 37). The ortho-chlorophenol reductive (o-CP) dehalogenase from *D. dehalogenans* is a membrane-associated enzyme that mediates electron transfer from donor to the halogenated substrate. The enzyme contains one [4Fe-4S] cluster, one [3Fe-4S] and one cobalamin per monomer (32). The gene encoding o-CP dehalogenase, *cprA*, is present in the *cpr* (chlorophenol reduction) gene cluster.

2.4.2 Role of cpr gene cluster in dehalorespiration

The *cpr* gene cluster in *D. dehalogenans* encodes proteins involved in the dehalorespiration process and consists of a total of 8 genes: *cprT*, *cprK*, *cprZ*, *cprE*, *cprB*, *cprA*, *cprC* and *cprD*, organized into four transcription units (Figure 2.4). All the cpr genes, except *cprAB*, are expressed constitutively. *CprB* and *cprA* are transcribed together. C*prB* has been predicted to encode an integral membrane protein that might serve as a membrane anchor for CprA. C*prA* encodes the o-CP dehalogenase pre-protein containing an amino terminal twin arginine (RR) signal sequence (S/TRRXFLK), which is a common feature of the reductive dehalogenases and is thought to play a role in the maturation and translocation of periplasmic proteins (32).

C*prC* and *cprD* are constitutively transcribed as bicistronic transcripts. CprC contains six transmembrane helices and has similarities with membrane-bound NosR/NirI regulators, while the *cprD* gene product is similar to GroEL-type chaperones. C*prK*, *cprZ*, *cprE* are transcribed as a tricistronic message (*cprKZE*). *CprE* potentially encodes a GroEL-type chaperone similar to *cprD*, while *cprZ* has no similarity to any known protein. C*prK* encodes a transcriptional regulatory protein that is responsible for the transcription of all

of the transcripts in the gene cluster and is the focus of section I of this thesis. *CprT* is transcribed in the opposite direction from all other genes in the cluster. C*prT* encodes a protein that is similar to a trigger factor peptidyl prolyl isomerase, and is considered to be involved in protein folding (27).

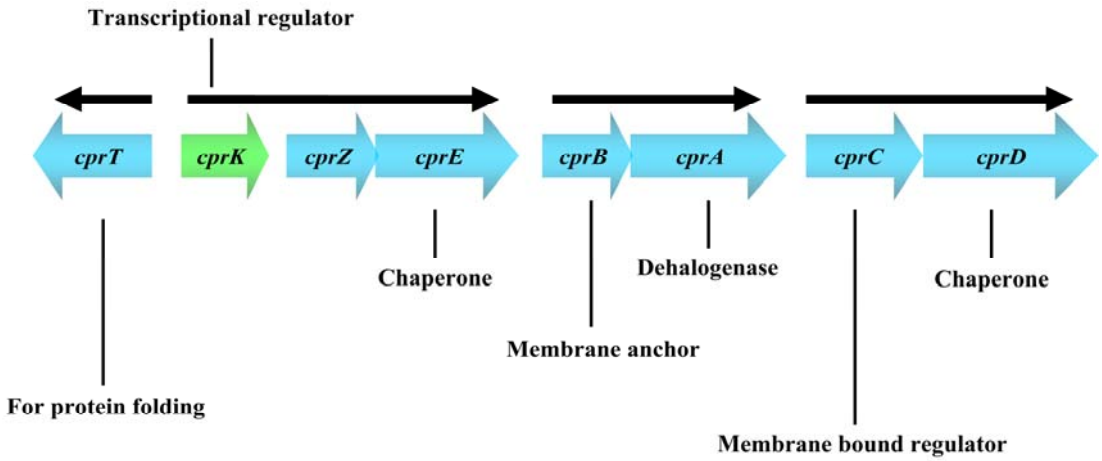

Figure 2.4: Gene organization and putative CprK-dependent promoter regions in the *cpr* gene cluster of *D. dehalogenans*. Arrows indicate the direction of transcription of each of the four transcription units. Functions/putative functions are indicated below or above of each gene.

Figure 2.5 provides an overall picture of the roles of the *cpr* gene cluster in expression and maturation of CprA in *D. dehalogenans*. CprC, CprD, CprE and CprT are proposed be involved in protein folding and maturation of CprA. CprK regulates the expression of CprA; while CprB probably anchors CprA into the membrane.

2.5 CprK: a transcriptional regulator of dehalorespiration

CprK is a transcriptional regulator of the *cpr* gene cluster that encodes proteins involved in the degradation of aromatic compounds (e.g. CHPA) and belongs to the CRP-FNR

(cAMP Receptor Protein-Fumarate Nitrate reduction Regulatory protein) superfamily of transcriptional regulators.

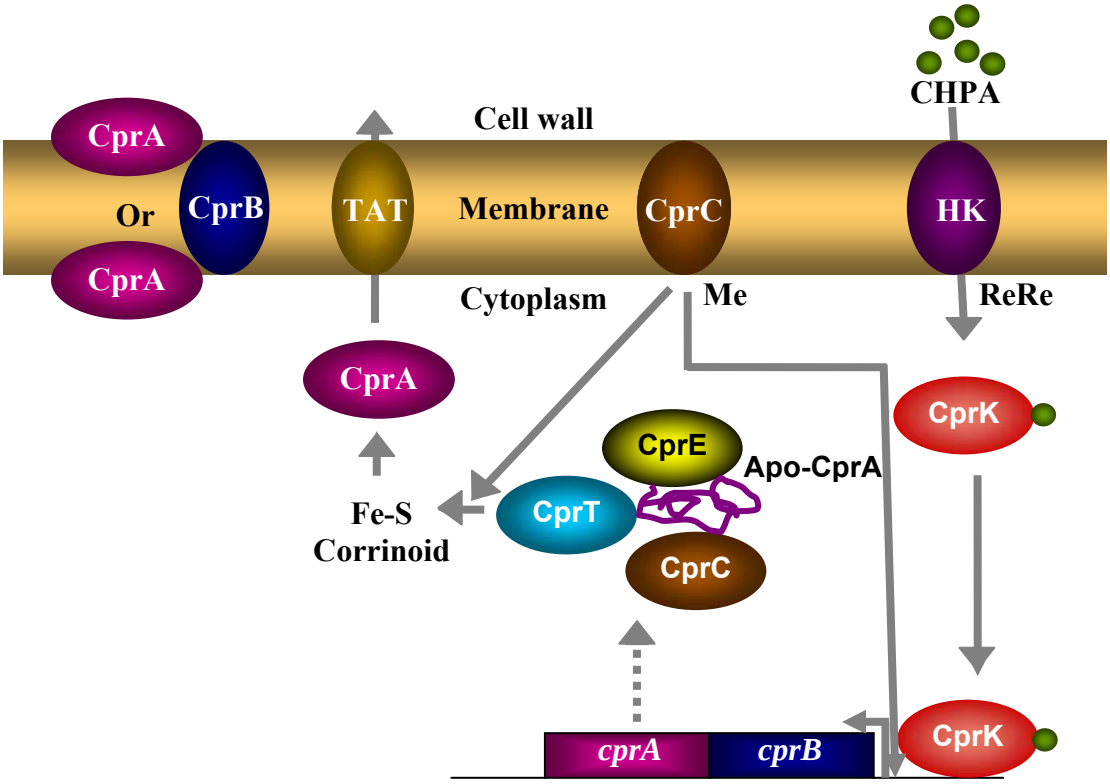

Figure 2.5: **Model for the roles of *cpr* gene cluster products in expression and maturation of CprA.** HK: histidine kinase with response regulator (ReRe). TAT: twin arginine specific complex. Me: metal ion that may be involved in the control of gene expression and is incorporated in mature reductive dehalogenase (CprA). CprA could be outside or inside of the cytoplasmic membrane. This figure is modified from Villemur et al., 2006 (34).

2.5.1 Characteristics of CRP-FNR family: CRP-FNR is a very large family of transcriptional regulators with over 1200 family members. All members of this family are DNA binding proteins that predominantly act as activators of transcription, but negative regulation has also been observed by some of the members. Members of this family respond to a broad spectrum of intracellular and exogenous signals such as cAMP, anoxia, oxidative and nitrosative stress, nitric oxide, CO, 2-oxoglutarate and temperature.

CRP, one of the main members, is involved in amino acid and sugar metabolism, transport processes, protein folding, pilus synthesis and toxin production (15). Transcriptional regulators of this family are characterized by the presence of an N-terminal effector binding domain and a C-terminally located helix-turn-helix (HTH) motif for DNA binding (16). It is believed that the HTH domain is one of the most ancient, conserved features of the transcription regulators (16) and was probably already present in the last universal common ancestor (1).

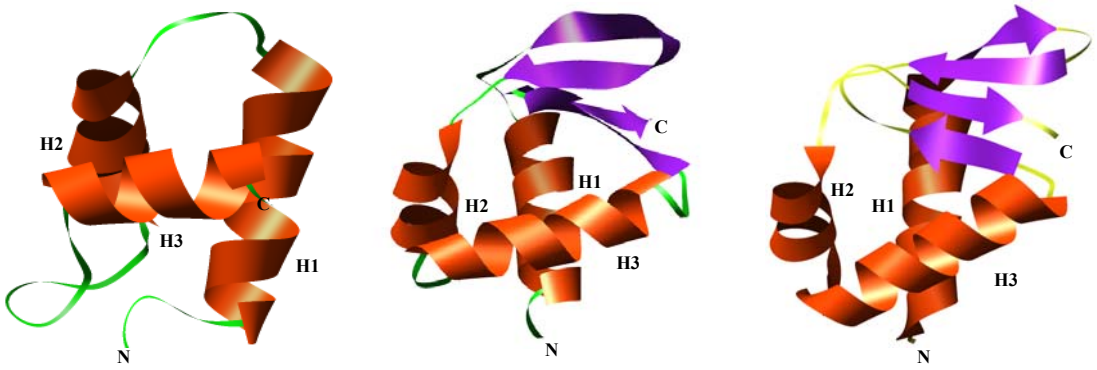

A. **B.** **C.**

Figure 2.6: **The HTH domain**. Salient structural features of a simple HTH domain (A), wHTH domain of the CRP-like group (B) and DNA binding domain of CprK (C). This figure was created in CHIMERA using the PDB Ids of the above described proteins; A-1k78, B-1cgp, and C-2h6c.

The basic HTH domain is comprised of three α-helices as shown in Figure 2.6.A. Sequence and structural analysis reveals that the loop between the first and second helices can accommodate insertions, but a sharp turn between the second and third helices, a characteristic feature of the HTH domain, has never been found to have insertions. The third helix, known as the recognition helix, forms the principal DNA-protein interface by inserting itself into the major groove of the DNA (3, 4). One of the

modifications of the HTH domain, the winged HTH (wHTH) domain, usually contains a C-terminal β-strand hairpin extension that is called the wing (3, 5). Further modifications in the basic wHTH motif are possible. One of the subsets of the wHTH forms a CRP-like group (Figure 2.6.B), which is actually a four-stranded version of the wHTH domain. Along with the C-terminal β-hairpin, this group also has another β-hairpin in the linker region between the first and second helices of the HTH domain. The DNA binding domain of CprK falls in the same category (Figure 2.6.C).

2.5.2 Characteristics of CprK

2.5.2.1 Sequence and structure: This thesis focuses on CprK from *D. dehalogenans*. CprK is a newly identified member of the CRP-FNR family of transcriptional regulators (27). CprK shows low sequence similarity (30-40%) with CRP and FNR, but has a characteristic wHTH domain and an N-terminal cAMP-like effector binding domain, which places CprK in the CRP-FNR family of transcriptional regulators. Its wHTH motif is very small but has a significant number of conserved residues (Figure 2.7). On the other hand, the effector binding domain, the largest domain of the protein, has very few residues that are conserved with CRP and FNR (Figure 2.7). The diversity in the effector binding domain likely accounts for the recognition of different effector molecules among the family members.

Most members of this family have only 1 or 2 cysteine residues with the exception of FNR, which has five cysteine residues and CprK that has five cysteine residues (Cys11, Cys105, Cys111, Cys161 and Cys200) (Figure 2.7). The presence of a higher number of cysteine residues suggests a possible functional importance for the protein; for example,

Figure 2.7: **Multiple sequence alignment of CprK with other representative members of the CRP-FNR family.** Dd: *D. dehalogenans* (NCBI ID: AAF67815), EC: *E. coli* [NCBI ID: POACJ8 (CRP) and POA9E5 (FNR)], Rr: *R. rubrum* (NCBI ID: 1FT9B). Cysteines are shown in red color font. Blue rectangle indicate the N-terminal effector binding domain and red rectangle outlines the contiguous wHTH motif, and the green rectangle covers the C-helix according to the CprK sequence. Seqence alignment was done in NCBI.

the four cysteine residues conserved at the N-terminus of FNR are involved in ligation of an 4Fe-4S cluster (6). The CprK sequence does not contain the N-terminal conserved cysteines found in FNR. This is consistent with the finding that CprK does not contain a metal cluster, which is also supported by the lack of absorption in the 350 nm to 420 nm region (24). Interestingly, most of the cysteine residues in CprK are involved in redox regulation of the protein as described in Chapter 3.

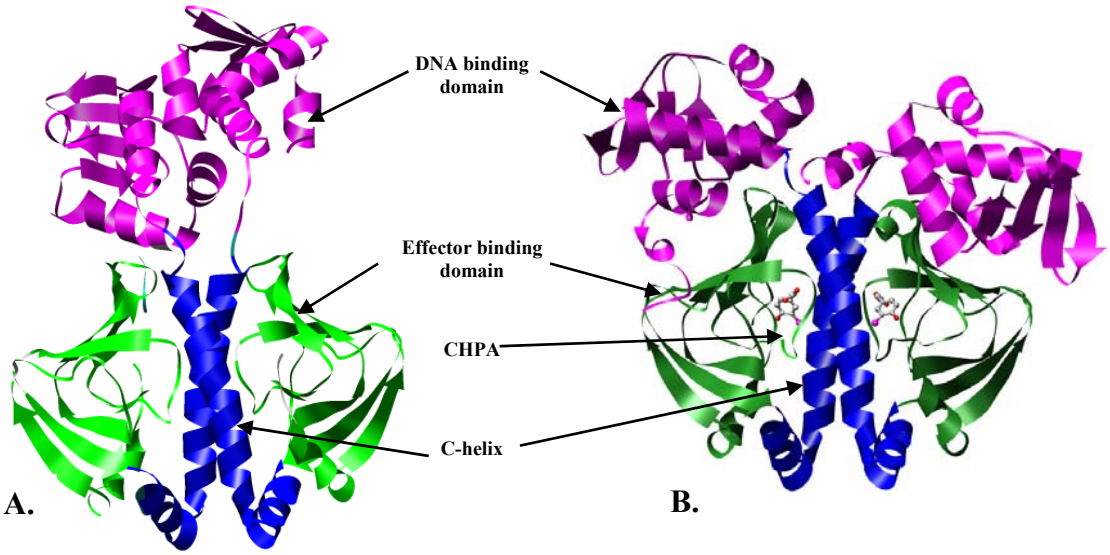

Figure 2.8: Crystal structures of CprK. Crystal structures of reduced (A) and oxidized (B) CprK from *D. dehalogenans* and *D. hafniense* respectively.

The crystal structures of reduced CprK (*D. dehalogenans*) in the absence of CHPA (PDB ID: 2h6b) and of the oxidized protein (*D. hafniense*) with CHPA (PDB ID: 2h6c) have been solved at 2.9 Å and 2.2 Å resolution, respectively and both are dimers (13). Similar to CooA, the DNA binding domains are swapped between the two monomers in the crystal structures of CprK (Figure 2.8). The N-terminal effector-binding domain has CHPA bound to it. The C-helix that connects the DNA and effector-binding domains also

provides the interface for dimerization (Figure 2.8). A significant difference in the three-dimensional arrangement of the DNA binding domain was observed in the reduced versus the oxidized proteins. In the oxidized protein, the DNA binding domain is at an approximately 110° angle from the C-helix, while in the reduced protein, the DNA binding domain is placed approximately parallel to the C-helix.

2.5.2.2 Intrinsic and biophysical properties: CprK is a cytoplasmic protein and is 232 amino acids long. The fulllength protein, described in this thesis, was expressed in *E. coli* cells with a C-terminal 6X-His tag. The pI of CprK is 5.74 and its molecular weight is 26.65 kDa; however, the molecular weight of 6x His-tagged CprK is 27,947.1+/- 2.7 Da, as analyzed by mass spectrometry analysis, which is in agreement with the predicted amino acid sequence (24).

2.5.2.3. DNA binding properties: CprK was characterized in 2004 as the first transcriptional regulator of dehalorespiration. Some of the experimentally demonstrated DNA binding properties of CprK (28) are as follows. CprK has been shown to bind DNA in the presence of CHPA. DNA footprinting analysis revealed that CprK protected a 14 bp pseudopalindromic sequence as shown in Figure 2.9.A. This sequence is similar to the consensus sequences recognized by CRP and FNR (Figure 2.9).

However, a electrophoretic mobility shift assay (EMSA) showed that a minimum of 32 bp are required for a gel shift in the *in vitro* assay, thereby extending the DNA length by few more residues on both sides of the 14 bp protected region (AGA TAA AAG **TTA ATA CGC ACT AA**T ACT TGT GT). The approximate K_d for CprK for DNA is 190 ± 30 nM as determined in EMSA studies (24). However, the binding analysis done under

the same conditions by the anisotropy method indicated much lower K_d value; 14 ± 3 nM (Gupta and Ragsdale, University of Michigan, unpublished data).

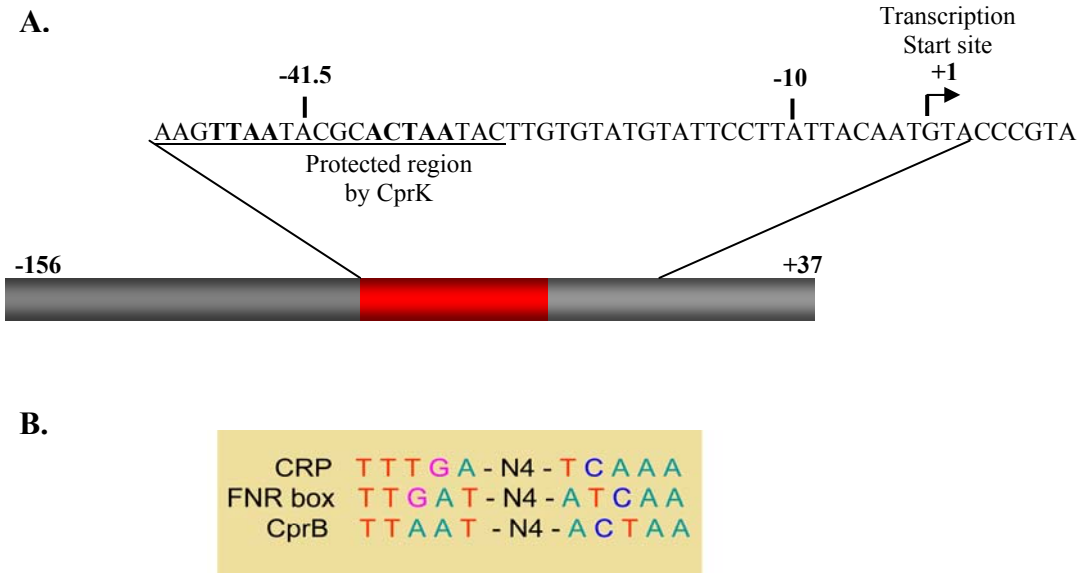

Figure 2.9: DNA binding sequence of CprK. A. CprK binding site in the *cprB* promoter region, as determined by DNase1 footprinting analysis. B. A comparison of the CRP and FNR binding sites on DNA with the CprK binding site (24).

2.5.2.4. Effector binding properties: The effector molecule for CprK from *D. dehalogenans* is CHPA and is required for CprK to bind DNA. Many other effector molecules, such as 3-chlorophenylacetate, 4-hydroxyphenylacetate, 3-chloro-4-hydroxybenzoate, 3-chlorobenzoate, 3, 5-dichloro-4-hydroxy benzoate and 2, 4-dichlorobenzoate, were also tested by EMSA for binding to CprK. However, no significant binding or mobility shift was observed (24). This suggests that the chlorine group and the hydroxyl group are important for specific interactions between CHPA and CprK.

2.6 References

1. Aravind L, Anantharaman V, Balaji S, Babu MM, Iyer LM. 2005. The many faces of the helix-turn-helix domain: transcription regulation and beyond. *FEMS Microbiol Rev* 29: 231-62

2. Benigni R. 2005. Structure and Activity Relationship Studies of Chemical Mutagens and Carcinogens: Mechanistic Investigations and Prediction Approaches. *Chemical Reviews* 105: 1767-800

3. Brennan RG. 1993. The winged-helix DNA-binding motif: another helix-turn-helix takeoff. *Cell* 74: 773-6

4. Brennan RG, Matthews BW. 1989. The helix-turn-helix DNA binding motif. *J Biol Chem* 264: 1903-6

5. Clark KL, Halay ED, Lai E, Burley SK. 1993. Co-crystal structure of the HNF-3/fork head DNA-recognition motif resembles histone H5. *Nature* 364: 412-20

6. Crack J, Green J, Thomson AJ. 2004. Mechanism of oxygen sensing by the bacterial transcription factor fumarate-nitrate reduction (FNR). *J Biol Chem* 279: 9278-86

7. DeWeerd K, Mandelco, L., Tanner, R., Woese, C., Sulflita, J. 1990. Desulfomonile tiedjei, new genus, new species, a novel anaerobic, dehalogenating, sulfate-reducing bacterium. *Arch. Microbiol.* 154: 23-30

8. El Fantroussi S, Naveau H, Agathos SN. 1998. Anaerobic Dechlorinating Bacteria. *Biotechnology Progress* 14: 167-88

9. Fetzner S. 1998. Bacterial dehalogenation. *Appl Microbiol Biotechnol* 50: 633-57

10. Gribble GW. 1994. The natural production of chlorinated compounds. *Environ. Sci. Technol.* 28: 311A-8A

11. Holliger C, Regeard, C., Diekert, G. 2004. *Dehalogenation by anaerobic bacteria. In dehalogenation*: Springer US

12. Janssen DB, Dinkla IJT, Poelarends GJ, Terpstra P. 2005. Bacterial degradation of xenobiotic compounds: evolution and distribution of novel enzyme activities. *Environmental Microbiology* 7: 1868-82

13. Joyce MG, Levy C, Gabor K, Pop SM, Biehl BD, et al. 2006. CprK crystal structures reveal mechanism for transcriptional control of halorespiration. *J Biol Chem* 281: 28318-25

14. Kimbrough R, D. 1989. *Halogenated Biphenyls, Terphenyls, Naphthalenes, Dibenzodioxins and Related Products*

15. Kolb A, Busby S, Buc II, Garges S, Adhya S. 1993. Transcriptional Regulation by cAMP and its Receptor Protein. *Annual Review of Biochemistry* 62: 749-97

16. Korner H, Sofia HJ, Zumft WG. 2003. Phylogeny of the bacterial superfamily of Crp-Fnr transcription regulators: exploiting the metabolic spectrum by controlling alternative gene programs. *FEMS Microbiol Rev* 27: 559-92

17. Luijten ML, Weelink SA, Godschalk B, Langenhoff AA, van Eekert MH, et al. 2004. Anaerobic reduction and oxidation of quinone moieties and the reduction of oxidized metals by halorespiring and related organisms. *FEMS Microbiol Ecol* 49: 145-50

18. Mackiewicz M, Wiegel J. 1998. Comparison of Energy and Growth Yields for Desulfitobacterium dehalogenans during Utilization of Chlorophenol and Various Traditional Electron Acceptors. *Appl. Environ. Microbiol.* 64: 352-5

19. Milliken CE, Meier GP, Watts JEM, May HD. 2004. Microbial Anaerobic Demethylation and Dechlorination of Chlorinated Hydroquinone Metabolites Synthesized by Basidiomycete Fungi. *Appl. Environ. Microbiol.* 70: 385-92

20. Mohn WW, Tiedje JM. 1992. Microbial reductive dehalogenation. *Microbiol Rev* 56: 482-507

21. Niggemyer A, Spring S, Rosenzweig RF. 2001. Isolation and characterization of a novel As(V)-reducing bacterium: implications for arsenic mobilization and the genus Desulfitobacterium. *Appl Environ Microbiol* 67: 5568-80

22. Oberg G. 2002. The natural chlorine cycle--fitting the scattered pieces. *Appl Microbiol Biotechnol* 58: 565-81

23. Paul D, Pandey G, Pandey J, Jain RK. 2005. Accessing microbial diversity for bioremediation and environmental restoration. *Trends in Biotechnology* 23: 135-42

24. Pop SM, Kolarik RJ, Ragsdale SW. 2004. Regulation of anaerobic dehalorespiration by the transcriptional activator CprK. *J Biol Chem* 279: 49910-8

25. Smidt H, de Vos WM. 2004. ANAEROBIC MICROBIAL DEHALOGENATION. *Annual Review of Microbiology* 58: 43-73

26. Smidt H, Song D, van der Oost J, de Vos WM. 1999. Random Transposition by Tn916 in Desulfitobacterium dehalogenans Allows for Isolation and Characterization of Halorespiration-Deficient Mutants. *J. Bacteriol.* 181: 6882-8

27. Smidt H, van Leest M, van der Oost J, de Vos WM. 2000. Transcriptional Regulation of the cpr Gene Cluster in ortho-Chlorophenol-Respiring Desulfitobacterium dehalogenans. *J. Bacteriol.* 182: 5683-91

28. Song B, Palleroni NJ, Hâggblom MM. 2000. Description of strain 3CB-1, a genomovar of Thauera aromatica, capable of degrading 3-chlorobenzoate coupled to nitrate reduction. *International Journal of Systematic and Evolutionary Microbiology* 50: 551-8

29. Utkin I, Dalton DD, Wiegel J. 1995. Specificity of Reductive Dehalogenation of Substituted ortho-Chlorophenols by Desulfitobacterium dehalogenans JW/IU-DC1. *Appl Environ Microbiol* 61: 1677

30. Utkin I, Woese C, Wiegel J. 1994. Isolation and characterization of Desulfitobacterium dehalogenans gen. nov., sp. nov., an anaerobic bacterium which reductively dechlorinates chlorophenolic compounds. *Int J Syst Bacteriol* 44: 612-9

31. van de Pas BA, Jansen S, Dijkema C, Schraa G, de Vos WM, Stams AJM. 2001. Energy Yield of Respiration on Chloroaromatic Compounds in Desulfitobacterium dehalogenans. *Appl. Environ. Microbiol.* 67: 3958-63

32. van de Pas BA, Smidt H, Hagen WR, van der Oost J, Schraa G, et al. 1999. Purification and molecular characterization of ortho-chlorophenol reductive dehalogenase, a key enzyme of halorespiration in Desulfitobacterium dehalogenans. *J Biol Chem* 274: 20287-92

33. van Eekert MH, Schraa, G. 2001. The potential of anaerobic bacteria to degrade chlorinated compounds. *Water Sci Technol* 44: 49-56

34. Villemur R, Lanthier M, Beaudet R, Lépine F. 2006. The Desulfitobacterium genus. *FEMS Microbiology Reviews* 30: 706-33

35. Vogel TM CC, McCarty PL. 1987. *Transformations of halogenated aliphatic compounds*. *Environ. Sci. Technol.* 21: 722-36

36. Wiegel J, Wu Q. 2000. Microbial reductive dehalogenation of polychlorinated biphenyls. *FEMS Microbiology Ecology* 32: 1-15

37. Wiegel J, Zhang X, Wu Q. 1999. Anaerobic dehalogenation of hydroxylated polychlorinated biphenyls by Desulfitobacterium dehalogenans. *Appl Environ Microbiol* 65: 2217-21

38. Wohlfarth G, Diekert G. 1997. Anaerobic dehalogenases. *Current Opinion in Biotechnology* 8: 290-5

Chapter 3

DUAL ROLES OF AN ESSENTIAL CYSTEINE RESIDUE IN ACTIVITY OF A REDOX REGULATED BACTERIAL TRANSCRIPTIONAL ACTIVATOR

The content of this chapter has been published in J Biol Chem. 2008 Oct 17;283(42):28721-8: **Gupta N and Ragsdale SW**. "Dual roles of an essential cysteine residue in activity of a redox-regulated bacterial transcriptional activator".

Acknowledgement
The work was partly supported by NSF Grant GM 39451 to SWR and some of the instrumentation used in early parts of this study was purchased with funds from an NIH grant (1P20RR17675) to help support the Biophysics Core Instrumentation Core of the Redox Biology Center at the University of Nebraska. The costs of publication of this article were defrayed in part by the payment of page charges. This article must therefore be hereby marked "advertisement" in accordance with 18 U.S.C. Section 1734 solely to indicate this fact. We are enormously indebted to Dr. Ari Gafni for providing advice and for letting us use his CD instrument, to Dr. Joseph A. Schauerte and Kathleen Wisser for assistance with CD experiments, and Dr. Bruce Palfrey for letting us use his spectrofluorometer and for helpful discussions.

3.1 Abstract

CprK from *Desulfitobacterium dehalogenans* is the first characterized transcriptional regulator of anaerobic dehalorespiration and is controlled at two levels: redox and effector binding. Redox regulation of CprK occurs through a thiol/disulfide redox switch, which includes two classes of cysteine residues. Under oxidizing conditions, Cys11 and Cys200 form an intermolecular disulfide bond, while Cys105 and Cys111 form an intramolecular disulfide *in vitro*. Here, we report that Cys11 is involved in redox inactivation *in vivo*. Upon replacement of Cys11 with serine, alanine, or aspartate, CprK loses its DNA binding activity. C11A is unstable; circular dichroism studies demonstrate that the stability and overall secondary structures of CprK and the C11S and C11D variants are similar. Furthermore, effector binding remains intact in the C11S and C11D variants. Nevertheless, fluorescence spectroscopic results reveal that the tertiary structures of the C11S and C11D variants differ from that of the wild type protein. Thus, Cys11 plays a dual role in its involvement in a redox switching mechanism and in maintaining the correct tertiary structure that promotes DNA binding.

3.2 Introduction

Desulfitobacterium dehalogenans, one of the most extensively studied reductive dehalogenating bacteria, was identified thirteen years ago (32). It is an anaerobic, gram positive bacterium with low G+C content (33). *D. dehalogenans* can use 3-chloro-4-hydroxyphenylacetate (CHPA) and several other chlorinated aromatic compounds, including polychlorinated biphenyls, as electron acceptors (36, 37) in an energy yielding process called dehalorespiration (27, 32). In the absence of chlorinated aromatics, this organism can also utilize sulfite, thiosulfate, fumarate and nitrite as electron acceptors (32).

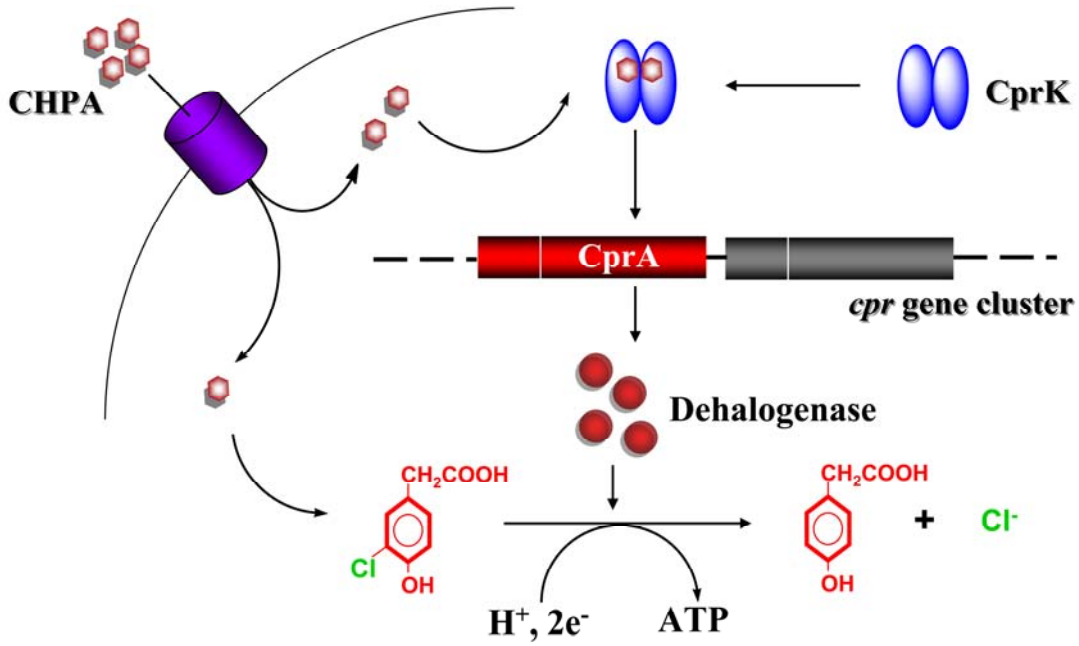

Figure 3.1: CprK and dehalorespiration. In presence of CHPA (3-chloro-4-hydroxyphenylacetate), CprK becomes activated upon binding of CHPA. Activated CprK induces the expression of genes in the *cpr* gene cluster including *cprA*. *cprA* encodes for the dehalogenase enzyme that exploits CHPA as substrate and catalyzes the dehalogenation of CHPA. This process of dehalogenation generates ATP for the cell.

Genes that encode proteins involved in dehalorespiration are present within the *cpr* gene cluster. The *cpr* gene cluster contains eight genes, *cprT, cprK, cprZ, cprE, cprB, cprA, cprC,* and *cprD*, which are located in five transcriptional units (*cprK*, *cprT*, *cprZE*, and *cprBA* or *cprBACD*) controlled by three promoters (28). CprK is constitutively expressed at low levels and acts as a transcriptional regulator for the *cpr* gene cluster (21). Induction of the *cpr*A gene results in production of the dehalogenase enzyme, which catalyzes the reductive dehalogenation of chlorinated aromatic compounds (Figure 3.1).

CprK has a C-terminal winged helix-turn-helix (wHTH) DNA binding motif (1) and an N-terminal effector binding motif. CHPA binds to the effector domain in CprK, which triggers a conformational change (8) that promotes the interaction of CprK with a nearly palindromic DNA sequence called a "dehalobox" (2) that is located in the promoter regions of the *cprT*, *cprZ*, and *cprB* genes in the *cpr* gene cluster (21). The effector (CHPA) can bind to CprK in both the reduced and oxidized states, but the protein must be in the reduced state to bind DNA (13, 20). Thus, dehalorespiration is regulated at the transcriptional level by effector binding and by the redox state of the protein. As shown in Figure 3.2, transcription occurs only under reducing conditions and when the effector is present.

CprK from *D. dehalogenans* has five cysteine residues: Cys11, Cys105, Cys111, Cys161 and Cys200. All cysteines except Cys161 are redox-sensitive and are involved in redox regulation of CprK. Upon oxidation, CprK loses DNA binding activity (21) due to the formation of an inter-molecular disulfide bond between Cys11 and Cys200 and/or an intra-molecular disulfide bond between Cys105 and Cys111 as our lab reported

previously (20). Based on the crystal structures of oxidized *D. hafniense* CprK1 and reduced *D. dehalogenans* CprK, an inactive state is stabilized by linkage of the effector domain to the DNA binding domain by the intermolecular disulfide bond. In addition, mass spectrometric studies reveal that several regions of the structure exhibit enhanced dynamics upon reduction (13).

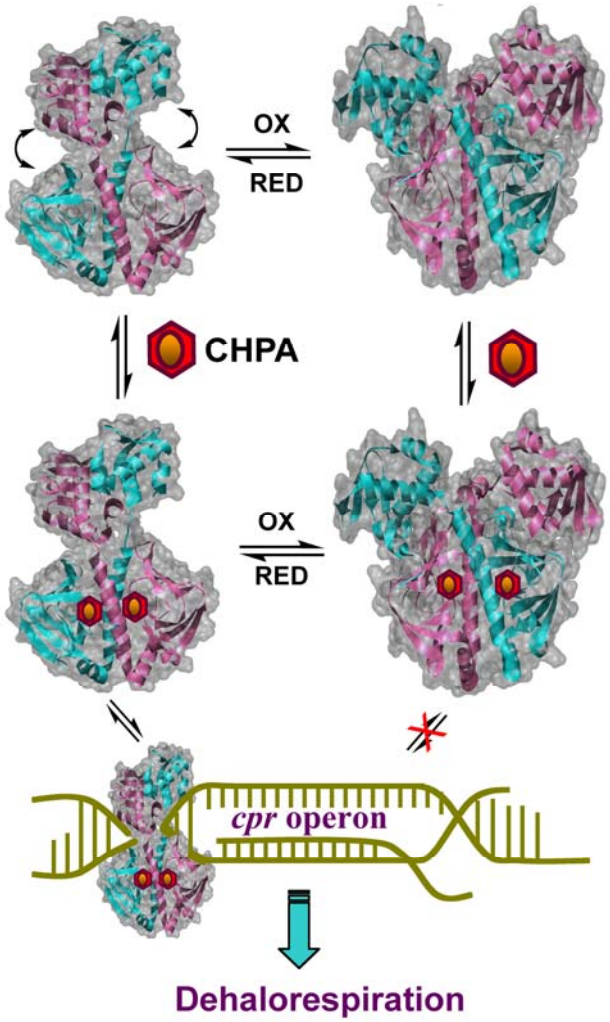

Figure 3.2: Regulation of CprK. CprK can exist in a thiol-oxidized state, containing an intermolecular disulfide linkage between Cys11 and Cys200 and an intramolecular disulfide linkage between Cys105 and Cys111, or a thiol-reduced state, in which all these Cys residues are in the thiol(ate) form. Oxidized and reduced CprK bind the effector (CHPA) with similar affinity. The oxidized state of CprK has low affinity for DNA; while the reduced form with effector binds DNA with high affinity and positively regulates expression of the *cpr* gene cluster. The products of this gene cluster are involved in catalysis of dehalorespiration (8).

The physiological relevance of the disulfide bond between Cys11 and Cys200 in redox regulation has been questioned (2). Here, we show that the intermolecular disulfide bond between Cys11 and Cys200 is observed *in vivo* upon exposure of *E. coli* cells overexpressing CprK to oxidative stress conditions. We also show that replacement of Cys11 with Ser or Asp results in a stable but inactive protein. The results of fluorescence spectroscopic studies and electrophoretic mobility shift assays (EMSA) reveal that the C11D and C11S variants can still bind effector with high affinity, but are unable to bind DNA. Changes in the fluorescence spectrum of the variants reveal that the loss of DNA binding activity in the Cys11 variants is related to a change in the tertiary structure of the protein. Thus, Cys11 plays a dual role in maintaining the correct structure for DNA binding and in redox regulation of CprK.

3.3 Experimental procedures

3.3.1 Cloning, overexpression, and purification of CprK: DNA isolation and manipulation were performed by standard techniques (23). Plasmid DNA was purified with a QIAprep spin miniprep kit (Qiagen, Valencia, CA). Construction of the overexpression plasmid and purification of CprK were described previously (21).

3.3.2 Site-directed mutagenesis of CprK: Cys11 was substituted with alanine, serine, and aspartate residues by performing site-directed mutagenesis according to the QuikChange protocol from Stratagene (La Jolla, CA). The pQE60:*cprK* plasmid was the template for PCR and the primers were purchased from Integrated DNA Technologies. The DNA sequences of all PCR-generated DNA fragments were confirmed using dye terminator chemistry and automated sequencing of both DNA strands with a Beckman/Coulter CEQ2000XL 8-capillary DNA sequencer at the Genomics Core Research Facility (University of Nebraska, Lincoln, NE).

3.3.3 Construction of strains for lacZ reporter assays: To measure *in vivo* activity of CprK, a two-plasmid reporter system was constructed, in which an arabinose-inducible *cprK* gene on one plasmid and a *cpr* promoter-lacZ fusion on another plasmid were cotransformed into an *ara*$^{-}$ *E. coli* strain. Wild type (WT) CprK was cloned into the *pBAD-Myc-HisA* expression vector (Invitrogen, Carlsbad, California), generating pBAD/Myc/HisA::cprK. To express the native protein lacking the His-tag, the native stop codon was included before the sequence that encodes the His-tag. Cys11 variants were generated by site-directed mutagenesis in the same construct. A *cpr* promoter-*lacZ* fusion was generated by cloning the promoter region of *cprB* into the EcoRI cloning site of

pRS551 (26) to yield *pRS551::PcprB*, which was used to transform the *ara*$^{-}$ *E. coli* strain LMG194 (Invitrogen, Carlsbad, California). Then, the *pBAD/Myc/HisA::cprK* construct and the corresponding C11A, C11S, and C11D variants were transformed into the LMG194 cells containing *pRS551::PcprB* to generate the two-plasmid reporter system. The pBAD system provides tight control of CprK expression (6), and the *E. coli* strain provides a background that lacks dehalorespiration genes.

3.3.4 Assay of *in vivo* activity of CprK: Promoter activity was measured *in vivo* by the β-galactosidase assay. Overnight cultures were grown aerobically at 37 °C in RM medium plus 50 μM CHPA, 0.2 % arabinose, 100 μg/ml ampicillin, and 34 μg/ml chloramphenicol. When required, diamide (1 mM final concentration) was added to the culture at an $O.D._{600}$≈0.2. Growth was stopped during the exponential phase by placing the cultures on ice when the $O.D._{600}$ reached 0.4 to 0.6. After 20 min, 500 μl of Z buffer (60 mM $Na_2HPO_4.7H_2O$, 40 mM $NaH_2PO_4.H_2O$, 10 mM KCl, 1 mM $MgSO_4$, and 50 mM β-mercaptoethanol, pH 7.0), 50 ml of 0.1% SDS, and 2 drops of chloroform were added to 500 μl of culture and the solution was incubated at 28 °C for at least 5 min when 200 μl of 4 mg/ml O-nitrophenyl-β-D-galactoside (ONPG) (final concentration, 0.8 mg/ml) was added. The reaction was stopped by adding 500 μl of 1 M Na_2CO_3 when the reaction mixture began to turn yellow, and the time of reaction was recorded. The absorbances at 420 nm and 550 nm were then measured to calculate the promoter activity in Miller Units as described (12). Each reaction was performed in quadruplicate.

3.3.5 *In vivo* intermolecular disulfide bond detection: *E. coli* strains containing the *cprK* gene were grown in LB media at 37 °C. At an $A_{600\ nm}$ of ~0.6, a 0.5 ml sample was

centrifuged and the cell pellet was immediately frozen in liquid nitrogen. Diamide (1 mM, final) was added to the rest of the culture and 0.5 ml samples were collected from the culture after 5, 10, 30 and 60 min, centrifuged, and frozen as just described. Next day, non-reducing loading buffer (60 mM Tris-Cl, pH 6.8, 1% SDS, 10% glycerol, 0.01% bromophenol blue) was added to the cell pellets at varying volumes to provide samples with equal final cell density (based on the absorbance at 600 nm). Finally, 10 µl of each sample was loaded on a 15% SDS-PAGE gel and immunoblotted with an anti-CprK antibody. After electrophoresis, proteins were transferred to a PVDF membrane, which was first incubated with primary rabbit anti-CprK antibody (Cocalico Biologicals Inc., Reamstown PA) that had been purified by chromatography on a CprK-actigel ALD superflow affinity column (Sterogene Bioseparations Inc., Carlsbad, CA). The membrane was then treated with secondary antibody (goat anti-rabbit IgG conjugated to horseradish-peroxidase, Sigma-Aldrich), and the presence of CprK was detected by chemiluminescence, using the protocol recommended by the manufacturer (Sigma-Aldrich).

3.3.6 Electrophoretic mobility shift assay (EMSA): EMSAs were performed as described (21) with increasing amounts of IRDye 700 labeled oligonucleotides (LI-COR, Inc, Lincoln). Data were analyzed by infrared imaging with an ODYSSEY infrared imager (LI-COR).

3.3.7 Liquid chromatography mass spectrometry (LCMS) analysis: The intact protein was analyzed at the Mass Spectrometry Core Facility (University of Nebraska, Lincoln) by an LC-MS/MS system comprised of a Shimadzu (SCL-10A) HPLC system, a 4000

Qtrap (ABS) mass spectrometry system, and a turbo ion-spray source probe. Protein samples (20 ml) were loaded onto a Micro-Tech Scientific C_{18} column (1.0 (ID) x 50 mm (length), 5 μm (particle size)) by a PE 200 Autosampler and eluted at a flow rate of 100 μl/min at room temperature with a gradient of 0.3% formic acid in H_2O (Solvent A) and 0.3% formic acid in acetonitrile (Solvent B). The percentage of Solvent B was increased linearly from 10-70% over a 5 min elution time. The data were acquired and processed with Analyst 1.4.1 software. Data was acquired in the Q1 (quadrupole one) positive ion mode as the mass range (m/z) of 850-1150 amu (atomic mass units) was scanned in 4 sec. The total run time for each sample was 20 min. The molecular mass of the protein was calculated by analyzing several multiply charged peaks with the Bayesian Protein Reconstruct option in Bioanalyst 1.4.1 software.

3.3.8 Intrinsic fluorescence quenching and circular dichroism (CD) analysis: For the CHPA binding assay shown in Fig. 3.6, 180 to 500 nM CprK was analyzed by fluorescence spectroscopy with a Shimadzu RF-530 1 PC Spectrofluorophotometer (Columbia, MD) at room temperature as described (20, 37). All fluorescence data were corrected for the inner filter effect (10). The intrinsic tryptophan fluorescence spectra of wild-type CprK, C11S, and C11D variants shown in Fig. 3.9 were recorded on an OLIS RSM1000F (OLIS, Inc., Bogart, GA).

Binding of CHPA to CprK causes quenching of intrinsic tryptophan fluorescence of CprK. Dissociation constants were calculated by fitting the fluorescence quenching data to Equation 1 or 2, where K_d represents the dissociation constant for the ligand (L, CHPA), [L] is the total ligand concentration, [P] equals the total protein concentration,

ΔF is the observed fluorescence quenching, F_0 equals the initial fluorescence, and ΔF_{max} is the maximum quenching that would be observed at infinite ligand concentrations. These equations assume a single binding site on CprK for CHPA. The [L] in Equation 1, which describes a standard one-site binding isotherm, should be free ligand, and because the free ligand concentration is unknown, we assumed that the free and total ligand concentrations are equal. However, when the [L] is in the range of the K_d, the fraction of bound ligand becomes significant; therefore, the data were also fit to quadratic Equation 2, which accounts for ligand depletion at low CHPA concentrations. We also estimated the free ligand concentration by subtracting bound ligand ([P] * $\Delta F/F_{max}$] from [L], and fit this data to Equation 1.

$$\Delta F = (\Delta F_{max} * L)/([L] + K_d) \qquad (1)$$

$$\frac{\Delta F}{F_0} = \frac{\Delta F_{\max}}{2F_0[P]}\left[\left([P]+[L]+K_d\right) - \sqrt{\left([P]+[L]+K_d\right)^2 - 4[P][L]}\right] \qquad (2)$$

The different one-site treatments gave similar dissociation constants, while a two-site model [$\Delta F = (\Delta F_{max} * L)/([L] + K_{d1}) + (\Delta F_{max} * L)/([L] + K_{d2})$] gave a K_{d1} in the low nanomolar range with high errors and a K_{d2} that was similar to the K_d value obtained from the one-site model. The R^2 values were also slightly better for the one-site model. Thus, we conclude that binding of CHPA to CprK follows a one-site binding model.

CD measurements were performed at 4 °C with a JASCO J-715 instrument (Jasco Inc., MD). Spectra were scanned from 260 to 190 nm at a speed of 50 nm/min with a data pitch of 1 nm. Forty scans at a 2 sec response time and a 5 nm bandwidth were averaged

for each sample. For secondary structure analysis, experiments were performed in a 0.1 mm path length cell with 0.7 mg/ml CprK in 10 mM potassium phosphate buffer, pH 7.5. The melting temperature of CprK was determined by measuring the CD spectrum of 0.2 mg/ml protein (in 50 mM Tris, 300 mM NaCl, pH-7.5) over a temperature range of 20 °C to 80 °C in a 1 mm path length cell. Data were obtained in millidegrees and converted into molar ellipticity by JASCO software. The Continll program (22) within the CDpro software (29) was used for secondary structure analysis.

3.4 RESULTS

3.4.1 Evidence for *in vivo* disulfide bond formation between Cys11 and Cys200

E. coli strains overexpressing CprK were grown in the presence or absence of diamide and samples were collected at 1, 5, 10, 30 and 60 min. Samples were prepared for non-reducing SDS-PAGE analysis followed by Western blot analysis to identify the oligomeric state of CprK, omitting DTT, as described in the Experimental Procedures section. When cells were treated in the absence of oxidant, CprK was predominantly in the monomeric state (Figure 3.3.A, lane 1). However, when the cells were treated with 1 mM diamide, CprK was rapidly converted from the monomeric to the dimeric form (lanes 2 to 6). Dimer formation was also observed when cells were treated with hydrogen peroxide (Figure 3.3.B).

Treatment of the C11S variant with diamide did not result in dimer formation (Figure 3.3.C). Similarly, the C200S variant remained predominantly in the monomeric state after treatment with diamide (Figure 3.3.D), with a small proportion of the dimeric form, as was observed in earlier *in vitro* experiments (20). Another band in the 15-20 kDa region appeared in the C200S variant, which might reflect a degradation product. In summary, these results indicate that *in vivo* Cys11 and Cys200 exist as the free thiol(ates) under normal growth conditions, and that they form an intermolecular disulfide bond when exposed to oxidants.

Mass spectrometric analyses of the purified Cys11 variants revealed that the C11S and C11D variants are full-length proteins just like the wild-type CprK (Figure 3.4), with the only observed differences being due to the site-directed amino acid replacements.

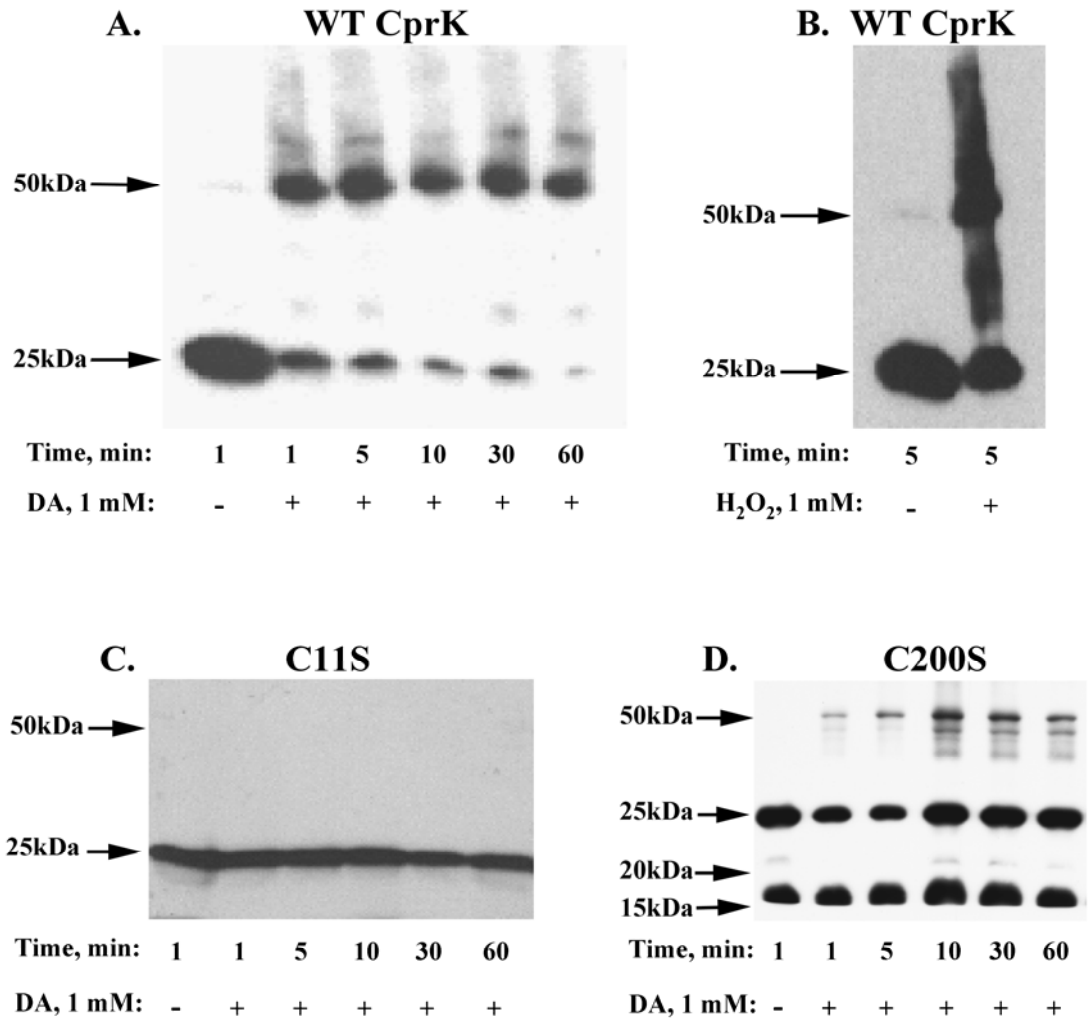

Figure 3.3: *In vivo* Cys11-Cys200 disulfide bond formation upon treatment of cells with oxidants. Exposure of cells containing wild-type CprK to (A) 1 mM DA or (B) 1 mM hydrogen peroxide or after treatment of (C) the C11S variant and (D) the C200S variant to 1 mM DA followed by separation on non reducing SDS-PAGE and Western blot analysis. The membranes were immunoblotted with anti-CprK antibody and stained as described in experimental procedures.

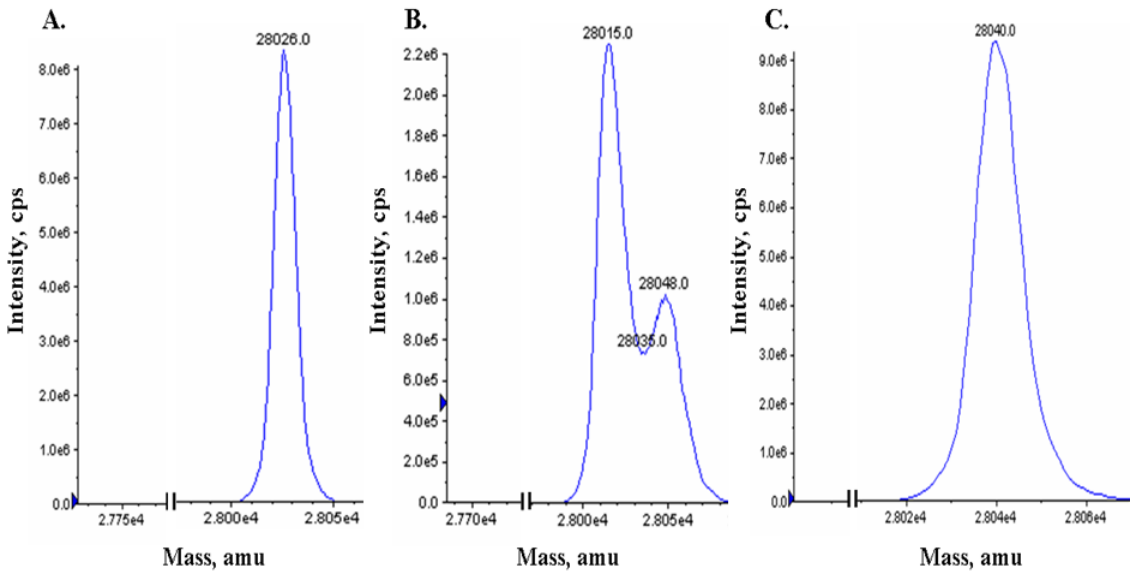

Figure 3.4: Parent ion analysis of CprK by mass spectrometry. Mass spectrometric analyses confirmed that CprK and variants are full-length proteins, with wild-type CprK (A) showing a mass of 28026.0 Da, C11S (B) of 28015.0 Da, and C11D (C) of 28040.0 Da.

3.4.2 Substitution of Cys11 with Ser/Asp inactivates CprK

To analyze the role of Cys11, *in vivo* β-galactosidase and *in vitro* DNA binding assays were performed with the C11S and C11D variants. Attempts to purify the C11A variant failed, whereas the C11D and C11S variants could be purified at levels of 10-20 mg/liter of culture. EMSA assays were performed on the wild-type and variant forms of CprK in the presence of effector. Neither the C11S nor C11D variants showed any mobility shift of *pcprB* (Figure 3.5.A and 3.5.B).

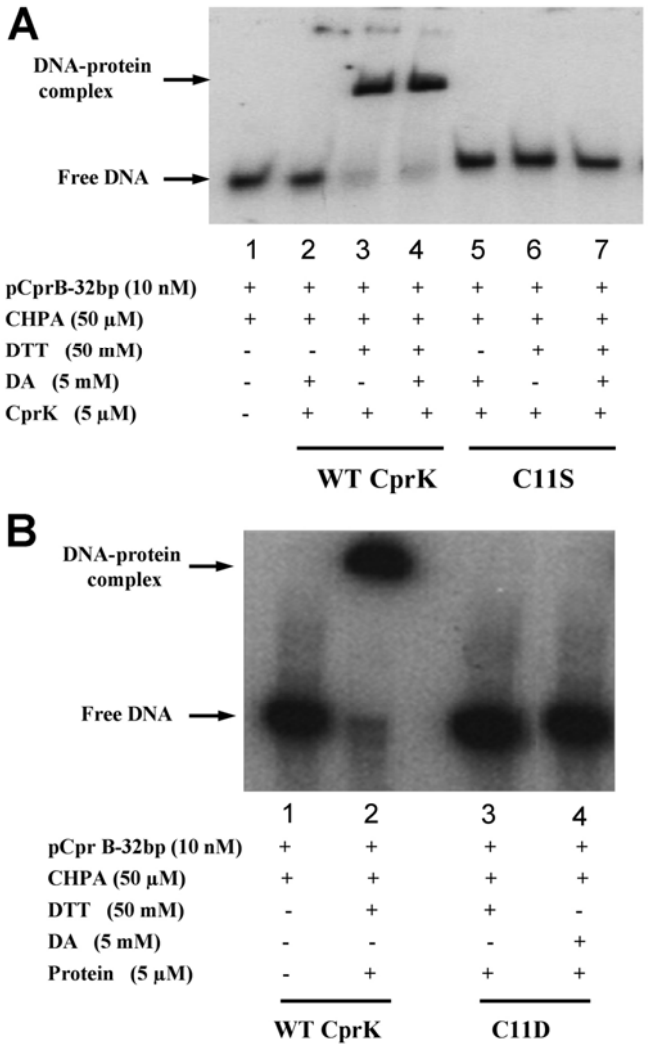

Figure 3.5: Loss of *in vitro* DNA binding activity of Cys11 variants. (A) EMSA experiments after incubation of wild-type CprK (lanes 1-4) or C11S (lanes 5-7) with DNA in the presence of DA (lane 2, 5), or DTT (lanes 3, 6) or DTT+DA (lanes 4, 7). (B) EMSA experiments comparing wild-type CprK with C11D. Lane 2 has wild-type CprK with 50 mM DTT. Lanes 3 and 4 have the C11D variant with 50 mM DTT and 5 mM DA respectively. Lane 1 in (A) or (B) is a control that lacks protein.

Similarly, *in vivo* analysis by the *cprB* promoter-*lacZ* fusion assay demonstrated that the C11S, C11A and C11D variants were severely compromised in DNA binding, with 2-3% β-galactosidase activity of the wild-type protein (Figure 3.6). Diamide-treated wild-type CprK showed 10% activity, indicating that oxidative stress inactivates CprK *in vivo* and

that the reducing conditions within the cell compete with diamide oxidation to restore the active protein. Diamide treatment of C11A, C11S, and C11D variants further decreased the DNA binding activity to background levels. Because formation of the Cys11-Cys200 disulfide bond is prevented in these variants, the additional decrease in activity could result from oxidation of Cys105 and Cys111 to form an intramolecular disulfide bond.

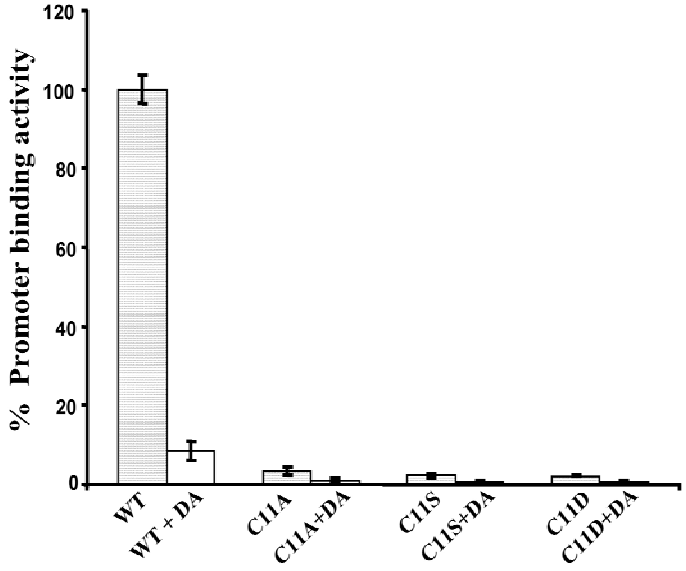

Figure 3.6: *In vivo* DNA binding activity of Cys11 variants. *E. coli* strains expressing wild-type CprK or the Cys11 variants were incubated with no (filled bar) or 1 mM DA (open bar) and promoter activity was measured by the β-galactosidase assay as described under experimental procedures. Activity is expressed as percentage of Miller units exhibited by the variant compared to that of wild-type CprK. Data are shown as mean ± SD and are representative of three separate experiments, each performed in quadruplicate.

3.4.3 Loss of DNA binding activity but unimpaired effector binding of the Cys11 variants

In order to determine if inactivity of the C11S and C11D variants is due to loss of effector or of DNA binding, effector binding affinity was measured by intrinsic tryptophan fluorescence (Figure 3.7).

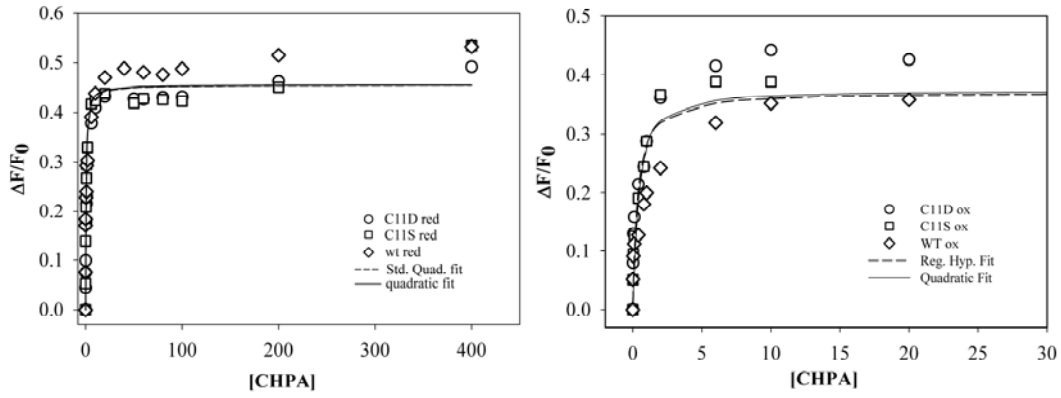

Figure 3.7: Effector binding affinity of WT and the Cys11 variants. Fluorescence intensities for the oxidized (right) and reduced (left) wild-type (◊), C11D (○), and C11S (□) variants were measured, as described previously (8). The dashed and solid lines represent the fits to one-site binding models according to Eqs. 1 and 2, respectively, as described in experimental procedures. The effector concentration is given in μM units.

As shown in Table 3.1 and Figure 3.7, the oxidized and reduced states of CprK, as well as the Cys11 variants bind CHPA with high affinity, and the data for the wild-type and Cys11 variant proteins are virtually superimposable. The binding data for the wild-type protein and the Cys11 mutants, best fit to a single binding site model. The ranges of K_d values are 0.29-0.49 μM and 0.34-0.68, for the oxidized and reduced proteins. In fact, composite fits that include all the data for wild-type and mutants (oxidized or reduced) give standard deviations that are similar to those for the individual fits. In addition, similar K_d values are obtained by fitting the data to the standard binding isotherm given in Equation 1 (dashed line, Fig. 3.7) as with the more rigorous quadratic Equation 2 (solid line) that takes ligand depletion at low CHPA concentrations into account. Therefore, based on the composite fits, the K_d value for CHPA of the oxidized and reduced states of CprK are between 0.3 μM and 0.5 μM.

Protein	Redox State	K_d (μM)[1]
WT	Reduced	0.52 ± 0.18
	Oxidized	0.49 ± 0.16
C11D	Reduced	0.68 ± 0.11
	Oxidized	0.31 ± 0.14
C11S	Reduced	0.34 ± 0.11
	Oxidized	0.29 ± 0.11
Combined[2]	Reduced	0.50 ± 0.09
	Oxidized	0.30 ± 0.09

Table 3.1: Dissociation constants for the complex between CprK (and variants) and CHPA. [1]These values were calculated by fits to Equation 2, which accounts for ligand depletion at low concentrations of CHPA. [2]These values were obtained by fitting the combined data sets for WT, C11S, and C11D.

Because the CprK variants with substitutions at Cys11 retain high affinity for CHPA, the inactivity of these variants was presumed to result from loss of DNA binding ability. We compared the affinity of the Cys11 variants for DNA to that of the wild type protein by performing EMSA at increasing DNA concentrations. The C11S variant requires greater than 50-fold more DNA to obtain the same amount of CprK-DNA complex as with the wild-type protein (Figure 3.8). Thus, only marginal activity is observed when the thiol of Cys11 is replaced by a hydroxide (in C11S). With the C11D variant (data not shown), no gel shift was observed even at 500 nM DNA, indicating either that the negative charge or the increased steric bulk of Asp at residue 11 strongly inhibits DNA binding. Thus, CprK's promoter binding activity appears to require the Cys11 thiol(ate) functionality.

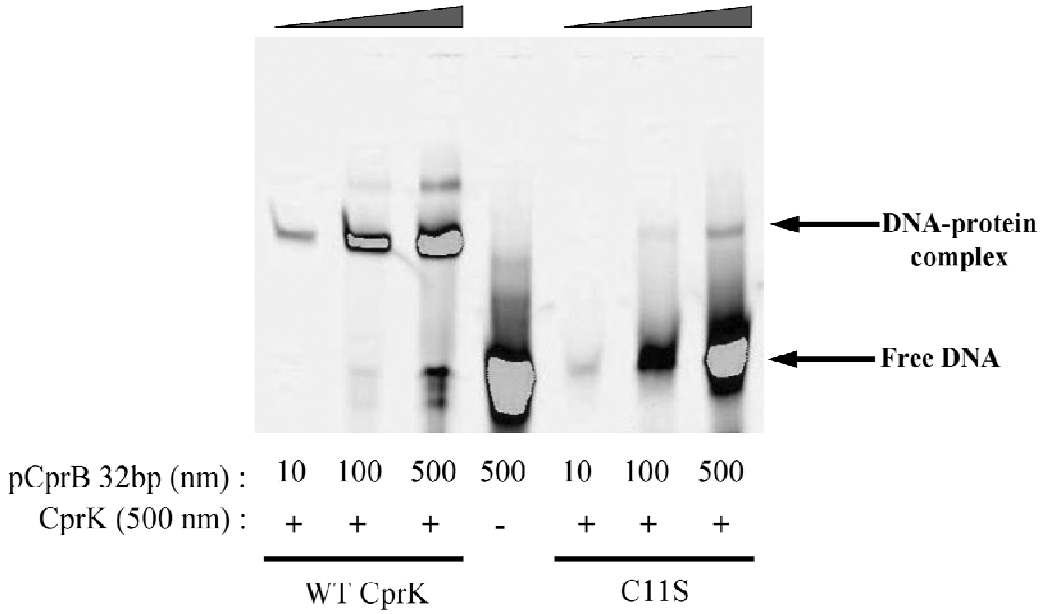

Figure 3.8: Effect of increasing DNA concentration on DNA binding activity of C11S. Wild-type CprK (lane1 to 3) and the C11S variant (lanes 5-7) were incubated with 10 nM to 500 nM DNA containing the *cpr* promoter. Lane 4 was a control that lacked protein.

3.4.4 Loss of DNA binding activity may reflect a change in tertiary structure of CprK

Although the first 18 amino acid residues were disordered and not seen in the crystal structure of the reduced protein, the structure of oxidized CprK reveals Cys11 to be positioned near the DNA binding domain (Figure 3.9) (8). To explore the reason behind the loss of DNA binding activity of the Cys11 variants, fluorescence spectroscopy and circular dichroism experiments were performed. We expected to detect the changes, if any, in the tertiary structure, secondary structure or thermal stability of variants.

To determine if loss of DNA binding activity in the Cys11 variants is associated with a change in the structure of CprK, intrinsic tryptophan fluorescence spectra were recorded of oxidized and DTT-reduced CprK and of the Cys11 variants (Figure 3.10).

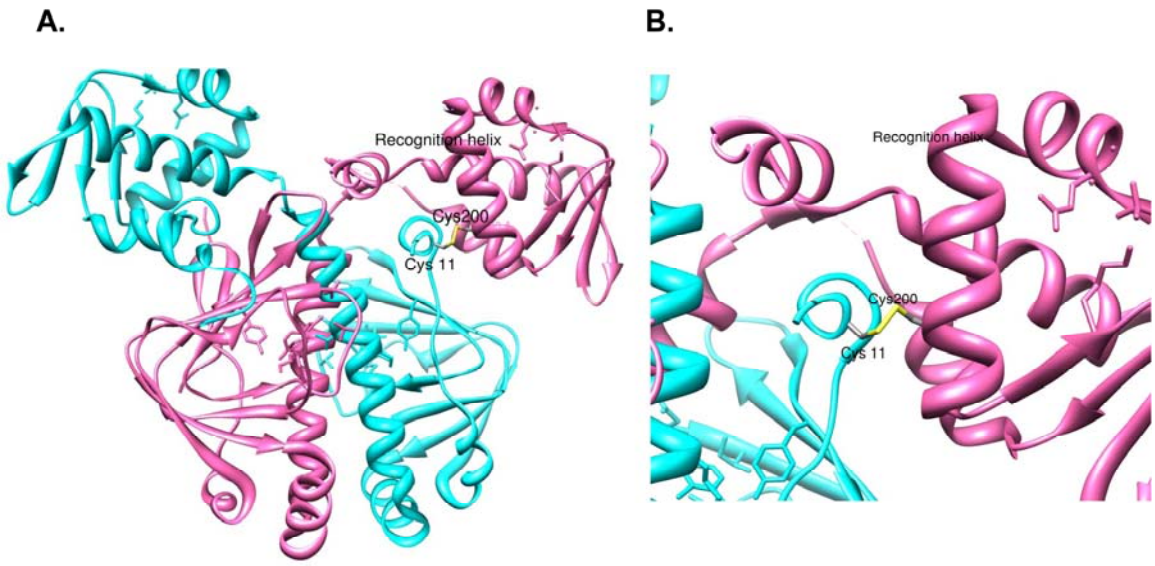

Figure 3.9: Cys11 in the crystal structure of oxidized CprK. The crystal structure of oxidized *D. hafniense* CprK (A), focusing on the helix-turn-helix DNA binding domain (B). Cys11 and other residues (Cys200) predicted to be in the recognition helix, based on the structure of the CRP-DNA complex (8), and are colored according to element. This figure was generated from PDB ID: 2h6b in CHIMERA.

As observed earlier, reduction of CprK leads to quenching of intrinsic tryptophan fluorescence (20), indicating that the single Trp at position 106 becomes more solvent exposed upon reduction (Figure 3.10.A & B). The fluorescence spectra of the DTT-reduced forms of C11S and C11D coincide, with a significantly lower intensity than that of the reduced wild-type protein (Figure 3.10.B). These results indicate that the tertiary structures of the reduced Cys11 variants (at least in the region of Trp106) are different from that of wild-type CprK.

The fluorescence spectrum of the oxidized C11S variant is similar to that of the reduced state of wild-type CprK (Figure 3.10.A), indicating that Trp106 in C11S is already rather solvent exposed in the oxidized protein. The fluorescence spectrum of oxidized C11D is

similar to that of oxidized wild-type CprK (Figure 3.10.A), while reduction of C11D leads to a marked (~40%) quenching of fluorescence (Figure 3.10.B).

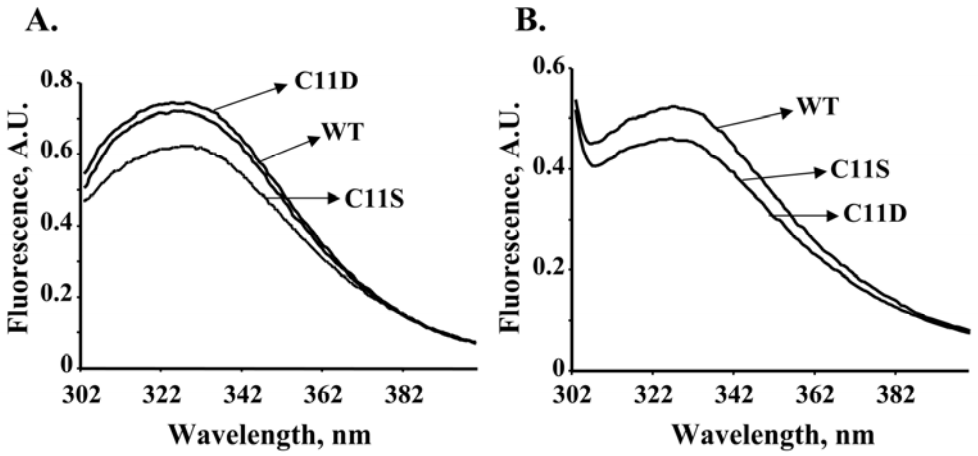

Figure 3.10: Intrinsic fluorescence spectrum of CprK. Spectra were recorded for wild-type CprK, C11S and C11D in 50 mM Tris-HCl, 300 mM NaCl pH 7.5 (A), or the same buffer containing 50 mM DTT (B). Data presented here are representative of three different experiments.

Based on CD analysis, substitutions at Cys11 cause only marginal changes in secondary structure (Figure 3.11 and Table 3.2), which are within or near the error limits of the experiment. Table 3.2 shows the results obtained from the secondary structure analysis for wild type CprK and the Cys11 variants. The normalized root-mean-squared deviation values for all of the fits are below 0.1, which indicates that the experimental data are well fit by parameters calculated by the Contin ll program.

Stabilities of the Cys11 variants in the oxidized state were also measured by recording the CD spectrum at 222 nm in the temperature range between 20 °C and 80 °C (Figure 3.12). The actual melting temperature (T_m) could not be accurately determined as the thermal unfolding curves were irreversible. The wild-type protein gave an approximate T_m of 54

°C, while the variants exhibited transitions at slightly lower temperatures, indicating that they have similar or only slightly decreased, stability.

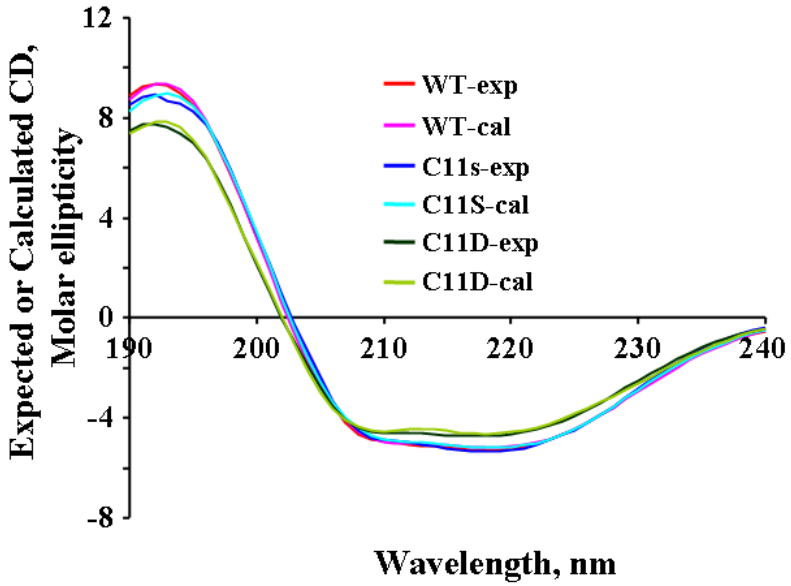

Figure 3.11: Circular dichroism analysis. Superimposed CD spectra of WT, C11S and C11D variants. Data presented here are representative of three independent experiments. Samples were prepared in 10 mM potassium phosphate buffer, pH 7.5.

Protein	α-helix	β-sheet	Turn	Unordered	NRMSD
WT	0.421	0.167	0.154	0.258	0.018
C11S	0.409 (2.8 %)	0.159 (4.8 %)	0.150 (2.6 %)	0.281	0.026
C11D	0.415 (1.4 %)	0.139 (16.7%)	0.159 (3.2 %)	0.296	0.028
X-ray	0.42	0.26	-	-	-

Table 3.2: Secondary structure analysis of wild-type CprK and variants. Secondary structure fractions are shown here as analyzed by the Continll program (CDPro software) in comparison with the secondary structure fractions based on the X-ray structure (PDB entry 2h6b) of wild-type CprK. Variation from the secondary structure content of wild-type is given in parentheses after the measured secondary structure contents of variants.

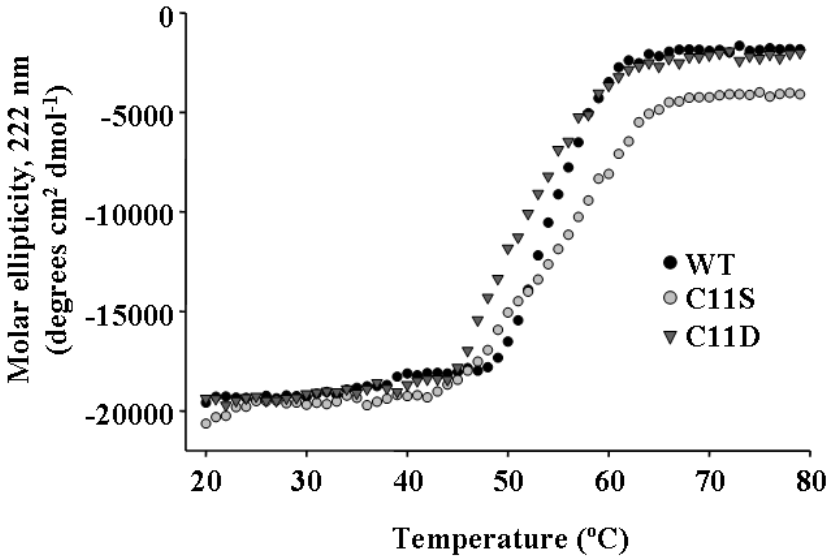

Figure 3.12: Stability of wild-type CprK and Cys11 variants. Melting curves of wild-type and variant proteins were obtained by recording the CD at 222 nm from 20 °C to 80 °C in a buffer containing 50 mM Tris, 300 mM NaCl, and pH 7.5.

3.5 Discussion

Upon binding its effector (CHPA), CprK induces the expression of genes involved in the use of chlorinated aromatic compounds as electron acceptors. Besides providing energy for the microbe, dehalorespiration helps to rid the environment of xenobiotics (like polychlorinated biphenyls) that constitute a significant health risk. Previous *in vitro* studies indicate that CprK contains two thiol/disulfide redox switches that regulate transcriptional activity of CprK: one involving Cys11 and Cys200 that, in the oxidized state, forms an intermolecular disulfide linkage and another involving Cys105 and Cys111 that forms an intramolecular disulfide bond (20).

Redox regulation of CprK activity has been proposed to prevent expression of CprA under oxidative conditions (21). CprA catalyzes reductive dehalogenation through a mechanism involving oxygen-sensitive iron-sulfur clusters and the low valent Co(I) state of cobalamin (9). Here we describe further studies indicating that the intermolecular thiol/disulfide switch is formed in the *E. coli* cytoplasm under oxidative stress conditions. Exposure of *D. dehalogenans* to such oxidative conditions would likely occur commonly in this microaerophile, as it does in the facultative anaerobe *E. coli*. Since it would be wasteful to produce CprA under oxidative conditions, it would be advantageous for the cells to exert redox control of transcription of the *cpr* gene cluster.

Thus, as shown in Figure 3.2, CprK is proposed to exert a two-tier mode of regulation of dehalorespiration involving a redox switch at one level and an effector-binding switch at another level. The studies described here also provide evidence that Cys11 plays a dual

role in transcriptional activation: as part of the intermolecular redox switch and in maintaining an optimal structure of CprK's DNA binding domain.

Formation of either the intramolecular or the intermolecular disulfide bond appears to be sufficient to inhibit transcriptional activation, since variants containing substitutions at Cys105, Cys111, or Cys200 (or Cys161, which does not appear play a redox role) retain redox-sensitivity and bind DNA and effector with affinities similar to those of the wild-type protein (data not shown). Thus, formation of either the intramolecular or the intermolecular disulfide bond appears to reversibly inactivate CprK. Surprisingly, as shown in this paper, substitution of Cys11 with Ala, Ser, or Asp results in a protein that is unable to activate transcription *in vivo* or to bind the *cpr* promoter DNA *in vitro*, even under reducing conditions and at saturating concentrations of effector. Thus, beyond its involvement in the intermolecular redox switch, Cys11 plays an additional role in transcriptional activation. These results differ from studies in which C11S of the related CprK1 from *D. hafniense* was shown to retain DNA binding activity (2). Based on DNA sequence and mass spectrometric analysis, we are certain that the only mutation in these variants is at Cys11 and the redox inactivity is observed in forms of CprK containing (*in vitro*) and lacking (*in vivo*) the His-tag sequence. Thus, it is difficult to harmonize our results with those described earlier (2), except to suggest that CprK1 in *D. hafniense* may exhibit different redox properties than CprK from *D. dehalogenans*. For example, Cys105 is absent in *D. hafniense*.

As shown in Figure 3.9, Cys11 (in the oxidized protein) is very close to the recognition helix of the wHTH DNA binding domain in CprK that binds to the dehalobox promoter

sequence. Furthermore, binding of DNA protects the recognition helix (a 14-amino acid peptide including residues 182-196) from limited proteolysis (13). Although Cys11 is not observed in the structure of the reduced protein, reduction of CprK increases the overall structural dynamics of CprK in the region of Cys11 (13). Other regions that were shown to undergo local changes upon effector binding include the long C-helix that connects the DNA and effector binding domains and Arg152, which is in a proposed hinge region that may transmit the effector-binding signal to the DNA binding domain.

By comparing the activities of CprK variants with Ala, Ser, or Asp substitution at Cys11, we expected to be able to determine whether Cys11 is involved in hydrophobic, H-bonding, or ionic interactions that are important for transcriptional activation. However, all three variants share similarly low abilities to activate transcription (Figure 3.6). Although the C11A variant could not be purified for *in vitro* studies, C11S, C11D, and wild-type CprK are all stable proteins that can be purified in large quantities and studied by various biochemical methods. As with the wild-type protein, both oxidized and reduced states of the C11S and C11D variants have a single high affinity (0.3-0.7 μM) binding site for the effector (Figure 3.7) Similarly, the crystal structure revealed a single CHPA molecule bound at the effector binding site of CprK (8). A single site binding model was used to fit the effector binding data for the related CprK from *D. hafniense* (8). In summary, our results indicate that Cys11 does not play a major role in effector binding.

Upon replacing Cys11 with serine, the DNA binding activity of CprK decreases more than 50-fold (Figure 3.8). Because the thiol and hydroxyl groups in the side chains of Cys

and Ser are similar in size and H-bonding ability, a H-bonding interaction(s) involving the neutral thiol of Cys11 does not explain the importance of this residue in transcriptional activation. Some redox-active thiols have unusually low pKa values; thus, to test the hypothesis that Cys11 may function as an ionized thiolate, the DNA binding activity of the C11D variant was tested. Although C11D retains high effector binding capacity, it exhibits no detectable DNA binding (Figure 3.7). These results suggest that the thiol(ate) function of Cys11 plays a crucial and very specific role in DNA binding.

Based on studies of a related transcriptional activator (CprK1) from *D. hafniense* and two variants (C11S and C200S), the disulfide bond between Cys11 and Cys200 in redox regulation was concluded to lack physiological relevance (2). Gabor et al. hypothesized that, if the Cys11-Cys200 disulfide bond was important *in vivo*, replacement of either Cys11 or Cys200 with serine would result in a redox-insensitive active state of CprK. Since, in aerobically grown *E. coli*, the level of transcriptional activation mediated by the C11S variant was similar to that of wild-type CprK1, it was concluded that the Cys11-Cys200 disulfide bond was not present in the cytoplasm of aerobically cultivated *E. coli* cells. However, the results described here clearly demonstrate the formation of the Cys11-Cys200 disulfide bond under oxidative stress conditions in the cytoplasm of *E. coli*, with an ambient redox potential of ~-250 mV (18, 31), which is similar to the redox potential of the ox/red couple for glutathione (i.e., between -240 (25) and -263 mV (15), the major redox buffer in most cells. Although the redox potentials for the intramolecular and intermolecular thiol/disulfide switches in CprK have not yet been determined, the redox potential of disulfide bonds in proteins vary over a wide range (-122 mV to -470 mV) (18). Thus, we suggest that transcriptional control by CprK is subject to

thiol/disulfide regulation, like a number of processes in prokaryotes and eukaryotes, including transcriptional regulation by OxyR(3), glutathione biosynthesis (34), cell cycle progression (24), heme binding by heme oxygenase-2 (39), iron metabolism by FurS (17), DNA binding by NF- kB (16), and thioredoxin/thioredoxin reductase-dependent reactions (30, 40).

Crystallographic (7) and site-directed mutagenesis (5) studies of bovine papillomavirus-1 E2 demonstrated that Cys340 is required for transcriptional activation through interactions between its sulfhydryl group and two bases in its target DNA. Like CprK, the E2 protein is subject to redox regulation, with its transcriptional activity lost upon oxidation (14). Similar results were obtained with NF-kB, where it loses DNA binding activity upon alkylation of a Cys residue in the DNA binding domain (11).

Fluorescence spectroscopic results demonstrate that the tertiary structures of the Cys11 variants are different from that of wild-type CprK, in both the reduced and oxidized states. Furthermore, the thiol/disulfide transition in CprK results in a substantial change in conformation, especially affecting the DNA binding domain, as observed in the crystal structures of the oxidized and reduced proteins (8), by limited proteolysis studies (13), and by fluorescence spectroscopy (Figure 3.10). An important structural role for Cys11 is also supported by the observations that the C11A variant cannot be purified and that the C11S and C11D variants are slightly less stable than the wild-type protein. Functional and structural roles for cysteine have been demonstrated in various proteins (4, 19, 35, 38) where cysteine plays a role in activity, in maintaining an active dimer, and in thermal stability. In the case of CprK, perhaps the charged Asp, being larger than the cysteine

residue, interferes with protein-DNA interactions by either direct stereoelectronic effects or by indirect effects on protein packing near the recognition helix. However, the position of Cys11 in active reduced CprK is not known (8). It is hoped that further structural studies will lead to a better understanding of the nature of interactions involving Cys11 that promote DNA binding.

3.6 References

1. Aravind L, Anantharaman V, Balaji S, Babu MM, Iyer LM. 2005. The many faces of the helix-turn-helix domain: transcription regulation and beyond. *FEMS Microbiol Rev* 29: 231-62

2. Gabor K, Verissimo CS, Cyran BC, Ter Horst P, Meijer NP, et al. 2006. Characterization of CprK1, a CRP/FNR-type transcriptional regulator of halorespiration from Desulfitobacterium hafniense. *J Bacteriol* 188: 2604-13

3. Georgiou G. 2002. How to flip the (redox) switch. *Cell* 111: 607-10

4. Giese NA, Robbins KC, Aaronson SA. 1987. The role of individual cysteine residues in the structure and function of the v-sis gene product. *Science* 236: 1315-8

5. Grossel MJ, Sverdrup F, Breiding DE, Androphy EJ. 1996. Transcriptional activation function is not required for stimulation of DNA replication by bovine papillomavirus type 1 E2. *J Virol* 70: 7264-9

6. Guzman LM, Belin D, Carson MJ, Beckwith J. 1995. Tight regulation, modulation, and high-level expression by vectors containing the arabinose PBAD promoter. *J Bacteriol* 177: 4121-30

7. Hedges SB, Bogart JP, Maxson LR. 1992. Ancestry of unisexual salamanders. *Nature* 356: 708-10

8. Joyce MG, Levy C, Gabor K, Pop SM, Biehl BD, et al. 2006. CprK crystal structures reveal mechanism for transcriptional control of halorespiration. *J Biol Chem* 281: 28318-25

9. Krasotkina J, Walters T, Maruya KA, Ragsdale SW. 2001. Characterization of the B12- and iron-sulfur-containing reductive dehalogenase from Desulfitobacterium chlororespirans. *J Biol Chem* 276: 40991-7

10. Kubista M, Sjoback R, Eriksson S, Albinsson B. 1994. Experimental correction for the inner-filter effect in fluorescence spectra *Analyst* 119: 417-9

11. Lambert C, Li J, Jonscher K, Yang TC, Reigan P, et al. 2007. Acrolein inhibits cytokine gene expression by alkylating cysteine and arginine residues in the NF-kappaB1 DNA binding domain. *J Biol Chem* 282: 19666-75

12. M. JH. cold spring harbor, NY: Cold spring harbor laboratory

13. Mazon H, Gabor K, Leys D, Heck AJ, van der Oost J, van den Heuvel RH. 2007. Transcriptional activation by CprK1 is regulated by protein structural changes induced by effector binding and redox state. *J Biol Chem* 282: 11281-90

14. McBride AA, Klausner RD, Howley PM. 1992. Conserved cysteine residue in the DNA-binding domain of the bovine papillomavirus type 1 E2 protein confers redox regulation of the DNA-binding activity in vitro. *Proc Natl Acad Sci U S A* 89: 7531-5

15. Millis KK, Weaver KH, Rabenstein DL. 1993. Oxidation/reduction potential of glutathione. *The Journal of Organic Chemistry* 58: 4144-6

16. Nishi T, Shimizu N, Hiramoto M, Sato I, Yamaguchi Y, et al. 2002. Spatial redox regulation of a critical cysteine residue of NF-kappa B in vivo. *J Biol Chem* 277: 44548-56

17. Ortiz de Orué L, Tröller, Schrempf. 2003. Amino acid residues involved in reversible thiol formation and zinc ion binding in the<SMALL> Streptomyces reticuli</SMALL> redox regulator FurS. *Molecular Genetics and Genomics* 268: 618-27

18. Ostergaard H, Henriksen A, Hansen FG, Winther JR. 2001. Shedding light on disulfide bond formation: engineering a redox switch in green fluorescent protein. *EMBO J* 20: 5853-62

19. Pajares MA, Corrales FJ, Ochoa P, Mato JM. 1991. The role of cysteine-150 in the structure and activity of rat liver S-adenosyl-L-methionine synthetase. *Biochem J* 274 (Pt 1): 225-9

20. Pop SM, Gupta N, Raza AS, Ragsdale SW. 2006. Transcriptional activation of dehalorespiration. Identification of redox-active cysteines regulating dimerization and DNA binding. *J Biol Chem* 281: 26382-90

21. Pop SM, Kolarik RJ, Ragsdale SW. 2004. Regulation of anaerobic dehalorespiration by the transcriptional activator CprK. *J Biol Chem* 279: 49910-8

22. Provencher SW, Glockner J. 1981. Estimation of globular protein secondary structure from circular dichroism. *Biochemistry* 20: 33-7

23. Sambrook J. F.E. M, T. 1989. *Molecular cloning: A laboratory manual*. Cold spring harbor, NY: Cold spring Harbor laboratory

24. Savitsky PA, Finkel T. 2002. Redox regulation of Cdc25C. *J Biol Chem* 277: 20535-40

25. Schafer FQ, Buettner GR. 2001. Redox environment of the cell as viewed through the redox state of the glutathione disulfide/glutathione couple. *Free Radical Biology and Medicine* 30: 1191-212

26. Simons RW, Houman F, Kleckner N. 1987. Improved single and multicopy lac-based cloning vectors for protein and operon fusions. *Gene* 53: 85-96

27. Smidt H, de Vos WM. 2004. Anaerobic microbial dehalogenation. *Annu Rev Microbiol* 58: 43-73

28. Smidt H, van Leest M, van der Oost J, de Vos WM. 2000. Transcriptional regulation of the cpr gene cluster in ortho-chlorophenol-respiring Desulfitobacterium dehalogenans. *J Bacteriol* 182: 5683-91

29. Sreerama N, Woody RW. 2000. Estimation of protein secondary structure from circular dichroism spectra: comparison of CONTIN, SELCON, and CDSSTR methods with an expanded reference set. *Anal Biochem* 287: 252-60

30. Staples CR, Gaymard E, Stritt-Etter AL, Telser J, Hoffman BM, et al. 1998. Role of the [Fe4S4] cluster in mediating disulfide reduction in spinach ferredoxin:thioredoxin reductase. *Biochemistry* 37: 4612-20

31. Taylor MF, Boylan MH, Edmondson DE. 1990. Azotobacter vinelandii flavodoxin: purification and properties of the recombinant, dephospho form expressed in Escherichia coli. *Biochemistry* 29: 6911-8

32. Utkin I, Woese C, Wiegel J. 1994. Isolation and characterization of Desulfitobacterium dehalogenans gen. nov., sp. nov., an anaerobic bacterium which reductively dechlorinates chlorophenolic compounds. *Int J Syst Bacteriol* 44: 612-9

33. Villemur R, Lanthier M, Beaudet R, Lepine F. 2006. The Desulfitobacterium genus. *FEMS Microbiol Rev* 30: 706-33

34. Vitvitsky V, Mosharov E, Tritt M, Ataullakhanov F, Banerjee R. 2003. Redox regulation of homocysteine-dependent glutathione synthesis. *Redox Rep* 8: 57-63

35. Waterman MR. 1974. Role of cysteine residues in hemoglobin structure and function: transfer of p-mercuribenzoate from alpha subunits to beta subunits during tetramer formation. *Biochim Biophys Acta* 371: 159-67

36. Wiegel J, Wu Q. 2000. Microbial reductive dehalogenation of polychlorinated biphenyls. *FEMS Microbiology Ecology* 32: 1-15

37. Wiegel J, Zhang X, Wu Q. 1999. Anaerobic dehalogenation of hydroxylated polychlorinated biphenyls by Desulfitobacterium dehalogenans *Appl Environ Microbiol* 65: 2217-21

38. Yang Y, Chen M, Kesterson RA, Jr., Harmon CM. 2007. Structural insights into the role of the ACTH receptor cysteine residues on receptor function. *Am J Physiol Regul Integr Comp Physiol* 293: R1120-6

39. Yi L, Ragsdale SW. 2007. Evidence that the heme regulatory motifs in heme oxygenase-2 serve as a thiol/disulfide redox switch regulating heme binding. *J Biol Chem* 282: 21056-67

40. Zhong L, Arner ES, Holmgren A. 2000. Structure and mechanism of mammalian thioredoxin reductase: the active site is a redox-active selenolthiol/selenenylsulfide formed from the conserved cysteine-selenocysteine sequence. *Proc Natl Acad Sci U S A* 97: 5854-9

SECTION II

Chapter 4

Rev-erbβ, A TRANSCRIPTIONAL REGULATOR OF CIRCADIAN RHYTHM, GROWTH AND METABOLISM

4.1 Nuclear receptors

Transcription initiation in eukaryotes requires a group of proteins that assemble into a large complex that includes RNA polymerase, general transcription factors (TFIIA-H), coactivators, chromatin remodelers, histone acetylases, histone deactetylases, kinases and methylases. These proteins are important for transcription, however, regulation of transcription (activation or repression) and the choice of specific initiation sites i.e. genes for transcription are controlled by transcription factors. One of the largest groups of transcription factors in animals is represented by nuclear receptors. The nuclear receptor superfamily includes related but diverse arrays of transcription factors, which are capable of exerting transcriptional regulation in the nucleus in response to various intracellular and extracellular signals (36, 72). There are 48 nuclear receptors encoded in human genome; however, only 27 of them have known endogenous ligands. The remaining 21 belong to the category of orphan nuclear receptors (6, 74). The widespread relevance of nuclear receptors/orphan nuclear receptors to almost all aspects of human

physiology, including metabolism, homeostasis, development and disease, has made them promising pharmacological targets (36, 41). In fact, almost 15% of current drugs target nuclear receptors (48), which make them the third largest target for the pharmaceutical industry after G protein coupled receptors and kinases (51).

Nuclear receptors have two defining structural and functional features; first an N-terminal (sometimes, centrally located) conserved zinc finger DNA-binding domain (DBD) and second, a ligand binding domain (LBD) located at the C-terminus. The complete domain organization of a nuclear receptor is described in figure 4.1. The N-terminal domain is also called the hypervariable or A/B domain, which contains transcriptional activation function which is independent of ligand, and is termed as AF-1 (64). The sequence and length of the A/B domain is highly variable among nuclear receptors.

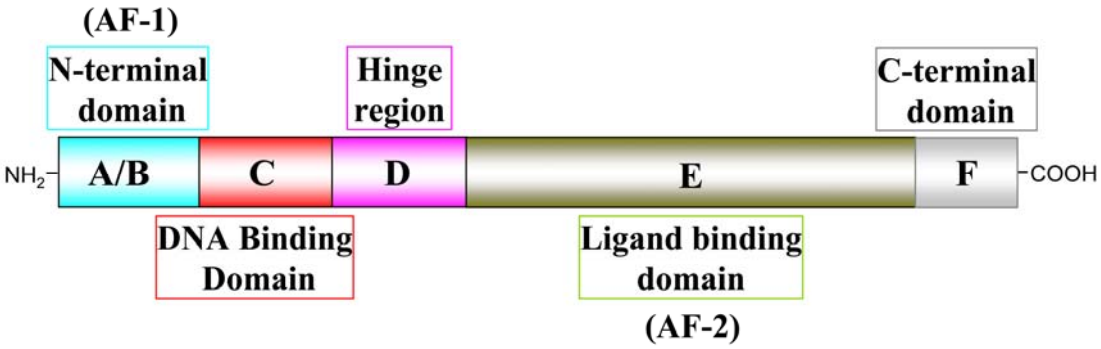

Figure 4.1: **General domain organization of nuclear receptors**. Nuclear receptors, in general, have five domains (A/B, C, D, E and F) as depicted in the figure.

Moreover, the A/B domain is the most frequent site of alternative splicing and contains a variety of kinase recognition sequences. DBD (or C domain) is the most conserved domain with two zinc fingers. It recognizes the hexanucleotide response element in the target promoter of nuclear receptors. The first Zn- finger contains the proximal-/P-box, an

alpha helix, which is responsible for specific recognition of the core half site of the response element. The second Zn-finger is comprised of the distal or D-box, which is also an α-helix. The D-box can mediate receptor dimerization, which is an important function because most nuclear receptors bind to their responsive elements as homodimers (e.g. GR, ER) or heterodimers (e.g. TR, RAR). However, NGF1-B, ROR are the example of some nuclear receptors which bind to their target as monomers. The response elements for nuclear receptors may be direct repeats (DR_x, AGGTCA-N_x-AGGTCA, where N is any nucleotide and acts as spacer; x could be any number of residues from 0-10), everted repeats (ER_x, ACTGGA-N_x-AGGTCA) or inverted repeats (IR_x, AGGTCA-N_x_ACTGGA). The DBD is followed by a flexible hinge region, called domain D that has a poorly defined function. The second characteristic domain of nuclear receptors is the LBD (domain E), which is preceded by domain D and is moderately conserved. This domain has an interior hydrophobic pocket for ligand binding and also contains ligand-regulated transcriptional activation function-2 (AF-2). This function is mainly attributed to the 12^{th} helix present on the extreme C-terminus of the domain that helps in co-activator/co-repressor recruitment. Coactivators/corepressors interact with LBD via hydrohphobic interaction mediated by a helical LXXLL motif in co-activators/co-repressors. Moreover, the LBD along with the DBD can provide an interface for dimerization (41). The F domain, which is present at the C-terminus of nuclear receptors, has no confirmed function and has variable length among nuclear receptors (3, 29, 57).

Rev-erbβ and Rev-erbα are heme-regulated nuclear receptors that control the expression of a number of important target genes involved in metabolism and circadian rhythm. They are unique members of the superfamily of nuclear receptors because they: i) use

heme as a ligand that helps in recruiting corepressor and, ii) lack the 12th helix in the ligand binding domain responsible for AF-2. Although this thesis focuses on human Rev-erbβ, both Rev-erbβ and Rev-erbα are discussed in this chapter, because they appear to have overlapping functional properties.

4.2 Occurrence and expression profile

Rev-erbα (also known as EAR1 or THRA1 or THRAL or ear-1 or hRev) and Rev-erbβ (also known as BD73 or EAR-1R or RVR) are the only two members of the Rev-erb group (Group D) and belong to thyroid hormone receptor-like subfamily of nuclear receptors (Nuclear receptors nomenclature committee, 1999). The gene encoding Rev-erbβ is located on chromosome-3, while Rev-erbα is encoded by a gene present on chromosome-17 in humans (72).

Rev-erbβ, and Rev-erbα, are conserved among vertebrates and extensively expressed during development and in adult life. Both, Rev-erbβ and Rev-erbα are known to be present at moderate levels in most human tissues, and have a high expression in metabolically active tissues such as liver, adipose tissue, skeletal muscle, and brain (8, 18, 20, 33, 43, 50). In particular, in mouse, Rev-erbα (97.4 % sequence identity to human) exhibits elevated expression in testis and skeletal muscles, while Rev-erbβ shows higher expression in the central nervous system. Thus, the wide expression of Rev-erbβ and Rev-erbα, in different tissues and different developmental phases of life, indicates broad roles of these factors in cell proliferation and physiology (6).

Moreover, Rev-erbs are clock-controlled genes and show a circadian pattern of expression, with peak levels in the middle of the day (16, 65). This circadian pattern of

expression can be attributed to their role in circadian circuitry, described later in this chapter.

4.3 Isoforms

The *rev-erbα* gene encodes two splice variants in human and rat. The larger isoform encodes a 614-amino acid protein, while the second isoform encodes 508 amino acids. Transcription initiation from an internal promoter generates the shorter isoform. The two isoforms differ only in their N-terminal A/B domain (56).

Rev-erbβ also exists in two different isoforms in human; Rev-erbβ1 and Rev-erbβ2, which are 579 and 504 amino acids long respectively. Rat is also reported to have two isoforms of Rev-erbβ (578 and 383 amino acids long) that may originate by alternate splicing. (20, 54).

4.4 Domain organization

Rev-erbs have domain organizations that are atypical of nuclear receptors.. They have an N-terminal variable domain (A/B region), followed by a highly conserved DNA binding domain (DBD, C region), a hinge region (D region) and a C-terminal ligand binding domain (E region). Rev-erbs lack the F domain, which is not uncommon among nuclear receptors. Sequence identity between Rev-erbα and β is very high in the DBD (98%) and moderate in the LBD (74%). The major differences between Rev-erbs occur in the N-terminal domain (29% sequence identity) and in the hinge region (31% sequence identity) (18) (Figure 4.2).

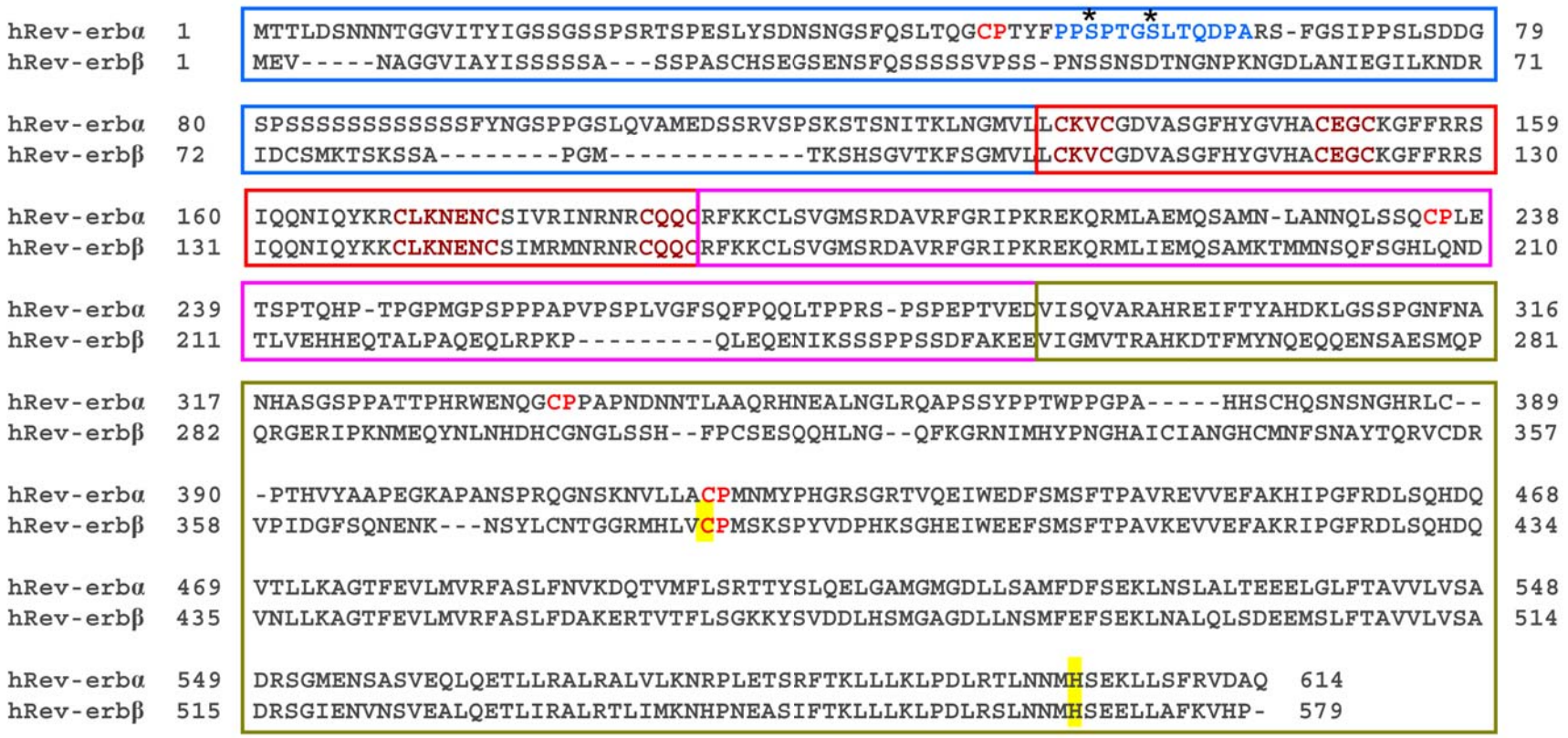

Figure 4.2: Sequence alignment of human Rev-erbα and Rev-erbβ. Domain organization is based on the Rev-erbα sequence a follows; A/B domain (cyan box), DBD (red box), hinge/D domain (magenta box) and LBD (olive green). The blue fonts in the A/B represents the phosphorylation site in Rev-erbα and * indicates the serine residues that get phosphorylated. Conserved CXXC and CX motives involved in binding of two Zn molecules are in maroon fonts inside the DBD. Residues involved in heme ligation are highli yellow. HRMs are also illustrated throughout the sequence and are indicated with red fonts. The sequence alignment was performed BLAST tool in NCBI; NCBI Ids of the sequences used in this alignment are as follows; Rev-erbα-CAE75563.1 and Rev-erbβ-NP_00511

Overall, the A/B domains of Rev-erbs are serine rich (Figure 4.3), which is a site for posttranslational modification by GSK3β (described later). The DBD has two C4-type zinc fingers, which are characterized by four cysteines coordinating one zinc molecule with no further sequence similarity. The nuclear localization signal (NLS) of Rev-erbs is located within the DBD, which is unusual in the nuclear receptor family (11).

4.5 Mechanism of action:

Nuclear receptors can repress or activate transcription of target genes via different mechanisms. Three basic mechanisms of transcriptional regulation have been described and are as follows: Type I nuclear receptors reside in the cytoplasm and translocate into the nucleus after dissociation from heat shock proteins and dimerization following ligand binding. In the nucleus they bind to their promoter consisting of inverted repeats and enhance transcription of their target genes. Examples of this class of nuclear receptors includes androgen receptors, estrogen receptors etc. In contrast, type II receptors are retained in the nucleus irrespective of the occupancy of the ligand binding domain and, bind as heterodimers to their promoters. In general, co-repressors bind to these types of unliganded nuclear receptors and convey a repressive signal to the transcription assembly. Then, once the ligand is bound to the ligand binding domain, conformational changes occur in the nuclear receptor, which in turn release the co-repressor and recruits the co-activator. Representative of this class of nuclear receptors are retinoic acid receptor and retinoid X receptor. Type III class of nuclear receptors are constitutive transcriptional activators and act in a ligand-independent manner. They bind to their

response elements as monomers and are categorized as orphan nuclear receptors whose endogenous ligands are unknown such as SF-1 (31, 39, 70).

Rev-erbs belong to the type II category of nuclear receptors and are constitutively bound to their responsive elements (RevREs; Rev-erb-responsive elements, see section 4.6.1 for detail), after translocation from the cytoplasm to the nucleus (68). However, unlike type II nuclear receptors, Rev-erbs recruit co-repressor (NCoR) upon liagnd (heme) binding to the LBD. They are unable to repress the target genes unless heme is bound to their LBD (44, 68). Upon binding of heme, Rev-erb recruits nuclear co-repressor (NCoR) and, in turn, NCoR recruits histone deacetylase (HDAC3 for Rev-erbα and HDAC1 for Rev-erbβ) that results in transcriptional silencing of target genes (47) (Figure 4.3).

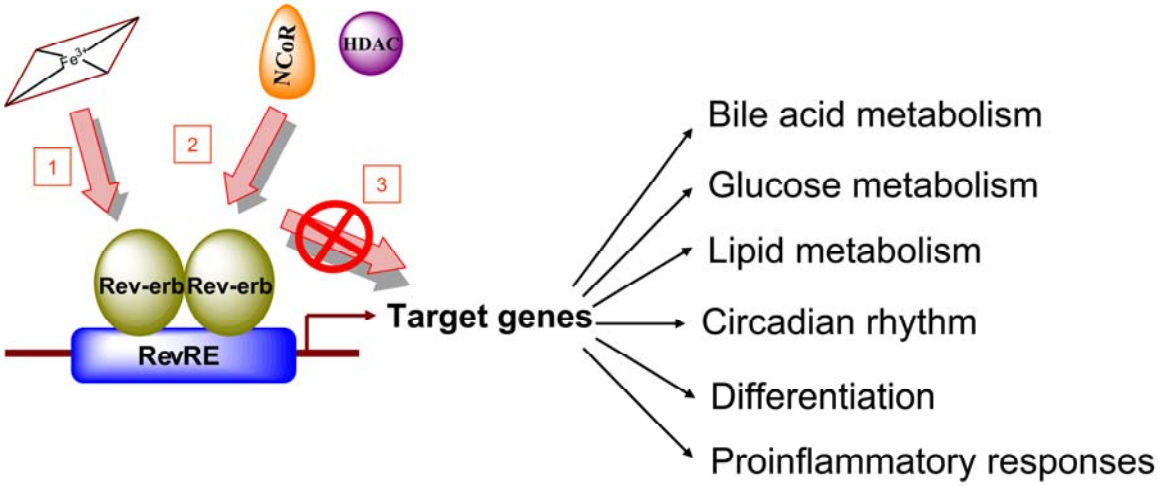

Figure 4.3: Transcriptional repression mechanism of Rev-erbs. This figure is based on Burris T P, 2008. Mol Endocrinol (10).

Rev-erbs are dominant transcriptional repressors and they suppress trans-activation mediated by retinoid related orphan receptors (RORs). Both Rev-erbs and RORs compete for the same DNA binding site and modulate expression of the same target genes such as

Bmal1 (1, 23, 28). However, both Rev-erbs and RORs show a circadian pattern of expression with a 180º phase difference (10).

Not much information is available about the mechanism of derepression of Rev-erb target genes. Two independent studies have revealed the role of Tip60α and ZNHIT-1 in derepression of Rev-erbβ mediated repression. Tip60α and ZNHIT-1 are both recruited to the apoCIII promoter by Rev-erbβ, which then results in the removal of Rev-erbβ–induced inhibition. While Tip60α, a histone acetyltransferase, interacts with and acetylates an RxKK motif in the DBD of Rev-erbβ, ZNHIT-1 interacts via its FxLL motif with the LBD of Rev-erbβ and predicted to act via recruitment of a chromatin remodeling complex (61, 62). Sauve and colleagues have also shown *in vitro* interaction of Rev-erbs with a novel activator, CIA (NCOA5) in yeast two-hybrid assay. CIA interacts with nuclear receptors in an AF-2 independent manner and is predicted to act both as an activator and a repressor (52).

Functions of Rev-erbα and Rev-erbβ are quite redundant and are required for rhythmic expression of Bmal1 and other target genes (35). Intriguingly, the role of individual Rev-erbs and their preferential requirement in circadian regulation has not been well documented. A comparative study done by Yang and colleagues has demonstrated that peak expressions of rhythmic Rev-erbα and Rev-erbβ are at different Zeitgeber Times (ZT). They compared the expression profiles of Rev-erbα and Rev-erbβ in four different murine metabolic tissues (white adipose tissues, brown adipose tissue, liver and muscle). Expression of Rev-erbα always peaked at ZT4, similar to most of the other nuclear

receptors in these tissues, while Rev-erbβ lagged 4 hrs behind and showed a peak expression at ZT8 (65).

Rev-erbα and Rev-erbβ, both bind to same responsive element and thus should control expression of the same genes; however, only limited studies have examined the differential role(s), if any, of both Rev-erbs in gene regulation. Given that the expression levels of Rev-erbα and Rev-erbβ vary in most tissues (28) and that peak expression varies in different metabolic tissues (65), the requirement for Rev-erbα and Rev-erbβ could be spatial and time dependent. It will also be interesting to find out the intricate mechanisms by which Rev-erbs act as positive or negative regulators when bound to the same evolutionarily conserved DNA binding site. For example Rev-erbβ, in general, acts as negative regulator of genes includingBmal1, however, acts as a positive activator of the srebp1c gene described in section 4.8.

4.5.1 DNA binding properties

Rev-erbs bind to two different but closely related promoter sequences, RORE (ROR-responsive elements) and Rev-DR2 (Rev-erb direct repeat separated by two nucleotides). RORE is not strongly conserved and its consensus is PuAPuNT**PuGGTCA**. Thus, RORE is comprised of a classic hexanucleotide response element (bold letters, shown above), plus a 5′ A/T rich extension (6, 27, 30). The C-terminal extension of the DBD of Rev-erbα has been shown to interact with this A/T-rich 5′ extension of a hexanucleotide half site (PuGGTCA) that is required for high affinity binding (73). In general, both the Rev-erbα monomers bind independently to two relatively widely-spaced ROREs and recruit one NCoR. Rev-erbβ also requires two distant ROREs in order to suppress target genes

(62). Intriguingly, a monomeric Rev-erbα bound to a single RORE cannot recruit NCoR. (30, 69, 70) but can repress target genes by competing with RORs (23, 27, 28).

Rev-erbs can also bind cooperatively as homodimers to RevDR2 (30, 70), which are composed of a RORE at the 5′ end and a classic PuGGTCA element (a direct repeat of the hexanucleotide of RORE) at the 3′ terminus, and these two elements are separated by two nucleotides (always CT) (30). Quantitative analyses have shown cooperative binding of DBD of Rev-erbβ to Rev-DR2 with a 50% fractional saturation at 270 nM (54)

In both the above cases, the Rev-erb monomer binds to an extended hexanucleotide half-site sequence via a PuGGTCA motif. Moreover, a recognition helix at the C-terminal part of the first Zn-finger interacts with the major groove of DNA and makes specific contacts with the PuGGTCA motif. The second Zn-finger stabilizes the interaction with DNA via a second helix and additionally, allows dimerization in the presence of a partner (6, 53).

4.5.2 Ligand binding properties

Rev-erbs were thought to be constitutive repressors until heme was discovered as an endogenous ligand for Rev-erbs in two parallel and independent studies (44, 68). Heme was shown via different spectroscopic methods to bind reversibly to the LBDs of Rev-erbs. Moreover, heme binding increased the thermal stability of Rev-erbs, demonstrating the direct interaction of heme with Rev-erb. Dissociation constants (K_d) for heme were found between 2 to 6 μM for Rev-erbα and Rev-erbβ (44, 68).

Less is known about heme binding to Rev-erbα than to Rev-erbβ. The H602F mutant of Rev-erbα was unable to bind heme or to recruit NCoR and HDAC3 and was unable to

repress the target gene (44, 68). Therefore, it is plausible that His602 is a heme ligand for Rev-erbα as is His568, the analogous residue in Rev-erbβ whose ligation, along with Cys384, was clearly revealed by crystallographic studies (42). However, no further studies were done to determine whether the Rev-erbα heme is a penta- or hexa-coordinated.

Cys384, which is one of the heme ligands in Rev-erbβ, also is a part of heme regulatory motif (HRM), present in many heme binding proteins. A cysteine residue flanked by a proline forms the core of HRM (also called CP motif) and has been shown to responsible for heme mediated activity and stability of proteins harboring them (71). The Cys384 CP motif in Rev-erbβ and analogus CP motif in Rev-erbα are conserved among most of species that harbor these proteins. Interestingly, Rev-erbα possesses several additional CP motives (2 in the LBD, 2 in the A/B domain and in the D domain), which are absent in Rev-erbβ (Figure 4.3). However, the role, if any, of these additional CP motif is not known.

Further studies of heme ligation to Rev-erbβ have disclosed that the protein is capable of binding to both ferric and ferrous heme and that internal heme ligands can be replaced by other amino acids or diatomic gases (42). However, the physiological relevance of this ligand switching is not clear at this point.

Many synthetic ligands have also been identified for Rev-erbs. The first synthetic ligand, {1,1-dimethylethylethylN-[(4-chlorophenyl)methyl]-N-[(5-nitro-thienyl)methyl]glycinate }, was found soon after the discovery of heme as an endogenous ligand. This synthetic ligand acted as an agonist and reset the circadian rhythm in a phasic manner (EC_{50}=250

nM) in a cell-based assay (37). Recently, GSK4112/SR6452, a synthetic ligand, was also found as an agonist of heme and was shown to regulate NCoR binding (32). Furthermore, SR8278 was shown to behave as Rev-erbs antagonist (EC_{50}=470 nM) and caused derepression of target genes of Rev-erbs (31).

4.6 Regulation of expression and activity of Rev-erbs:

Expression of Rev-erbs is regulated at both transcriptional and post-translational levels (Figure 4.4). *Rev-erbs* are clock genes and their expression is controlled by different clock genes as well. Expressions of Rev-erbs are enhanced by BMAL1/CLOCK heterodimers and are indirectly suppressed via PER and CRY.

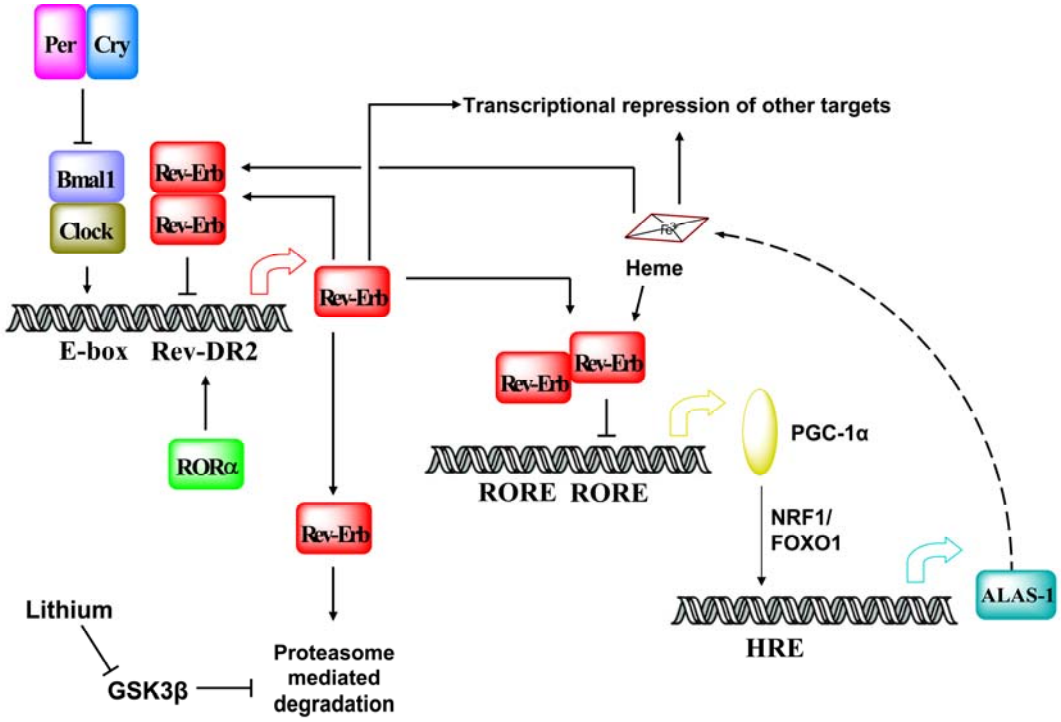

Figure 4.4: Regulation of expression/activity of Rev-erbs via different mechanisms. The figure is based either on the individual findings with Rev-erbα or Rev-erbβ and/or findings that applies to both of them (please refer to the text for detail). Promoter regions are represented by double helixes and names of the promoters are given beneath the helix. Proteins translated from the transcription products of genes under the influence of these promoters are shown in rectangles and indicated via arrow of the same color.

Rev-erbα is also able to modulate its own expression and activity via controlling the expression of PGC-1α (69). Rev-erbα downregulates the expression of PGC-1α, which is required for ROR-mediated induction of Rev-erbα expression. However, such an auto-regulation of Rev-erbβ is not known. Moreover, PGC-1α is also required for expression of δ-ALAS1 (δ-amino levulinate synthase1), a rate-limiting enzyme in heme biosynthesis. Thus, Rev-erbα controls the biosynthesis of its own ligand and therefore modulates its own activity.

At the post-translational level, Rev-erbα is stabilized via serine phosphorylation (FPP**S**^{55}PTG**S**^{59}LTQDPA) at its N-terminus by GSK3β, and this site is conserved in human, mouse and rat Rev-erbs (67). This is counterintuitive because GSK3β-mediated phosphorylation in general, targets proteins for proteasomal degradation (15). Phosphorylation via GSK3β stabilizes the Rev-erbα protein and inactivation of GSK3β results in ubiquitination leading to 26S proteasome-directed degradation of Rev-erbα. Interestingly, lithium, which is used for bipolar treatment, inhibits GSK3β and causes Rev-erbα protein level to diminish without affecting mRNA level (67).

In addition to the aforementioned global regulation of Rev-erbα, limited studies have shown liver-specific regulation of Rev-erbα. PPARα directly induces the expression of Rev-erbα in the hepatic system in the presence of the PPARα agonist, fibrates (26). Glucocorticoid down regulates the expression of Rev-erbα in liver via glucocorticoid receptor (55). Moreover, liver X receptor (LXR) α also induces Rev-erbα expression directly in human macrophages (22).

4.7 Role of Rev-erbs in different cellular processes

Rev-erbs regulate divergent cellular processes including circadian rhythm, metabolism, inflammation, growth and development (Table 1). The following two sections below describe genes regulated by either Rev-erbα or Rev-erbβ or both in different tissues and cellular processes.

4.7.1 Role in Circadian rhythm

Circadian rhythms are generated and sustained by transcriptional feedback loops contributed by clock genes (Figure 4.6). Brain and Muscle Arnt-Like protein 1 (BMAL1) and Circadian Locomoter Output Cycles Kaput (CLOCK) proteins form a heterodimeric complex and induce the expression of cryptrochrome (*cry1*, *cry2*) and period (*per1*, *per2* and, *per3*) genes. Once PER and CRY reach saturation levels, they inhibit BMAL1-stimulated expression via binding to the BMAL1/CLOCK heterodimer in the nucleus. RORs upregulate the expression of BMAL1. On the other hand, Rev-erbs cause the transcriptional silencing of the *bmal1* gene and are required for rhythmic expression of BMAL1 (10). Recent studies demonstrated that Rev-erbα also downregulates the expression of CLOCK and NPAS2 (CLOCK homolog in brain) (13, 14). Additionally, both Rev-erbα and Rev-erbβ can suppress the expression of Rev-erbα (1). Interestingly, expression of Rev-erbs is upregulated via RORα and the BMAL1/CLOCK heterodimer (Figure 4.6) (10). Hence, Rev-erbs form a negative feedback loop that connects the negative limb to the positive limb of the circadian rhythm.

4.7.2 Role in Metabolism

Rev-erbs are highly expressed in metabolic tissues, as mentioned above in sections 4.2.1. In these tissues, Rev-erbs control genes involved in glucose metabolism, fatty acid

metabolism, bile acid synthesis and heme biosynthesis. These target genes are described below in tissue specific manner.

Gene	Function/Pathways	Rev-erbα	Rev-erbβ	Reference
Bmal1	Clock gene	√	√	(10, 66)
Npas2	Clock gene	√		(14)
Clock	Clock gene	√		(13)
Rev-erbα	Clock gene	√	√	(1)
PGC-1α	Heme biosynthesis and others	√		(69)
Glucose-6-phosphatse	Gluconeogenesis	√		(68)
mir-122	Cholesterol and fatty acid metabolism	√		(25)
apoCIII	Fatty acid metabolism	√	√	(12, 50)
APOAI	Fatty acid metabolism	√		(59)
Srebp1c	Fatty acid synthesis		√	(46)
Cyp7A1	Bile acid synthesis	√	√	(40)
SHP	Bile acid synthesis	√		(17, 34)
E4BP4	Bile acid synthesis	√		(17, 34)
NF-κB	Inflammation	√		(38)
N-myc	Neural tumerogenesis	√	√	(19)
PAI-1	Fibrinolysis inhibition	√		(63)
α-fetoprotein	Embryogenesis	√	√	(7)

Table 4.1: List of various genes under control of Rev-erbs. (√) indicates whether Rev-erbα or Rev-erbβ is involved in regulation of the particular gene.

4.7.2.1 Skeletal muscle metabolism: Rev-erbβ regulates numerous genes in skeletal muscles such as myostatin involved in myogenesis (45) or FAT/CD36 and FABP3/4, which facilitate uptake of long chain fatty acids and low-density lipoproteins (45). While, Rev-erbβ, in general, is a negative transcriptional regulator, it can induce expression of

the *srebp1c* gene that plays a role in lipogenesis (46). No gene target for Rev-erbα in skeletal muscle has been described so far.

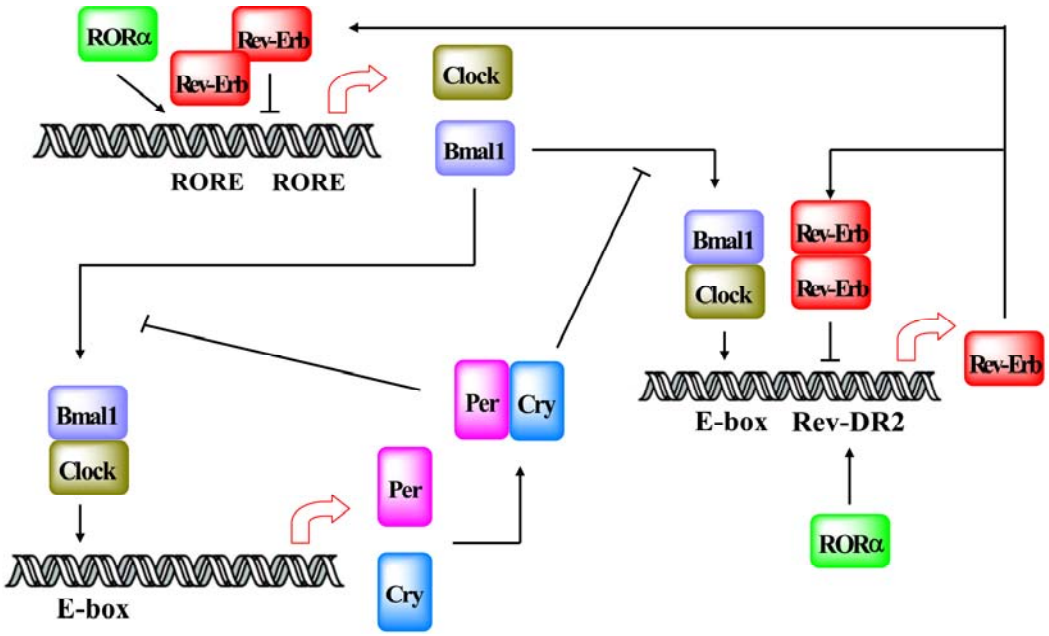

Figure 4.5: Molecular mechanism responsible for circadian oscillations. The figure is based either on the individual findings with Rev-erbα or with Rev-erbβ or findings that applies to both of them. The promoter regions are represented by double helixes and names of the promoters are given beneath the helix. The proteins translated from the transcription product of the genes under the influence of these promoters are shown in rectangles and are indicated by red arrows. This figure has been modified from Burris, T. P. Mol Endocrinol, 2008 (10).

4.7.2.2 Adipose tissues metabolism: Rev-erbα induces adipogenesis, although its exact target in adipose tissue is not known (60). The role of Rev-erbβ has not been well studied in adipogenesis. However, it is known that Rev-erbβ together with Rev-erbα is regulated in a biphasic manner upon induction of adipogenesis (47).

4.7.2.3 Liver metabolism: Besides regulating clock genes (described in section 4.7.1), Rev-erbα along with Rev-erbβ suppresses the expression of apolipoprotein CIII (apoCIII) in liver (12, 49). Thus, mice lacking Rev-erbα exhibit elevated levels of apoCIII with an

increase in serum triglycerides and VLDL (48). Rev-erbα also regulates the expression of Apolioprotein A1, a component of high density lipoprotein (HDL); however this regulation is species-specific and is observed in rats but not in humans (59). Rev-erbα also plays a role in gluconeogenesis by regulating expression of glucose-6-phosphatase (68).

Rev-erbα and Rev-erbβ positively regulate bile acid metabolism by maintaining the robust and circadian expression of cholesterol 7α-hydoxylase, (CYP7A1), the first and rate limiting enzyme in the bile acid production pathway (40). Additionally, both Rev-erbα and Rev-erbβ negatively regulate the expression of SHP and E4BP4, which are negative regulators of CYP7A1 (17, 34).

Recently, Rev-erbα was shown to regulate the highly abundant liver-specific microRNA, mir-122 (25), which appears to regulate cholesterol and fatty- acid metabolism in adult mouse liver (21). Furthermore, Elovl3 (present in both liver and adipose tissue), which encodes a very long chain fatty acid elongase, has recently been identified as a Rev-erbα target (2).

4.7.2.4 Heme biosynthesis: Biosynthesis of heme, which is a ligand for Rev-erbs, occurs in all cell types and therefore, has been described here separately. Interestingly, Rev-erbα regulates the synthesis of its own ligand. Heme biosynthesis, in general, is upregulated by NPAS2 and PGC-1α (coactivator). NPAS2 and PGC-1α induce the expression of ALAS1, a rate-limiting enzyme in heme biosynthesis. Rev-erbα, intriguingly, has been shown to down regulate both NPAS2 and PGC-1α and thus inhibit heme synthesis (14, 69).

In addition to above mentioned roles, Rev-erbs are also involved in the inflammation cascade, fibrinolysis and embryogenesis. For example, Rev-erbα mediates expression of inflammatory cytokines such as IL-6 and COX-2 via NF-κB trans-activation in vascular smooth muscle cells (38). In addition to have a role in inflammation, Rev-erbα also interferes with the fibrinolysis cascade by inhibiting RORα-mediated induction of the plasminogen activator inhibitor (PAI)-1, and may support the development of atherothrombosis (58, 63). Furthermore, Rev-erbs also play a role in embryonic development by regulating the expression of α-fetoprotein, which is expressed in the yolk sack, fetal liver and intestine (7).

Overall, Rev-erbs, which are clock genes, not only maintain the circadian rhythm of clock genes but also regulate huge numbers of metabolic genes and some genes involved in inflammation, growth and development. A causal relationship between altered circadian rhythm and metabolic disorders has already been observed. For example, disruption of clock genes causes dyslipidemia, insulin resistance and obesity, all leading to atherosclerosis (16). Therefore, Rev-erbs have been predicted to connect metabolism with circadian rhythm. Moreover, Rev-erbs might also be able to connect inflammatory responses, growth and development with circadian rhythm provided their widespread role in all these cellular processes. Therefore, study of regulation of Rev-erbs' will open new opportunities for understanding the circadian control of many physiological events.

4.8 References

1. Adelmant G, Begue A, Stehelin D, Laudet V. 1996. A functional Rev-erb alpha responsive element located in the human Rev-erb alpha promoter mediates a repressing activity. *Proc Natl Acad Sci U S A* 93: 3553-8

2. Anzulovich A, Mir A, Brewer M, Ferreyra G, Vinson C, Baler R. 2006. Elovl3: a model gene to dissect homeostatic links between the circadian clock and nutritional status. *J Lipid Res* 47: 2690-700

3. Bain DL, Heneghan AF, Connaghan-Jones KD, Miura MT. 2007. Nuclear receptor structure: implications for function. *Annu Rev Physiol* 69: 201-20

4. Barish GD, Downes M, Alaynick WA, Yu RT, Ocampo CB, et al. 2005. A Nuclear Receptor Atlas: macrophage activation. *Mol Endocrinol* 19: 2466-77

5. Barlev NA, Liu L, Chehab NH, Mansfield K, Harris KG, et al. 2001. Acetylation of p53 activates transcription through recruitment of coactivators/histone acetyltransferases. *Mol Cell* 8: 1243-54

6. Benoit G, Cooney A, Giguere V, Ingraham H, Lazar M, et al. 2006. International Union of Pharmacology. LXVI. Orphan nuclear receptors. *Pharmacol Rev* 58: 798-836

7. Bois-Joyeux B, Chauvet C, Nacer-Cherif H, Bergeret W, Mazure N, et al. 2000. Modulation of the far-upstream enhancer of the rat alpha-fetoprotein gene by members of the ROR alpha, Rev-erb alpha, and Rev-erb beta groups of monomeric orphan nuclear receptors. *DNA Cell Biol* 19: 589-99

8. Bonnelye E, Vanacker JM, Desbiens X, Begue A, Stehelin D, Laudet V. 1994. Rev-erb beta, a new member of the nuclear receptor superfamily, is expressed in the nervous system during chicken development. *Cell Growth Differ* 5: 1357-65
9. Brivanlou AH, Darnell JE, Jr. 2002. Signal transduction and the control of gene expression. *Science* 295: 813-8

10. Burris TP. 2008. Nuclear hormone receptors for heme: REV-ERBalpha and REV-ERBbeta are ligand-regulated components of the mammalian clock. *Mol Endocrinol* 22: 1509-20

11. Chopin-Delannoy S, Thenot S, Delaunay F, Buisine E, Begue A, et al. 2003. A specific and unusual nuclear localization signal in the DNA binding domain of the Rev-erb orphan receptors. *J Mol Endocrinol* 30: 197-211

12. Coste H, Rodriguez JC. 2002. Orphan nuclear hormone receptor Rev-erbalpha regulates the human apolipoprotein CIII promoter. *J Biol Chem* 277: 27120-9

13. Crumbley C, Burris TP. 2010. Direct regulation of CLOCK expression by REV-ERB. *PLoS One* 6: e17290

14. Crumbley C, Wang Y, Kojetin DJ, Burris TP. 2010. Characterization of the core mammalian clock component, NPAS2, as a REV-ERBalpha/RORalpha target gene. *J Biol Chem* 285: 35386-92

15. Doble BW, Woodgett JR. 2003. GSK-3: tricks of the trade for a multi-tasking kinase. *J Cell Sci* 116: 1175-86

16. Duez H, Staels B. 2008. Rev-erb alpha gives a time cue to metabolism. *FEBS Lett* 582: 19-25

17. Duez H, van der Veen JN, Duhem C, Pourcet B, Touvier T, et al. 2008. Regulation of bile acid synthesis by the nuclear receptor Rev-erbalpha. *Gastroenterology* 135: 689-98

18. Dumas B, Harding HP, Choi HS, Lehmann KA, Chung M, et al. 1994. A new orphan member of the nuclear hormone receptor superfamily closely related to Rev-Erb. *Mol Endocrinol* 8: 996-1005

19. Dussault I, Giguere V. 1997. Differential regulation of the N-myc proto-oncogene by ROR alpha and RVR, two orphan members of the superfamily of nuclear hormone receptors. *Mol Cell Biol* 17: 1860-7

20. Enmark E, Kainu T, Pelto-Huikko M, Gustafsson JA. 1994. Identification of a novel member of the nuclear receptor superfamily which is closely related to Rev-ErbA. *Biochem Biophys Res Commun* 204: 49-56

21. Esau C, Davis S, Murray SF, Yu XX, Pandey SK, et al. 2006. miR-122 regulation of lipid metabolism revealed by in vivo antisense targeting. *Cell Metab* 3: 87-98

22. Fontaine C, Rigamonti E, Pourcet B, Duez H, Duhem C, et al. 2008. The nuclear receptor Rev-erbalpha is a liver X receptor (LXR) target gene driving a negative feedback loop on select LXR-induced pathways in human macrophages. *Mol Endocrinol* 22: 1797-811

23. Forman BM, Chen J, Blumberg B, Kliewer SA, Henshaw R, et al. 1994. Cross-talk among ROR alpha 1 and the Rev-erb family of orphan nuclear receptors. *Mol Endocrinol* 8: 1253-61

24. Fu M, Wang C, Zhang X, Pestell RG. 2004. Acetylation of nuclear receptors in cellular growth and apoptosis. *Biochem Pharmacol* 68: 1199-208

25. Gatfield D, Le Martelot G, Vejnar CE, Gerlach D, Schaad O, et al. 2009. Integration of microRNA miR-122 in hepatic circadian gene expression. *Genes Dev* 23: 1313-26

26. Gervois P, Chopin-Delannoy S, Fadel A, Dubois G, Kosykh V, et al. 1999. Fibrates increase human REV-ERBalpha expression in liver via a novel peroxisome proliferator-activated receptor response element. *Mol Endocrinol* 13: 400-9

27. Giguere V, Tini M, Flock G, Ong E, Evans RM, Otulakowski G. 1994. Isoform-specific amino-terminal domains dictate DNA-binding properties of ROR alpha, a novel family of orphan hormone nuclear receptors. *Genes Dev* 8: 538-53

28. Guillaumond F, Dardente H, Giguere V, Cermakian N. 2005. Differential control of Bmal1 circadian transcription by REV-ERB and ROR nuclear receptors. *J Biol Rhythms* 20: 391-403

29. Halachmi S, Marden E, Martin G, MacKay H, Abbondanza C, Brown M. 1994. Estrogen receptor-associated proteins: possible mediators of hormone-induced transcription. *Science* 264: 1455-8

30. Harding HP, Lazar MA. 1993. The orphan receptor Rev-ErbA alpha activates transcription via a novel response element. *Mol Cell Biol* 13: 3113-21

31. Kojetin D, Wang Y, Kamenecka TM, Burris TP. 2010. Identification of SR8278, a synthetic antagonist of the nuclear heme receptor REV-ERB. *ACS Chem Biol* 6: 131-4

32. Kumar N, Solt LA, Wang Y, Rogers PM, Bhattacharyya G, et al. 2010. Regulation of adipogenesis by natural and synthetic REV-ERB ligands. *Endocrinology* 151: 3015-25

33. Lazar MA, Hodin RA, Darling DS, Chin WW. 1989. A novel member of the thyroid/steroid hormone receptor family is encoded by the opposite strand of the rat c-erbA alpha transcriptional unit. *Mol Cell Biol* 9: 1128-36

34. Le Martelot G, Claudel T, Gatfield D, Schaad O, Kornmann B, et al. 2009. REV-ERBalpha participates in circadian SREBP signaling and bile acid homeostasis. *PLoS Biol* 7: e1000181

35. Liu AC, Tran HG, Zhang EE, Priest AA, Welsh DK, Kay SA. 2008. Redundant function of REV-ERBalpha and beta and non-essential role for Bmal1 cycling in transcriptional regulation of intracellular circadian rhythms. *PLoS Genet* 4: e1000023

36. Mangelsdorf DJ, Thummel C, Beato M, Herrlich P, Schutz G, et al. 1995. The nuclear receptor superfamily: the second decade. *Cell* 83: 835-9

37. Meng QJ, McMaster A, Beesley S, Lu WQ, Gibbs J, et al. 2008. Ligand modulation of REV-ERBalpha function resets the peripheral circadian clock in a phasic manner. *J Cell Sci* 121: 3629-35

38. Migita H, Morser J, Kawai K. 2004. Rev-erbalpha upregulates NF-kappaB-responsive genes in vascular smooth muscle cells. *FEBS Lett* 561: 69-74

39. Nikolenko Iu V, Krasnov AN. 2007. [Nuclear receptors: structure and mechanisms of action]. *Genetika* 43: 308-16

40. Noshiro M, Usui E, Kawamoto T, Kubo H, Fujimoto K, et al. 2007. Multiple mechanisms regulate circadian expression of the gene for cholesterol 7alpha-hydroxylase (Cyp7a), a key enzyme in hepatic bile acid biosynthesis. *J Biol Rhythms* 22: 299-311

41. Olefsky JM. 2001. Nuclear receptor minireview series. *J Biol Chem* 276: 36863-4

42. Pardee KI, Xu X, Reinking J, Schuetz A, Dong A, et al. 2009. The structural basis of gas-responsive transcription by the human nuclear hormone receptor REV-ERBbeta. *PLoS Biol* 7: e43

43. Pena-de-Ortiz S, Jamieson GA, Jr. 1997. Molecular cloning and brain localization of HZF-2 alpha, a new member of the Rev-erb subfamily of orphan nuclear receptors. *J Neurobiol* 32: 341-58

44. Raghuram S, Stayrook KR, Huang P, Rogers PM, Nosie AK, et al. 2007. Identification of heme as the ligand for the orphan nuclear receptors REV-ERBalpha and REV-ERBbeta. *Nat Struct Mol Biol* 14: 1207-13

45. Ramakrishnan SN, Lau P, Burke LJ, Muscat GE. 2005. Rev-erbbeta regulates the expression of genes involved in lipid absorption in skeletal muscle cells: evidence for cross-talk between orphan nuclear receptors and myokines. *J Biol Chem* 280: 8651-9

46. Ramakrishnan SN, Lau P, Crowther LM, Cleasby ME, Millard S, et al. 2009. Rev-erb beta regulates the Srebp-1c promoter and mRNA expression in skeletal muscle cells. *Biochem Biophys Res Commun* 388: 654-9

47. Ramakrishnan SN, Muscat GE. 2006. The orphan Rev-erb nuclear receptors: a link between metabolism, circadian rhythm and inflammation? *Nucl Recept Signal* 4: e009

48. Raspe E, Duez H, Mansen A, Fontaine C, Fievet C, et al. 2002. Identification of Rev-erbalpha as a physiological repressor of apoC-III gene transcription. *J Lipid Res* 43: 2172-9

49. Raspe E, Mautino G, Duval C, Fontaine C, Duez H, et al. 2002. Transcriptional regulation of human Rev-erbalpha gene expression by the orphan nuclear receptor retinoic acid-related orphan receptor alpha. *J Biol Chem* 277: 49275-81

50. Retnakaran R, Flock G, Giguere V. 1994. Identification of RVR, a novel orphan nuclear receptor that acts as a negative transcriptional regulator. *Mol Endocrinol* 8: 1234-44

51. Rosen J, Marschke K, Rungta D. 2003. Nuclear hormone receptor assays for drug discovery. *Curr Opin Drug Discov Devel* 6: 224-30

52. Sauve F, McBroom LD, Gallant J, Moraitis AN, Labrie F, Giguere V. 2001. CIA, a novel estrogen receptor coactivator with a bifunctional nuclear receptor interacting determinant. *Mol Cell Biol* 21: 343-53

53. Terenzi H, Alzari PM, Zakin MM. 1998. Structural features involved in the formation of a complex between the monomeric or the dimeric form of the rev-erb beta DNA-binding domain and its DNA reactive sites. *Biochemistry* 37: 11488-95

54. Terenzi H, Cassia RO, Zakin MM. 1996. Expression, purification, and functional analysis of the DNA binding domain of the nuclear receptor Rev-erb beta. *Protein Expr Purif* 8: 313-8

55. Torra IP, Tsibulsky V, Delaunay F, Saladin R, Laudet V, et al. 2000. Circadian and glucocorticoid regulation of Rev-erbalpha expression in liver. *Endocrinology* 141: 3799-806

56. Triqueneaux G, Thenot S, Kakizawa T, Antoch MP, Safi R, et al. 2004. The orphan receptor Rev-erbalpha gene is a target of the circadian clock pacemaker. *J Mol Endocrinol* 33: 585-608

57. Vanden JP. 2009. Nuclear receptors: A brief overview. *Nuclear receptor resource*: 1-5

58. Vaughan DE. 2005. PAI-1 and atherothrombosis. *J Thromb Haemost* 3: 1879-83

59. Vu-Dac N, Chopin-Delannoy S, Gervois P, Bonnelye E, Martin G, et al. 1998. The nuclear receptors peroxisome proliferator-activated receptor alpha and Rev-erbalpha mediate the species-specific regulation of apolipoprotein A-I expression by fibrates. *J Biol Chem* 273: 25713-20

60. Wang J, Lazar MA. 2008. Bifunctional role of Rev-erbalpha in adipocyte differentiation. *Mol Cell Biol* 28: 2213-20

61. Wang J, Li Y, Zhang M, Liu Z, Wu C, et al. 2007. A zinc finger HIT domain-containing protein, ZNHIT-1, interacts with orphan nuclear hormone receptor Rev-erbbeta and removes Rev-erbbeta-induced inhibition of apoCIII transcription. *FEBS J* 274: 5370-81

62. Wang J, Liu N, Liu Z, Li Y, Song C, et al. 2008. The orphan nuclear receptor Rev-erbbeta recruits Tip60 and HDAC1 to regulate apolipoprotein CIII promoter. *Biochim Biophys Acta* 1783: 224-36

63. Wang J, Yin L, Lazar MA. 2006. The orphan nuclear receptor Rev-erb alpha regulates circadian expression of plasminogen activator inhibitor type 1. *J Biol Chem* 281: 33842-8

64. Warnmark A, Treuter E, Wright AP, Gustafsson JA. 2003. Activation functions 1 and 2 of nuclear receptors: molecular strategies for transcriptional activation. *Mol Endocrinol* 17: 1901-9

65. Yang X, Downes M, Yu RT, Bookout AL, He W, et al. 2006. Nuclear receptor expression links the circadian clock to metabolism. *Cell* 126: 801-10

66. Yin L, Lazar MA. 2005. The orphan nuclear receptor Rev-erbalpha recruits the N-CoR/histone deacetylase 3 corepressor to regulate the circadian Bmal1 gene. *Mol Endocrinol* 19: 1452-9

67. Yin L, Wang J, Klein PS, Lazar MA. 2006. Nuclear receptor Rev-erbalpha is a critical lithium-sensitive component of the circadian clock. *Science* 311: 1002-5

68. Yin L, Wu N, Curtin JC, Qatanani M, Szwergold NR, et al. 2007. Rev-erbalpha, a heme sensor that coordinates metabolic and circadian pathways. *Science* 318: 1786-9

69. Yin L, Wu N, Lazar MA. 2010. Nuclear receptor Rev-erbalpha: a heme receptor that coordinates circadian rhythm and metabolism. *Nucl Recept Signal* 8: e001

70. Zamir I, Zhang J, Lazar MA. 1997. Stoichiometric and steric principles governing repression by nuclear hormone receptors. *Genes Dev* 11: 835-46

71. Zhang L, Guarente L. 1995. Heme binds to a short sequence that serves a regulatory function in diverse proteins. *EMBO J* 14: 313-20

72. Zhang Z, Burch PE, Cooney AJ, Lanz RB, Pereira FA, et al. 2004. Genomic analysis of the nuclear receptor family: new insights into structure, regulation, and evolution from the rat genome. *Genome Res* 14: 580-90

73. Zhao Q, Khorasanizadeh S, Miyoshi Y, Lazar MA, Rastinejad F. 1998. Structural elements of an orphan nuclear receptor-DNA complex. *Mol Cell* 1: 849-61

74. Zhou XE, Suino-Powell KM, Xu Y, Chan CW, Tanabe O, et al. 2011. The orphan nuclear receptor TR4 is a vitamin A-activated nuclear receptor. *J Biol Chem* 286: 2877-85

Chapter 5

THIOL-DISULFIDE REDOX DEPENDENCE OF HEME BINDING AND HEME LIGAND SWITCHING IN THE NUCLEAR RECEPTOR, Rev-erbβ

Results described in this chapter have been published (except the limited proteolysis experiment) and the reference is as follows: **Gupta, N., and Ragsdale, SW. 2011. Thiol-Disulfide Redox Dependence of Heme Binding and Heme Ligand Switching in the Nuclear Hormone Receptor, Rev-erbβ.** *J. Biol. Chem.* 286(6):4392-403. Epub 2010 Dec 1.

5.1 Abstract

Rev-erbβ is a heme-binding nuclear hormone receptor that represses a broad spectrum of target genes involved in regulating metabolism, the circadian cycle and proinflammatory responses. Here, we demonstrate that a thiol-disulfide redox switch controls the interaction between heme and the ligand-binding domain of Rev-erbβ. The reduced dithiol state of Rev-erbβ binds heme five-fold more tightly than the oxidized disulfide state. By means of site-directed mutagenesis and by UV-visible and EPR spectroscopy, we also show that the ferric heme of reduced (dithiol) Rev-erbβ can undergo a redox-triggered switch from imidazole/thiol ligation (via His568 and Cys384, based on a prior crystal structure) to His/ neutral residue ligation upon oxidation to the disulfide form. On the other hand, we have found that a change in the redox state of iron has no effect on heme binding to the ligand-binding domain of the protein. The low dissociation constant for the complex between Fe^{3+}- or Fe^{2+}-heme and the reduced dithiol state of the protein (K_d ~ 20 nM) is in the range of the free intracellular heme concentration. We suggest that this thiol-disulfide redox switch is one mechanism by which oxidative stress is linked to circadian and/or metabolic imbalance. Heme dissociation from Rev-erbβ derepresses the expression of target genes in response to changes in intracellular redox conditions. We propose that oxidative stress leads to oxidation of cysteine(s), thus releasing heme from Rev-erbβ and altering its transcriptional activity.

5.2 Introduction

Rev-erbs are transcriptional repressors that are present in the nucleus and bind as a monomer to the Rev responsive element (RevRE) or as a dimer to a Rev-RE direct repeat, RevDR-2 (11, 57). Rev-erbs were considered to be the orphan nuclear receptors until recently, when the *Drosophila* ortholog of human Rev-erb (E75) (45) and then Rev-erbα (43, 68) and Rev-erbβ (43) were demonstrated to bind heme at their LBDs. Heme binding to Reb-erbs promotes recruitment of nuclear corepressor (NCoR) and histone deacetylase (HDAC) (39, 43, 67). Rev-erbα recruits HDAC3, while Rev-erbβ recruits HDAC1 (10, 43, 68). In turn, the Rev-erb-NCoR-HDAC complex facilitates the repression of target genes involved in glucose, lipid and bile acid metabolism, as well as in regulating the circadian cycle and the proinflammatory response (10, 46, 67). Therefore, Rev-erbα and Rev-erbβ have been proposed to link metabolism and inflammation to the circadian clock (4, 11, 27, 44). Because heme controls the activity of Rev-erb, understanding regulation of heme binding is of special significance.

Several recent studies have focused on the relationship between heme and Rev-erbs. Heme has long been implicated to play a key role in maintaining the circadian rhythm via binding to different circadian proteins such as NPAS2 and mPer2 (2, 63). Correspondingly, heme shows a circadian pattern of expression (24). Rev-erbβ has also been recently shown to bind heme and the X-ray crystal structure reveals Cys384 and His568 as axial ligands for the ferric heme (39), similar to the Drosophila homolog, E75 (7). A ligand switch appears to occur upon reduction of the Fe^{3+}-heme to Fe^{2+} with His 568 proposed to remain as one of the Fe^{2+} ligands. Raman and MCD data indicated the presence of one or two neutral ligands in the Fe^{2+} state (34).

Here, we show that a thiol-disulfide redox switch regulates binding of heme to the ligand-binding domain (LBD) of Rev-erbβ. Heme binds more tightly to the reduced dithiol state of Rev-erbβ, forming a complex with a dissociation constant that is similar to the low nanomolar intracellular concentration of free heme. Mass spectrometric and mutational analyses reveal that formation of the disulfide bond between Cys384 and Cys374 lowers the affinity for heme by ~5-fold. UV-visible and EPR spectroscopic studies with the purified protein and with *E. coli* cells expressing the Rev-erbβ LBD indicate that oxidation of Rev-erbβ also triggers a ligand switch converting His/Cys ligated heme to another six-coordinated heme ligated via His and an unknown neutral residue. Based on EPR spectra, the neutral ligand could be another His, Met or Lys. Increasing the pH above 10 also converts the His/neutral residue ligation state of the oxidized protein to His/Cys ligation. Our results indicate that the thiol/disulfide redox switch (but not the ligand switch) regulates heme affinity. Thus, the present study demonstrates a mechanism by which the redox status of Rev-erbβ can alter heme binding and may facilitate its ability to regulate the cyclic expression of metabolic and proinflammatory genes in response to changes in intracellular redox conditions.

5.3 Experimental Procedures

5.3.1 Protein expression and purification: In all experiments, the LBD (residues 247-579) of human Rev-erbβ was used. The wild-type Rev-erbβ LBD clone was generously provided by Thomas P. Burris (Scripps – Florida). The protein was expressed in a pET-46Ek/LIC vector as an N-terminal 6X his-tagged protein. All the cysteines were kept intact in the protein unless otherwise specified. *E. coli* cells were grown without any heme supplement, unless otherwise stated. The protein was purified using a Ni-NTA column (Qiagen, Valencia, CA) and was then dialyzed against a buffer containing 20 mM Tris-HCl, 300 mM NaCl, and 10% glycerol, pH 8.0 (Buffer A). No significant amount of heme remained bound to the protein after overnight dialysis as was confirmed by the pyridine hemochrome assay (1).

5.3.2 Site-directed mutagenesis of Rev-erbβ LBD: Site-directed mutagenesis was performed as described previously (16), and all clones were sequenced at the DNA Sequencing Core Facility (University of Michigan, Ann Arbor, MI).

5.3.3 Reduction and oxidation of Rev-erbβ LBD: Throughout, we refer to the disulfide and dithiol states of the Rev-erbβ LBD when we describe the "oxidized" and "reduced" protein; the redox state of the heme, i.e., Fe^{3+} or Fe^{2+}, is stated explicitly. To generate the fully reduced or fully oxidized form of the protein, the following methods were employed. To obtain the fully reduced protein, the Rev-erbβ LBD was first incubated with a 30-fold molar excess of TCEP (tris (2-carboxyethyl) phosphine) for 30 min on ice and then TCEP was removed on a Bio-Gel P-6 (Bio-Rad Laboratories Inc., Hercules, CA) column. Therefore no TECP was present while performing experiments with the

reduced protein. The number of free thiols in the reduced Rev-erbβ LBD was quantified by a 5, 5'-dithio-bis (2-nitrobenzoic acid) (DTNB) assay as described earlier (3, 13, 66). The TCEP treatment, incubation, chromatography, and assay were carried out inside an anaerobic chamber (Vacuum Atmospheres Co., Hawthorne, CA). Then, the protein was transferred to anaerobically closed vials/cuvettes or EPR tubes, thus, maintaining the reducing environment. To fully oxidize the protein, the reduced Rev-erbβ LBD was treated with 400 μM diamide; alternatively, the air-oxidized protein was used. Complete oxidation of thiols was verified by the DTNB assay before performing experiments with the oxidized protein.

5.3.4 Heme binding analysis: Heme titrations were performed by difference spectroscopy in a double beam spectrometer using 0.2 to 0.5 μM protein, as described earlier (66), except that the buffer contained Buffer B (20 mM Tris-HCl, 300 mM NaCl, and 10% glycerol, 3% DMSO, pH 8.0). In these titrations, the blank cuvette contained buffer, the sample cuvette had both protein and buffer, and heme from a 50 μM stock solution was added to both cuvettes. Because heme solutions are prone to dimerization and oligomerization, special precautions, as described earlier (66), were taken in preparation of the stock heme solutions that were used in the titrations. Briefly, hemin (Fe^{3+}-heme) stocks were prepared fresh for each use by dissolving hemin (Sigma) in 0.1 M NaOH and 5% DMSO, filtering with a 0.2 μm syringe filter (Amicon, Beverly, MA) and diluting to 50 μM by adding an aliquot into a solution of 20 mM Tris-HCl pH 8.0, 300 mM NaCl, 5 % DMSO, and 10% glycerol. In order to prepare Fe^{2+}-heme, the Fe^{3+} in the 50 μM hemin stock solution was reduced by adding 2.5 mM sodium dithionite in the

anaerobic chamber (Vacuum Atmospheres Co., Hawthorne, CA) and was handled anaerobically in vials and cuvettes that were sealed with rubber serum stoppers.

To determine the binding parameters, the data obtained from the heme (7) titrations were plotted and fit to an equation describing a single binding site (Equation 1), which is quadratic and is used when the K_d value is similar to the concentration of protein, because it accounts for the amount of bound ligand in the solution (66). Here, ΔA refers to the absorbance difference at 416, 424 and 428 nm between the sample (containing protein and added heme) and reference (containing only protein) cuvettes; $\Delta\varepsilon$ is defined as the difference in extinction coefficient between free and bound heme; and EL is the concentration of the heme-protein complex. EL was calculated from equation 2, where E_0 refers to the total protein concentration, L_0 to the total heme concentration, and K_d to the dissociation constant. Thus, the lines shown in the heme titrations are all theoretical fits of the data (the symbols) to these equations.

$$EL = 0.5(E_0+L_0+K_d - ((E_0+L_0+K_d)^2 - 4E_0*L_0)^{1/2}) \quad \text{[Equation 1]}$$

$$\Delta A = \Delta\varepsilon * EL \quad \text{[Equation 2]}$$

Surprisingly, for Rev-erbβ LBD, the apparent K_d value seemed to depend on the protein concentration. When the titration was performed at increasing concentrations of the oxidized protein (from 0.4 to 5 μM), the K_d value increased from 0.12 to 2 μM, similar to values reported earlier (see above). Likewise, variation in concentration of reduced protein from 0.3 to 5 μM resulted in an increase in the K_d from 23 nM to 0.9 μM. It is likely that aggregation of Rev-erbβ at higher protein concentrations is responsible for this non-ideal behavior in heme-binding experiments. Correspondingly, native gel

electrophoresis experiments with the oxidized LBD show high molecular weight species that are not present with the reduced protein or with reduced protein that has been freshly treated with diamide. When the concentration of the Rev-erbβ LBD was kept below 1 μM, K_d values in the 0.20 μM range for the oxidized protein and in the 23 nM range for the reduced protein were consistently observed. Thus, the high K_d values in the 2-6 μM range are likely to be artifactual. Furthermore, free heme concentrations in the cell are below 0.1 μM (15, 31, 49) and free heme levels above 1 μM are toxic (49). Thus, we continued our experiments using protein concentrations below 1 μM.

5.3.5 EPR spectroscopy: EPR spectra were recorded at 15 K on an X-band Bruker EMX spectrometer (Bruker Biospin Corp., Billerica, MA) containing an Oxford ITC4 temperature controller, a Hewlett-Packard model 5340 automatic frequency counter, and a Bruker gaussmeter. All EPR samples were prepared in Buffer A (see above). Samples were frozen with liquid nitrogen before the experiment.

5.3.6 Whole cell EPR spectroscopy: For *in vivo* detection of the Fe^{3+}-heme complex with Rev-erb, whole cell EPR experiments were performed. *E. coli* cells expressing the Rev-erbβ LBD were grown overnight at 25 ºC after induction with 1 mM IPTG and 10 ml of culture was centrifuged at 2977 x g for 10 min. The pellet obtained was resuspended in 100 μL of Buffer B, transferred to an EPR tube, and frozen in liquid nitrogen before obtaining the EPR spectrum.

5.3.7 Alkylation of cysteines: Samples of oxidized and reduced (with 10 mM TCEP) Rev-erbβ LBD (2 mg/ml) were subjected to a two-step alkylation protocol, as has been described previously (66). Briefly, samples were first treated with iodoacetamide (IAM)

in a denaturing buffer and then with 4-vinyl pyridine (VP) after reduction with 10 mM TCEP.

5.3.8 Mass-spectrometric analysis: Alkylated Rev-erbβ LBD samples were digested with trypsin and analyzed by mass-spectrometry in the Protein Structure Facility at The University of Michigan, Ann Arbor. LC-MS/MS was performed on a NanoAqcuity/Qtof Premier Instrument (Waters Inc., Milford, MA). See supplementary method for detail.

5.3.9 Quantification of redox states of the cysteines in Rev-erbβ LBD using the ICAT technique: OxICAT, a novel mass spectrometric method that couples thiol trapping with the ICAT technique to quantify oxidative thiol modifications, was performed. For trapping the redox states of purified Rev-erbβ LBD, 100 μg of oxidized Rev-erbβ LBD was applied to a two-step alkylation procedure with light/heavy ICAT reagents as described previously (30, 62). The alkylated protein was then digested with trypsin, and the cysteine-containing peptides, which are linked to biotin, were enriched on a cation-exchange cartridge followed by an avidin affinity cartridge (Applied Biosystems, Foster City, CA). The biotin tag, which was conjugated to the cysteine-containing peptides, was removed afterwards and then samples were analyzed by nano-liquid chromatography/tandem mass spectrometry at the Michigan Proteome Consortium to quantify the amounts of reduced (dithiol) protein containing the light ICAT and oxidized (disulfide) protein containing the heavy ICAT adduct. For determining the redox state of cysteines in Rev-erbβ LBD, different peptides were analyzed containing the cysteine(s) of interest. As expected, the high-resolution mass spectra consist of envelopes of multiple peaks reflecting the presence of 0.018% 2H, 1.11% 13C, 0.45% 15N, and

0.20% 18O in each peptide. The m/z ratios for the oxidized form of these peptides are 9 (for peptides containing single cysteine) and 18 (for the peptide with two cysteines) mass units larger than those for the reduced protein (17).

5.3.10 Protein preparation for spectroscopic analysis at different pHs: The protein was dialyzed in AMT (50 mM acetic acid, 50 mM MES and 100 mM triethanolamine, pH 8.0) buffer (12). Then heme-protein complex was prepared and UV-visible spectroscopy was performed. In these titrations, the blank cuvette contained buffer, the sample cuvette had both heme-protein complex and buffer, and NaOH from a 10 N stock solution was added to both cuvettes to obtain the spectra at different pHs. The EPR samples were prepared by adding 10 N NaOH to heme-protein complex in AMT buffer and frozen in liquid nitrogen before recording the spectra at 15K.

5.3.11 Limited proteolysis: Limited proteolysis of Rev-erbβ LBD was carried out by trypsin digestion. 20 µg of oxidized or reduced (prepared as described section 5.3.3) Rev-erbβ LBD in AMT buffer was modified by 2.2 mM iodoacetamide (Sigma) in 10 µl reaction in eppendorf tubes. Samples were incubated with iodoacetamide for 30 min in the dark. At the same time, trypsin was prepared in 50 mM acetic acid according to the manufacturer's direction (Promega). Then, the desired amount of trypsin was added to each tube and tubes were incubated at RT for 5 minutes. The reaction was quenched by adding 5X non-reducing SDS-PAGE loading buffer and freezing immediately. A 12% SDS-PAGE was run later to analyze the differences in the digestion patterns of the oxidized and reduced protein.

5.4 Results

5.4.1 Thiol-disulfide redox regulation of heme binding to Rev-erbβ

Heme binding studies were performed with the oxidized and reduced forms (assessed by the DTNB assay as described in the Experimental Procedures section) of the purified LBD of Rev-erbβ and were monitored by difference UV-visible spectroscopy. All heme titrations were performed in Buffer A (see experimental procedures for details), unless stated otherwise.

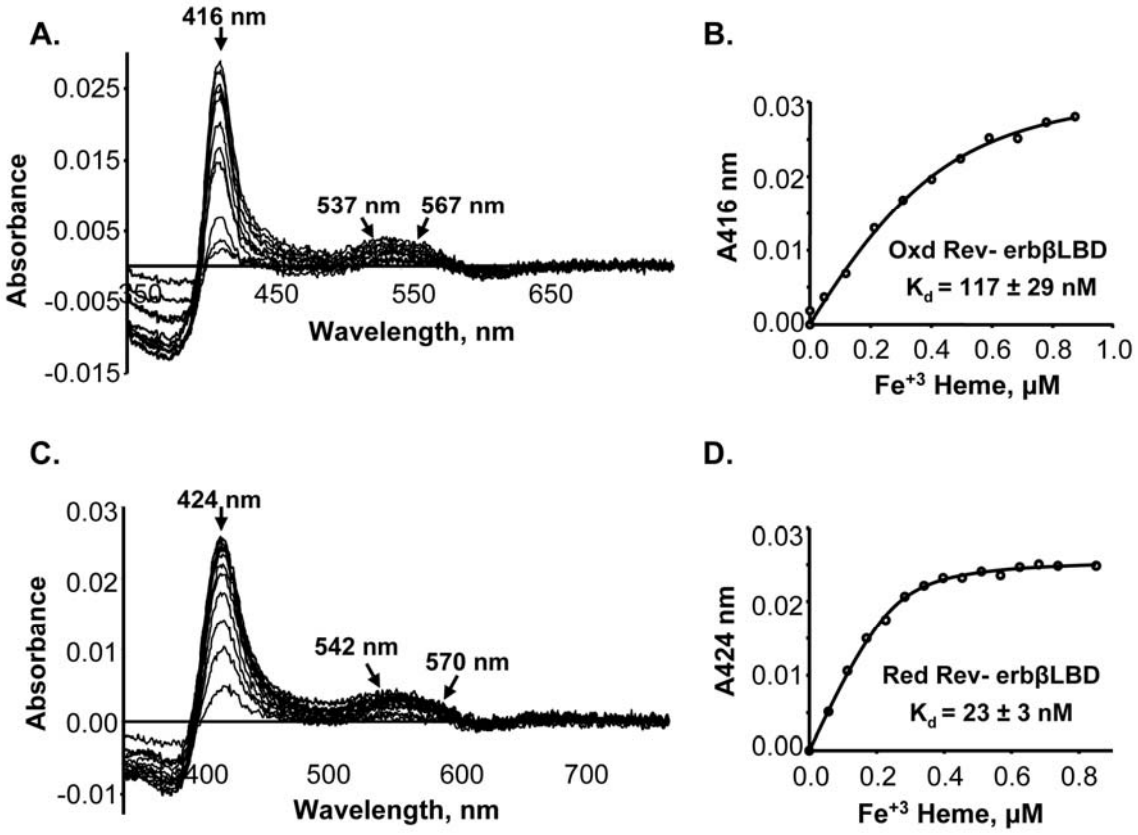

Figure 5.1: Redox-dependent binding of Fe^{3+}-heme to Rev-erbβ LBD: Difference absorption spectra and titration curves for oxidized (0.4 μM) (A and B, respectively) and reduced (0.3 μM) (C and D, respectively) Rev-erbβ LBD. Titration of reduced Rev-erbβ LBD with Fe^{3+}-heme was performed anaerobically to avoid thioloxidation during the experiment.

When the oxidized Rev-erbβ LBD was titrated with Fe^{3+}-heme, the difference spectra exhibited absorbance changes in the Soret region at 416 nm (Figure 5.1A) and in the alpha (567 nm) and beta (537 nm) bands. Titration of reduced Rev-erbβ LBD (after TCEP removal) with Fe^{3+}-heme resulted in shifts in the Soret peak to 424 nm, and the alpha and beta peaks to 570 nm and 542 nm (Figure 5.1C), which is characteristic of His/Cys axial ligands (7, 19).

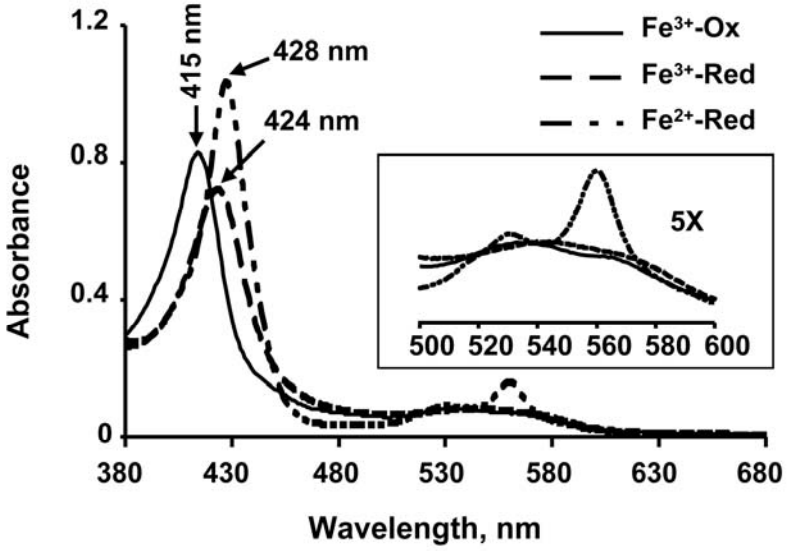

Figure 5.2: UV-visible spectra of the Rev-erbβ LBD-heme complexes in different redox-states. The spectra shown are of the complexes between oxidized LBD and Fe^{3+}-heme (Fe^{3+}-Ox), reduced LBD and Fe^{3+}-heme (Fe^{3+}-Red), and reduced LBD and Fe^{2+}-heme (Fe^{2+}-Red). The spectra were recorded in Buffer B with 10 μM protein and 9 μM heme. Inset: Five-fold vertical expansion of the spectral regions between 500-600 nm to better exhibit the alpha and beta peaks.

The UV-visible spectra of the oxidized and reduced protein-heme complexes are shown in figure 5.2, and show similar peaks shifts as observed in the difference spectra (Figure 5.1). The oxidized protein with bound Fe^{3+}-heme has its Soret band at 415 nm, while two long-wavelength peaks are at 566 and 534 nm. However, the TCEP-reduced protein

containing bound Fe^{3+}-heme exhibits a Soret peak at 424 nm and alpha and beta peaks at 571 and 541 nm, respectively. These spectral changes between the oxidized and reduced protein in the Fe^{3+}-heme state indicate that a ligand switch is associated with oxidation/reduction of the Rev-erbβ LBD (this conclusion is verified by the mutagenesis and EPR studies described below). By plotting the change in absorbance at 416 nm (for the oxidized LBD) or at 424 nm (for the reduced protein) versus the concentration of added Fe^{3+}-heme, typical hyperbolic profiles were obtained, indicating saturation binding. When the data for the oxidized protein were fit to Equation 1, the K_d value was 117 nM (Figure 5.1.B), significantly lower than the values of ~2 μM (43) or ~6 μM (39) reported earlier. Furthermore, the reduced protein binds Fe^{3+}-heme even more tightly, with a K_d value of 23 nM (Figure 5.1.D). Because the crystal structure identified His568 and Cys384 as heme ligands, we performed heme titrations of the H568R, H568A and C384A variants. The heme binding affinities of these variants, both in oxidized and reduced states, were significantly lower than those of the wild-type protein (Table 5.3). The K_d for the complex between heme and the H468R variant is about 20-fold higher than that for the H568A mutant, suggesting that this substitution may have an additional effect on the active site other than simply removal of the heme ligand.

Because the heme binding assays demonstrated that oxidation of the protein weakens affinity for heme, we used LC-MS/MS analyses to determine if Cys384 forms a disulfide bond and (if so) which residue it is linked to, as well as to evaluate the redox-status of all seven cysteines present in the LBD. Initially, we performed the LC-MS/MS analysis of the trypsin-digested oxidized protein and searched for the peptides carrying disulfide bonds. The result of this analysis is described in Table 5.1, which compares the predicted

molecular mass of each peptide (based on sequence) to the experimentally determined mass. The intensity values given in the table do not measure the absolute quantity of a peptide, but quantify the relative abundance under similar LC-MS/MS conditions. Intact disulfide bonds were found between Cys337-Cys343, Cys374-Cys384, and Cys355-Cys374 in their respective peptides. Two other disulfides, Cys301-Cys311 and Cys355-Cys384 were also detected but with very low ionization intensity. The disulfide bonds between Cys301-Cys311 and Cys337-Cys343 were present in single peptides. Because there are trypsin cleavage sites between the interlinked cysteine residues, the other three disulfide bonds connected two peptides. Nevertheless, all the detected disulfides appear to be intra-molecular, because no dimeric form of the protein was observed in non-reducing SDS-PAGE analyses of the oxidized protein.

Peptide	Sequence	Cys involved in disulfide	Oxidized		
			M_r (cal)[a]	M_r (obs)[b]	Intensity (cps)[c]
290-323**	NMEQYNLNHDH**C**GNGLSSHFP**C**SESQQHLNGQFK	301-311	3897.64	3897.69	6.24e4
326-353	NIMHYPNGHAI**C**IANGH**C**MNFSNAYTQR	337-343	3174.38	3174.36	6.13e4
354-369, 370-379	V**C**DRVPIDGFSQNENK NSYL**C**NTGGR	355-374	2901.31	2901.28	1.82e4
370-379, 380-388	NSYL**C**NTGGR MHLV**C**PMSK	374-384	2125.95	2125.90	1.90e4
354-369, 380-388**	V**C**DRVPIDGFSQNENK MHLV**C**PMSK	355-384	2862.33	2862.31	1.19e4

Table 5.1: Disulfide bonds analysis after mass-spectrometry of unmodified air-oxidized Rev-erbβ LBD. [a] relative molecular mass based on the matched peptide sequence; [b], observed m/z factored by z; [c] counts per second; **These peptides had very low ionization intensity.

LC-MS/MS was also performed on tryptic-digested products of the oxidized and reduced Rev-erbβ LBD that had been subjected to the two-step alkylation with iodoacetamide and vinyl pyridine, as previously described (41). This analysis further confirmed the involvement of all the above mentioned cysteines in disulfide bonds, in the oxidized state of the protein (Table 5.2). In the reduced protein, all Cys residues were modified by IAM, confirming that all Cys residues are in the thiol(ate) state in the reduced protein. In the oxidized protein, Cys301 and Cys311 from peptide 290-323 and Cys337 and Cys343 from peptide 326-353 showed only 4-VP modifications, indicating that these cysteines were involved in disulfide bond in the oxidized protein. However, peptides containing the other three cysteine residues (Cys355, Cys374 and, Cys384) were detected with both IAM and 4-VP modifications in different fractions. This might result from incomplete oxidation of the cysteines. Regardless, the peptide containing 4-VP-modified Cys 384 (peptide 380-388) was almost 50 times more abundant than that containing IAM modification. Moreover, the peptides containing Cys374-Cys384 was 1.6-fold more abundant than the peptides containing Cys355-Cys384. Thus, based on the above two mass-spectrometric analyses, we hypothesize that Cys384 may form a disulfide with either Cys374 or Cys355.

To test the above hypothesis about Cys384, we used the oxICAT method to quantify the redox state of cysteines in the oxidized protein. As described under Experimental Procedures, we treated Rev-erbβ LBD with the light ICAT reagent, reduced all existing oxidative thiol modifications and alkylated all newly reduced thiols with the heavy ICAT. Thus, a peptide containing a free Cys thiol(ate) will have an **m/z** value that is 9 units smaller than one containing a Cys that is engaged in a disulfide bond (17). Mass spectral

analysis of the affinity-purified tryptic peptide harboring Cys384 (MHLVC^{384}PMSK) reveals peaks at 1288.69 and 1297.65 (+9), with the major peak at 1297.65, resulting from labeling with one heavy ICAT molecule (Figure 5.3). Similarly, peptides containing Cys374 (NSYLC^{374}NTGGR) and Cys355 (VC^{355}DRVPIDGFSQNENK) showed major peaks at 1320.64 (+9) and 2057.02 (+9) from the addition of one heavy ICAT molecule (Figure 5.3). Thus, the majority of the oxidized protein contains oxidized forms of Cys 384 (89%), Cys374 (87%) and Cys355 (92%). In fact, all of the LBD peptides containing Cys residues showed major peaks with an increase in their mass by 9 or 18 Da, indicating that all cysteines in the oxidized state of the LBD are in the oxidized form (not shown).

Peptide	Sequence	Oxidized					Reduced				
		No.[a]		M_r (cal)[b]	M_r (obs)[c]	Intensity (cps)[d]	No.[a]		M_r (cal)[b]	M_r (obs)[c]	Intensity (cps)[d]
		IAM	4VP				IAM	4VP			
290-323	NMEQYNLNHDHCGNGLSSHFPCSESQQHLNGQFK	0	2	4322.90	4322.93	1.75e4	ND	ND	ND	ND	ND
326-353	NIMHYPNGHAICIANGHCMNFSNAYTQR	0	2	3386.55	3386.51	8.54e4	2	0	3290.44	3290.44	2.09e4
354-369	VCDRVPIDGFSQNENK	0	1	1924.91	1924.91	5.15e4	1	0	1876.86	1876.86	1.55e4
		1	0	1876.87	1876.87	4.10e3					
370-379	NSYLCNTGGR	0	1	1188.53	1188.54	4.69e2	1	0	1140.50	1140.50	4.07e2
		1	0	1140.50	1140.50	6.46e2					
380-388	MHLVCPMSK	0	1	1149.55	1149.51	1.14e5	1	0	1101.51	1101.50	8.84e5
		1	0	1101.51	1101.51	2.27e3					

Table 5.2: LC-MS/MS results of oxidized and reduced Rev-erbβ LBD after two-step alkylation. [a] number of cysteine residues modified; [b] relative molecular mass based on the matched peptide sequence; [c]observed m/z factored by z; [d] cps, counts per second; ND, peptide not detected; IAM, idoacetamide; 4VP, 4-vinylpyridine.

To determine which disulfides are involved in regulating heme binding, we generated C374S and C355S/C374S variants. Interestingly, mutation of Cys374 to Ser was sufficient for the loss of redox-dependent heme binding (Table 5.3). Both C374S and

C355S/C374S variants exhibited similar affinity for heme in both oxidized and reduced states. The C374S variant has binding constants of 12 nM and 13 nM for the oxidized and reduced states, respectively (Figure 5.4 top panel), while the C355S/C374S variant has binding constants of 13 nM and 24 nM for the oxidized and reduced proteins, respectively (Figure 5.4, bottom panels).

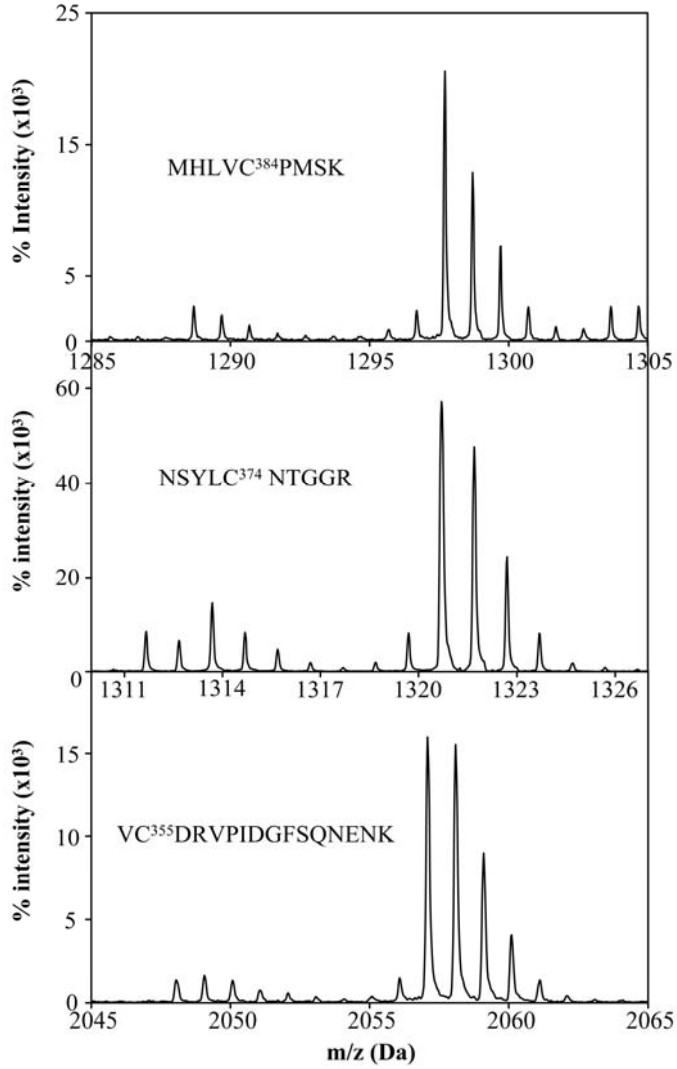

Figure 5.3: Oxidation of cysteines in oxidized Rev-erbβ LBD: OxICAT analysis of the redox state of purified and oxidized Rev-erbβ LBD reveals incorporation of heavy ICAT (^{13}C) in Cys384 (top panel), Cys374 (middle panel) and Cys355 (lower panel) in their respective peptides, which reflects that these cysteines are oxidized upon oxidation of the protein.

	Ox protein-Fe^{3+}heme				Red protein-Fe^{3+}heme				Red protein-Fe^{2+}heme			
	Soret	α	β	K_d (nM)	Soret	α	β	K_d (nM)	Soret	α	β	K_d (nM)
WT	416	567	537	117 ± 29	424	570	542	23 ± 3	428	560	530	16 ± 4
C374S	416	567	537	12 ± 4	424	570	542	13 ± 6	-	-	-	-
C355S/C374S	416	567	537	17 ± 5	424	570	542	24 ± 4	-	-	-	-
C384A	415	567	537	1010 ± 110	420	broad peak at 550		46 ± 14	428	560	530	209 ± 30
H568R	416	broad peak at 550		13090 ± 780	424	broad peak at 550		175 ± 44	431	563	536	1520 ± 490
H568A	416	broad peak at 550		713 ± 135	420	broad peak at 550		2291 ± 580	427	560	530	199 ± 54

Table 5.3: Redox-dependent heme binding properties of the wild-type and mutants.* Peaks from optical absorption spectra are given in nm. ** Ox = oxidized; Red = reduced

Altogether, mass-spectrometric and heme binding analyses demonstrate that disulfide bond formation between Cys384 and Cys374 is responsible for lower heme affinity of the oxidized Rev-erbβ LBD as compared to the reduced Rev-erbβ LBD.

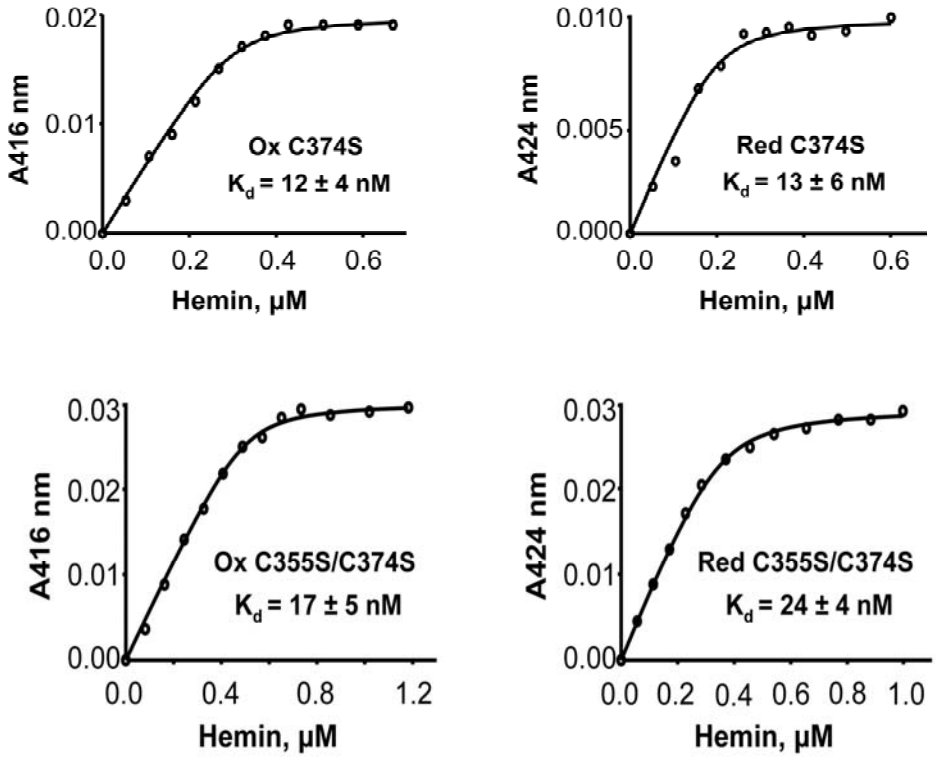

Figure 5.4: Loss of redox-dependent binding of Fe^{3+}-heme to the C374S variant: Fe^{3+}-heme titration curves of the oxidized (ox) and the reduced (red) C374S (top panel) and C355S/C374S (lower panel) variants. The titrations were performed in Buffer B (see Experimental Procedures). Titration of reduced Rev-erbβ LBD variant with Fe^{3+}-heme was performed anaerobically to avoid thiol-oxidation during the experiment.

5.4.2 A ligand switch occurs upon changing the thiol redox state

To further examine the nature of the ligand switch in the Rev-erbβ LBD predicted by the UV-visible absorption measurements, X-band EPR experiments were performed on the Fe^{3+}-heme-bound oxidized and reduced proteins (Figure 5.5). The EPR spectrum of the anaerobically prepared complex of the reduced protein and Fe^{3+}- heme manifests a rhombic spectrum with *g*-values of 2.49, 2.27, and 1.86. These *g* values are consistent with His and Cys axial ligation to a low-spin six-coordinate heme (Figure 5.5.A) (34). On the other hand, the predominant EPR spectrum of the complex between the oxidized protein and heme has *g* values (2.96, 2.27, and 1.52) that are characteristic of a low-spin six-coordinate Fe^{3+}-heme that is ligated by His and a neutral residue. The minor component (~30 %) consists of His/Cys ligation (*g* values of 2.49, 2.27, and 1.87) (Figure 5.5.A). The *g* values (2.96, 2.27, and 1.52) of the major species are fairly close to those assigned to a bis-His ligated heme (58); however, because the EPR spectra of His/Lys- or His/Met-coordinated heme are similar, the possibility of His/Met or His/Lys ligation can not be excluded (5). When Cys384 was mutated to Ala, as expected, the EPR spectrum of the oxidized C384A-heme complex exhibited pure His/neutral residue ligation (*g* values at 2.96, 2.27, 1.52), with no detectible $g = 2.48$ peak. On the other hand, EPR experiments of the reduced C384A-heme complex (Figure 5.5.C) did reveal low amounts of a low-spin EPR spectrum characteristic of His/Cys ligation (which might be provided from another unknown Cys) along with a $g = 2.0$ species of unknown origin.

Assuming that the EPR spectrum with *g* values at 2.96, 2.27, and 1.52 originates from bis/His ligation, we assessed whether His381, which is near Cys384, might be the ligand that replaces Cys384 in this ligand switch. However, as shown in Figure 5.6, the EPR

spectrum of the H381A variant is nearly identical to that of the wild-type protein, with no diminution in the $g = 2.96$ peak. To ensure that this His/neutral residue ligation is not due to an artifact resulting from the binding of one of the His residues in the His-tag, we removed this tag by proteolytic cleavage with enterokinase and performed EPR experiments on the oxidized protein. The EPR spectrum of the oxidized tagless variant is identical to that of the wild-type protein (Figure 5.6), demonstrating that the His-tag does not affect the ligation state of the heme.

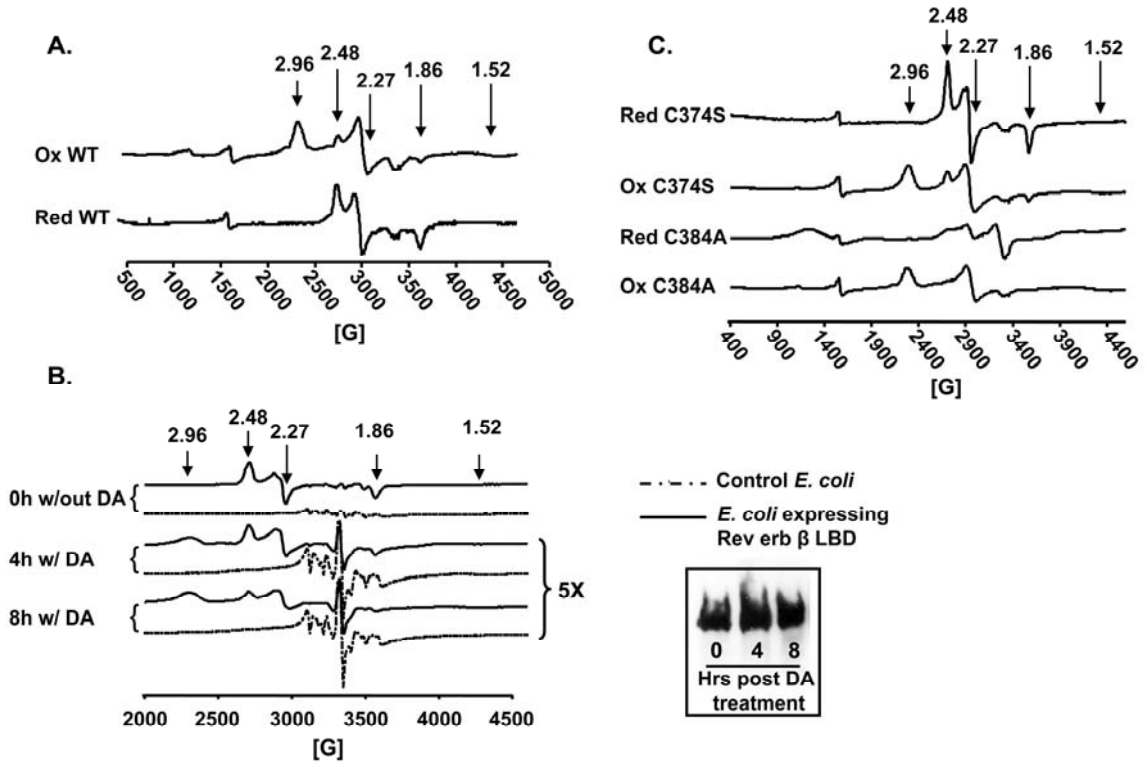

Figure 5.5: Ligand switching associated with a change in redox-state of Rev-erbβ LBD: **A**. EPR spectroscopic analysis of heme complexes with the reduced and oxidized proteins (complexes were prepared at a ratio of 1:1.5 of Fe^{3+}-heme: LBD). **B.** EPR analysis of *E. coli* over-expressing Rev-erbβ LBD (without or with oxidation by 30 mM diamide (DA) for 4 and 8 hours). **Inset**: Western blot analysis of the EPR samples from the diamide treatment at 0, 4 and 8 hrs using anti-penta His antibody. **C**. EPR analysis of C384A-heme and C374S-heme complexes as in panel A. Note: The *in vitro* experiments were performed in Buffer B. The minor peaks at g-values of 2.0 and 1.99 are from the buffer.

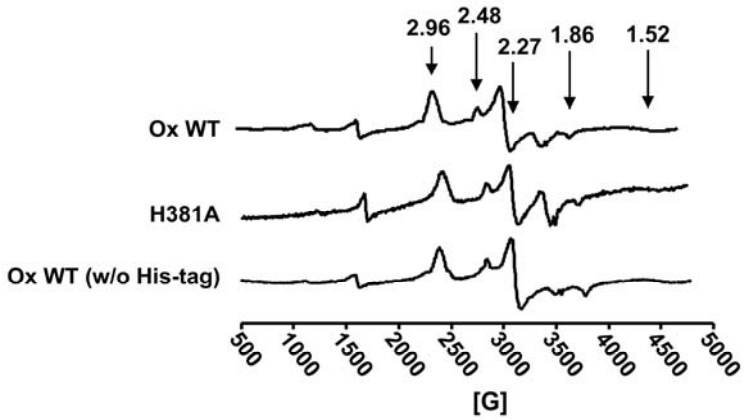

Figure 5.6: EPR analysis of oxidized Rev-erbβ LBDs: EPR spectra of the oxidized wild-type protein, the oxidized H381A variant and the tag less oxidized wild-type protein are nearly identical.

To further examine whether the LBD binds heme *in vivo* and whether the Cys-to-unknown neutral residue ligand switch occurs in growing cells, we performed whole-cell EPR analyses on *E. coli* cells overexpressing the Rev-erbβ LBD. One might criticize the use of a bacterial system for these studies; however, use of the oxICAT methodology revealed that the redox state of human heme oxygenase-2 under normoxic growth conditions, as well as the response to oxidative and reductive conditions, was similar whether the protein was expressed in *E. coli or* in the human embryonic kidney cell line (HEK293) (64). Even though the *E. coli* cells were grown without a heme precursor, the cells were amber colored (Figure 5.7.C), indicating that overexpression of the human Rev-erbβ LBD induces heightened production of heme in *E. coli*. The whole-cell EPR spectrum exhibited a single rhombic species with identical *g*-values (g = 2.48, 2.27, 1.86) to those obtained for the purified reduced LBD–Fe^{3+}-heme complex (Figure 5.5.B, 0 h), confirming that heme binds to the LBD through His/Cys ligation. This spectrum is absent when cells lacking the overexpression construct are similarly treated. When cells were treated with 30 mM diamide, a partial switch from His/Cys to His/neutral residue ligation

was observed. Initially, only the set of *g* values (2.48, 2.27, 1.86) characteristic of His/Cys ligation was detected; then, after 30 min, the spectrum of a His/neutral residue-ligated species appeared (*g* = 2.96, 2.27, 1.52). By 8 hrs, there was an equal mixture of the EPR spectra from the His/Cys- and His/neutral residue-ligated species (Figure 5.5.B). The amount of Rev-erbβ LBD was unchanged throughout the experiment (Figure 5.5.B inset). Thus, treatment of the cells with oxidants caused a Cys-to-neutral residue ligand switch, as observed for the purified protein. For control experiments, when either the H568R, H568A or C384A variants were overexpressed, the cells did not turn red (Figure 5.7.C) and the whole-cell EPR spectra revealed a pronounced *g*=4.3 spectrum, without detectible amounts of low-spin Fe^{3+}- heme (Figure 5.7.A), even when the growth medium was supplemented with δ-ALA (data not shown). Control *E. coli* cells, not expressing Rev-erbβ, also had the same peak (*g*=4.3), although with lower intensity. The *g*=4.3 EPR spectrum, which is characteristic of "extraneous" iron, probably derives from other iron proteins in the cell. Expression levels of the variants are similar to those of the wild-type Rev-erbβ LBD (Figure 5.7.B).

Because the mass-spectrometric results (above) demonstrated a disulfide linkage between Cys384 and Cys374, we hypothesized that mutating Cys374 would enable free Cys384 to ligate heme in the oxidized state of the protein. Thus, EPR experiments of the heme-bound C374S variant were performed. To our surprise, the variant showed an EPR spectrum that was similar to that of the wild-type protein, both in the reduced and oxidized states, although, the oxidized C374S variant exhibits slightly more Cys/His ligation (43%) than the corresponding wild-type protein (29%) (Figure 5.5.C). The EPR spectra of the C355S/C374S variant are similar to those of C374S (data not shown).

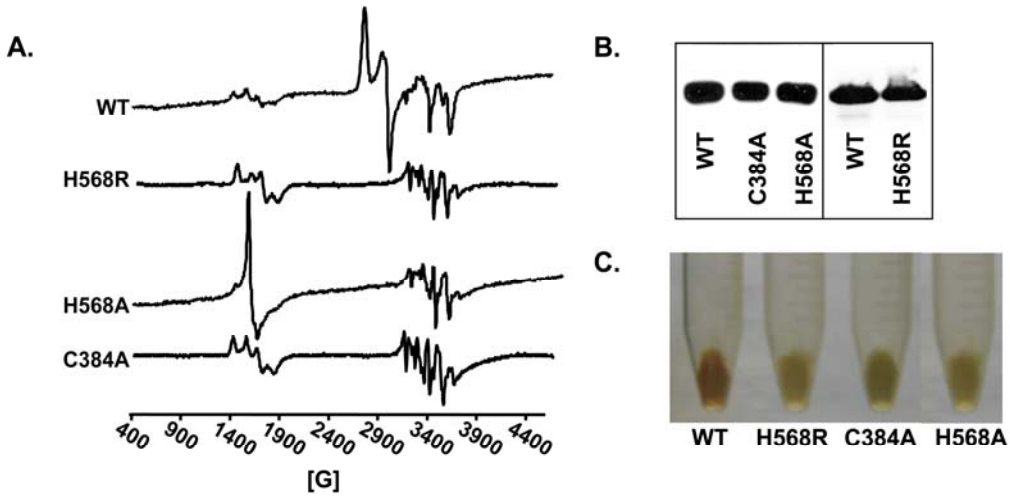

Figure 5.7: Whole cell EPR studies of heme binding to the His568R and C384A variants: Whole cell EPR analysis of *E. coli* cells overexpressing WT Rev-erbβ LBD, H568R, H568A and C384A variants, without any heme precursor (A) were performed as described in Experimental procedures. Expression levels of wild-type Rev-erbβ LBD and variants were similar, based on western blot analysis (B). The color of the pellet fraction from *E. coli* cells overexpressing Rev-erbβ LBD was deep red, while mutation of C384 to Ala produced a dark green pellet and mutation of H568 to Arg/Ala resulted in a cell paste that appears similar in color to that of *E. coli* cells lacking the expression plasmid (C).

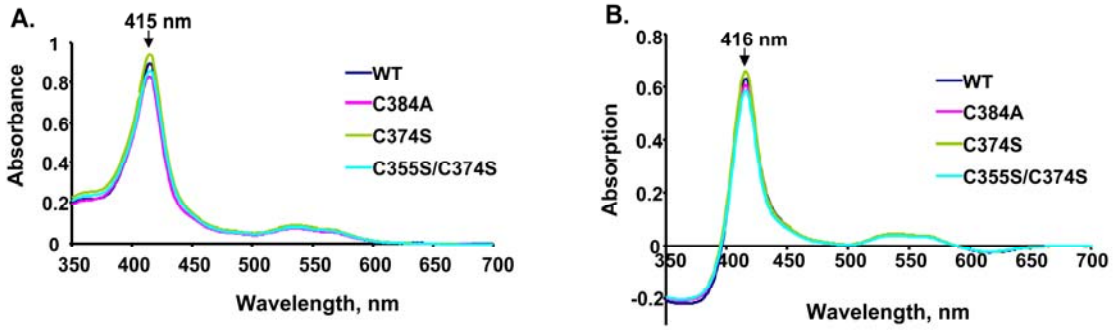

Figure 5.8: Absorption spectra of the oxidized Rev-erbβ LBD and variants: The absorption (A) and difference (B) absorption spectra of the oxidized Rev-erbβ LBD, C384A, C374S, and C355S/C374S variants. The spectral measurements were taken in Buffer B with 10 μM protein and 9 μM heme.

Overall, mutation of Cys374 resulted in the loss of the redox-dependence of heme binding, but not redox-dependent ligand switching. This indicates that oxidation of Cys384 (resulting in a disulfide bond with Cys374) is not solely responsible for the

ligand switch. Perhaps, oxidation of Cys384 induces a conformational shift that moves Cys384 away from the heme. This hypothesis is supported by the electronic absorption spectra (Figure 5.8.) of the oxidized wild-type, C384A, C374S and C355S/C374S proteins. Similar absorption spectra of wild-type and cysteine variants indicate similar heme ligation states (i.e., His/neutral residue) in the oxidized forms of these variants and the wild-type protein (Figure 5.8).

However, unlike the wild-type protein, the oxidized and reduced states of the C374S variant bind heme with similar affinities. Therefore, it is the redox switch (oxidation of Cys384), not the ligand switch (replacement of Cys384 with other neutral residue) that alters the heme binding affinity. It is plausible that a conformational change in the LBD, resulting from oxidation of Cys384, might block the heme binding site, thus, decreasing the affinity of the oxidized protein for heme. On the other hand, a conformational change induced by formation of the disulfide in the Rev-erbβ LBD might cause the ligand switching in the protein. The conformational change hypothesis was tested by limited proteolysis of the oxidized and reduced Rev-erbβ LBDs (Figure 5.9). The oxidized and reduced Rev-erbβ LBDs have markedly different digestion patterns indicating that they are in different conformational states. Initially with a lower amount of trypsin (reaction 2), the reduced state appears to undergo cleavage to form 4 major cleavage products along with some minor products. Subsequently, with the use of higher amount of typsin (reactions 3 to 5), these bands are ultimately degraded to two main cleavage products around 25 and 20 kDa. On the other hand, the oxidized protein shows only one major cleavage products with some minor products at the lowest trypsin (reaction 2) concentration unlike the reduced protein. The cleavage products between 25 to 37 kDa

regions are more stable in the oxidized protein as compared to the reduced protein at various trypsin concentrations used (reactions 1 to 5). When a very high concentration of trypsin was used (reaction 5), all cleavage products in the oxidized protein also accumulated in two main cleavage products at 25 and 20 kDa similar to the reduced protein with a minor cleavage product below the band at 25 kDa. Theses data show that the oxidized state of the protein is much more resistant to degradation as compared to the reduced protein. Non-overlapping digestion patterns of the oxidized and reduced proteins indicate dissimilar accessibility of trypsin to these two forms and thus predict their different conformation, at least, around trypsin digestion sites.

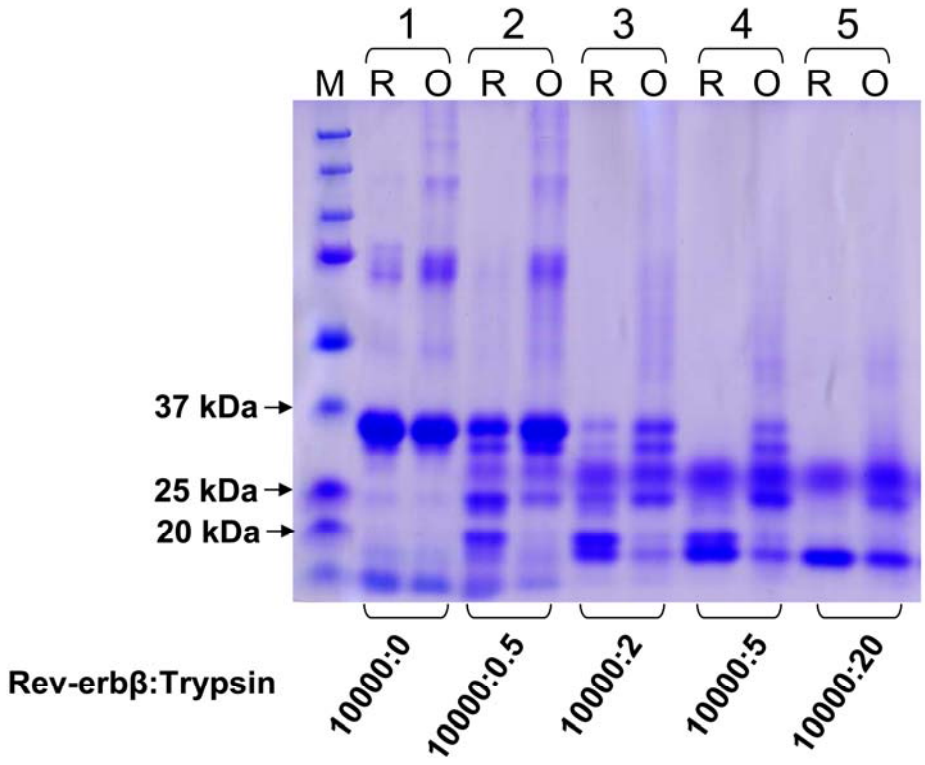

Figure 5.9: Limited proteolysis of oxidized and reduced Rev-erbβ LBD: SDS-PAGE analysis of products of trypsin mediated limited proteolysis of the reduced (R) and oxidized (O) Rev-erbβ LBDs. Conditions for limited proteolysis are specified in experimental procedures. Different ratios between the protein and trypsin used are given below the gel; M = molecular weight marker.

5.4.3 pH dependent ligand switch in the oxidized Rev-erbβ LBD

Apart from the redox-dependent ligand switch, the oxidized protein shows a pH-dependent switch from His/neutral residue to His/Cys ligation. At increasing pH values, the Soret peak of the wild-type oxidized protein showed a red-shift from 416 nm to 424 nm along with a significant decrease in intensity from pH 8 to pH 10 (Figure 5.10.A) and the color of the complex changed from dark red to green over the pH range from pH 8 to pH 10. The titrations could not be performed at lower pH values, because the protein precipitated below pH 7. Similar observations were made for the C374S variant (Figure 5.10.C). Similarly, EPR spectroscopic results indicate a ligand switch from His/neutral residue to His/Cys ligation above pH 10 for wild-type LBD (Figure 5.10.B) and for the C374S (Figure 5.10.D) variant. It is plausible that a base-induced cleavage of the Cys374-Cys384 disulfide bond occurs at pH 10, which releases Cys384 for ligation to the heme.

As the pH is increased, a minor amount of high-spin heme (g~6.2) is observed, as seen earlier with cytochrome b561 (58). In addition, a small amount of a low-spin species with a g value at 2.68 appears which could result from His /water ligation (66). Furthermore, a peak at g=4.3 is observed which is likely to reflect heme decomposition. Nevertheless, the physiological relevance of this pH-dependent ligand switching is not clear at this point.

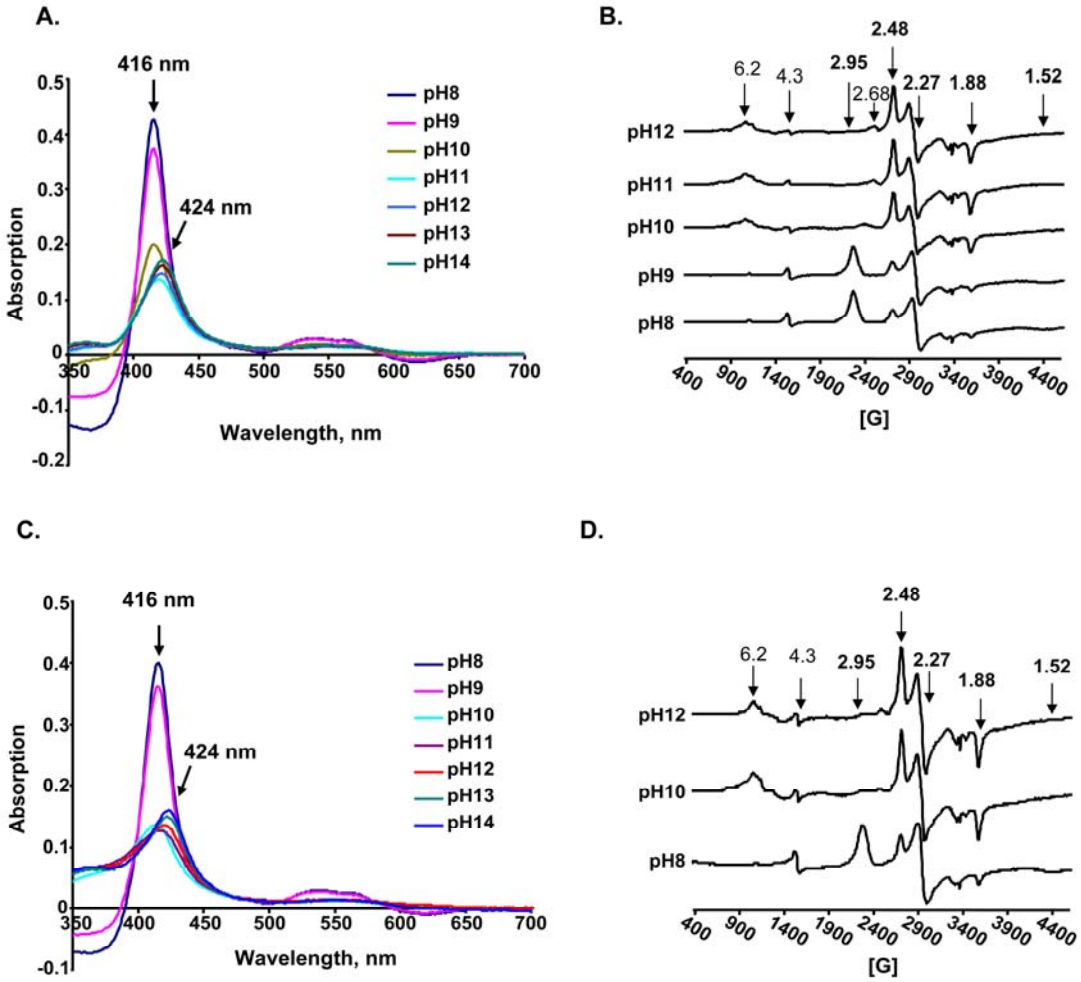

Figure 5.10: pH dependent ligand switching of oxidized Rev-erbβ LBD: Titration of the oxidized wild-type Rev-erbβ LBD (**A)** and the C374S variant (C) with NaOH shifts the Soret peak from 416 nm to 424 nm, indicating a ligand switch from His/neutral residue to His/Cys **B.** EPR analysis of the oxidized wild-type protein-heme (B) and the oxidized C374S mutant-heme (D) complexes also show ligand switching from His/neutral residue (2.96, 2.27 and 1.52) to His/Cys (2.48, 2.27 and 1.88) upon increasing the pH from 8 to 10. Note: AMT buffer was used in both the above analyses in order to provide higher stability to the protein at pH values above 8 (see experimental procedure).

5.4.4 No effect of change in iron redox state on heme binding affinity

Pardee et al. (39) recently showed that Rev-erbβ is capable of binding both Fe^{3+}- and Fe^{2+}-heme. We performed Fe^{2+}-heme titrations to determine if the reduced protein prefers Fe^{3+}- versus Fe^{2+}-heme. All titrations with Fe^{2+}-heme were performed in anaerobically

closed vials in the presence of 2.5 mM sodium dithionite to prevent oxidation of the Fe^{2+}-heme to Fe^{3+}. The absorption spectrum of Fe^{2+}-heme–reduced Rev-erbβ LBD complex is shown in figure 5.2. The spectrum has a Soret band at 428 nm and alpha and beta bands at 560 and 530 nm, respectively, indicating that the Cys ligand is released from the Fe^{2+}-heme (22, 26). Similarly, the difference spectrum of the complex between the reduced Rev-erbβ LBD and Fe^{2+}-heme exhibited a Soret peak at 428 nm along with the alpha (560 nm) and beta (530 nm) bands (Figure 5.11.A). Titration of the reduced Rev-erbβ LBD with Fe^{2+}-heme resulted in a sharply saturating binding isotherm (Figure 5.11.B), which, when fit to the quadratic equation (Eq 1) gave a K_d value in the low nM range (K_d = 15.8 ± 4.1 nM). This K_d value is similar to that obtained in the titration of the reduced form of the Rev-erbβ LBD with Fe^{3+}-heme (above). Thus, the reduced protein exhibits similar high affinity for Fe^{2+}- and Fe^{3+}-heme. Because dithionite, which is used to reduce the heme, also reduces the disulfide groups in the LBD, it is not possible to determine the K_d of the oxidized protein for Fe^{2+}-heme.

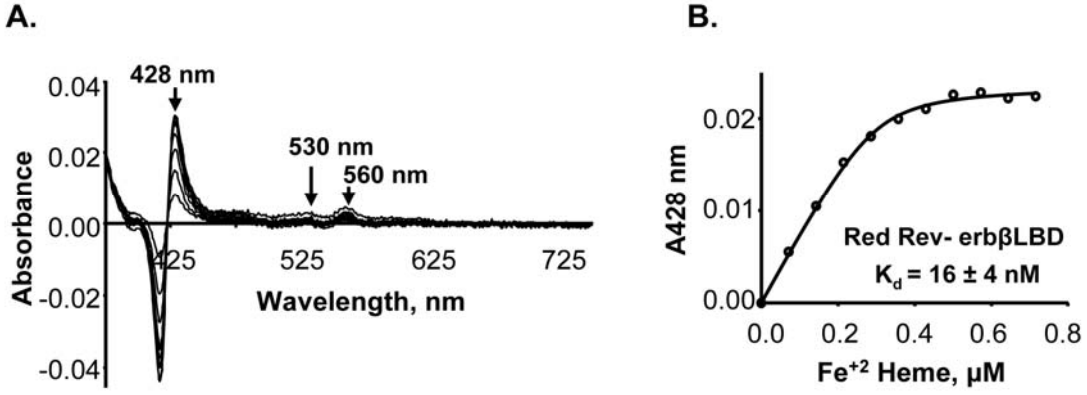

Figure 5.11: Similar affinity of reduced Rev-erbβ LBD towards Fe^{3+}- and Fe^{2+}-heme: The Rev-erbβ LBD (0.3 µM) was anaerobically titrated with Fe^{2+}-heme in Buffer B, in the presence of 2.5 mM dithionite. The Soret peak for Fe^{2+}-heme is at 428 nm and exhibits sharp alpha and beta peaks at 560 and 530 nm, respectively (A). The K_d values of the complexes of Fe^{3+}- and Fe^{2+}-heme with reduced Rev-erbβ LBD are 23 ± 2.7 nM (Figure 5.1.D) and 15.8 ± 4.1 nM (B), respectively.

Magnetic circular dichroism and resonance Raman spectroscopic experiments have revealed that the Fe^{2+}-heme bound to Rev-erbβ can exist in a five-coordinate environment with a single neutral ligand as well as a six-coordinate state with two neutral ligands (34). His568 has been postulated to remain as an axial ligand in the Fe^{2+}-state. To further examine the ligand environment of Fe^{2+}-heme, we determined the affinity of the H568R variant for Fe^{2+}-heme. Substitution of His568 by Arg severely diminished the affinity of the Rev-erbβ LBD for Fe^{2+} heme (K_d = 1.52 ± 0.49 μM). On the other hand, mutation of C384 to Ala had a more modest effect on the affinity (K_d = 210 ± 30 nM) for Fe^{2+}-heme (Table 5.3). These observations lend further support for the conclusion that in the Fe^{2+} state, His568 remains as an axial ligand, while Cys384 ligation might be lost. Dissociation of a thiolate anionic ligand upon reduction of Fe^{3+}-heme is a fairly common phenomenon (40).

5.5 Discussion

Rev-erbα and Rev-erbβ are heme-binding nuclear receptors that are highly expressed in the brain, liver, adipose tissue and skeletal muscle. The Rev-erbs exhibit circadian patterns of expression and play important roles in controlling the expression of genes constituting the primary transcriptional-translational feed back loop that regulates the vertebrate circadian clock (48, 54). This primary negative feedback loop involves a highly conserved suite of proteins (CLOCK, the CLOCK paralog NPAS2, BMAL1, Per1, Per2, Cry1 and Cry2*)* that are expressed within the suprachiasmatic nucleus (SCN) of the hypothalamus, the central circadian pacemaker in humans, as well as in peripheral tissues that are subject to circadian modulation. In this primary feed back loop, the CLOCK-BMAL1 heterodimer serves as a positive acting transcription factor that activates expression of the Cry and Per proteins, which feedback to repress the expression of BMAL1. In a secondary negative feedback loop, Rev-erb represses the expression of BMAL1 by binding to two ROR response elements in the BMAL1 promoter; yet expression of Rev-erb is activated by the CLOCK-BMAL1 heterodimer, which binds to E-boxes within the Rev-erb promoter (4, 29, 42). Transcriptional regulation through the primary and secondary circadian loops, coupled to post-translational modification and degradation of circadian clock proteins (29, 52), synchronizes to the daily light–dark cycle a wide range of metabolic and behavioral processes, including the sleep–wake cycle, feeding behavior, body temperature, and blood hormone levels (54).

Besides serving as a prosthetic group in enzymes, heme can act as a signaling molecule that regulates biochemical and physiological processes as diverse as enzyme and ion channel activity, DNA binding, signal transduction and protein complex assembly (36);

thus, heme is linked to the circadian cycle at several levels. Like Rev-erb, heme exhibits circadian patterns of expression, due at least in part to circadian regulation of ALA synthase, the rate-limiting enzyme in heme synthesis (24). Heme also modulates the activity of multiple nuclear receptors such as Hap1, HRI kinase, elF2α (36) and several key players involved in the circadian rhythm, including Rev-erbα and Rev-erbβ (8, 43, 63, 67). Heme binding to Rev-erb is required for efficient NCoR recruitment; thus, alterations in intracellular heme levels modulate the expression of BMAL1 in a manner suggesting that heme stabilizes the Rev-erb-NCoR complex (4).

The intracellular redox state has also been proposed to entrain the circadian oscillator by modulating the ability of the CLOCK:BMAL1 and NPAS2:BMAL1 heterodimers to bind DNA (48). One mechanism of redox-regulation of gene expression is by thiol-based redox modification of nuclear receptors (55). For example, upon treatment with thiol-oxidizing reagents, the ligand binding activity of the glucocorticoid receptor is severely impaired, but is restored by overexpression of thioredoxin (32, 55).

One mechanism by which proteins link redox- and heme-dependent regulation is by thiol-disulfide regulation of heme binding. For example, human heme oxygenase-2 and the BK channel contain redox switches that undergo reversible thiol-disulfide interconversion, with different heme binding affinities in the oxidized disulfide state and the reduced state (64-66). The HRM consists of a conserved Cys-Pro core sequence that is usually flanked at the N-terminus by basic amino acids and at the C terminus by a hydrophobic residue (35, 53, 69). Given that the LBD of Rev-erbβ contains an HRM motif ($HLVC_{384}PMSK$), in which Cys384 is a heme ligand (39), we hypothesized that Cys384 may be involved in

a ligand switch in which oxidation of this residue would abolish (or reduce) binding of Fe^{3+}-heme. Because heme binding to Rev-erb regulates the expression of target genes (39, 43, 67), such a redox and/or ligand switch could help explain how intracellular redox state and heme metabolism can control the circadian cycle. Furthermore, since the Cys residue appears to dissociate upon conversion to the Fe^{2+} state (39), we expected that the redox state of Cys384 would not affect binding of Fe^{2+} heme.

Our combined mutagenesis, spectroscopic (EPR and UV-visible) and mass spectrometric experiments provide novel insights into redox- and ligand-based changes in the LBD and lend support to the conclusions based on previous resonance Raman and crystallographic experiments that Cys384 and His568 can serve as the axial ligands to the heme in Rev-erbβ (34, 39). Based on heme titrations, the reduced state of the Rev-erbβ LBD binds Fe^{3+}-heme (K_d = 23 nM) with ~5-fold greater affinity than does the oxidized protein (K_d = 117 nM). This change in heme affinity appears to be associated with the reduction of the disulfide state of Cys384 (linked to Cys374) to the free thiolate state. With such a redox-coupled ligand switch, the Cys residue would only be available for heme ligation under reducing conditions within the cell. Mutagenesis studies further indicate that Cys384 is redox active, because the EPR spectra of the oxidized C384A variant, which has only His/neutral residue ligation to the heme, are similar to those of the diamide-oxidized wild-type Rev-erb β LBD. It is likely that His568 remains as one of the heme ligands in the oxidized protein, because mutation of His568 to either Ala or Arg markedly lowered heme binding affinity (Table 5.3). In an attempt to identify the other neutral residue that binds heme in the oxidized state, we performed EPR studies on mutants of the residue that seemed most likely to be involved in the ligand switch, e.g.,

His381, based on the crystal structure of the protein (39). However, the H381A variant exhibits an EPR spectrum that superimposes with that of the wild-type protein. Thus, the identity of the other neutral residue that can bind heme in the oxidized state of the protein is unknown.

The heme titrations quantitatively demonstrate that the reduced state of the purified LBD tightly binds heme at the low nanomolar concentrations of free heme present within the cell and the *in vivo* EPR and mutagenesis experiments confirm that the LBD tightly binds heme within growing cells. We used *E. coli* cells for this expression because obtaining sufficient numbers of mammalian cells for such an experiment is prohibitive and, at least from a redox perspective, the intracellular redox potential of *E. coli* is ~ -250 mV (38, 56), which is within the range of the ambient redox potential of mammalian cells, from -170 to -325 mV (9, 23). Furthermore, when heme oxygenase-2 was expressed in mammalian cells grown under different redox conditions, the measured ratios of oxidized/reduced thiols were similar to those observed when the protein was expressed in *E. coli* cells that had been treated under similar conditions (64). Therefore, we submit that this ex vivo EPR experiment is relevant and likely reflects the redox state of Rev-erbβ in mammalian tissues.

That the LBD binds heme with high affinity is also indicated by observation of the amber-color of *E. coli* cells that are overexpressing the LBD in the absence or presence of the heme precursor, δ-ALA. Similarly, when cytochrome b and NPAS2 are overexpressed, the bacterial cells exhibit the characteristic amber color of heme (8, 47). Earlier studies on heme binding to the Rev-erbβ LBD have yielded K_d values of 2 and 6

μM (39, 43), which are problematic because these values are much higher than the physiological concentration of free heme (< 100 nM) (37). Based on a 2 μM K_d value, at 100 nM free heme, ~95% of the Rev-erb population would be in the apo form. However, based on the published UV-visible spectra (including Soret peaks for the Fe^{3+}-heme-bound 415-420 nm) (34, 39, 43, 68), the previous studies were performed with a mixture of oxidized and reduced LBD. Our results also indicate that, besides the potential problems associated with working with mixed redox states of the LBD, the very high K_d values reported in prior studies result from protein aggregation at the high concentrations used in those experiments. Here, we show heme binding to the Rev-erbβ LBD at physiologically relevant heme concentrations and that heme affinity is redox regulated.

The EPR spectrum of the LBD-bound heme is easily observed in *E. coli* cells and the *g*-values, which are fingerprints for the heme ligation state, can be readily assigned. Thus, the mutagenesis and *in vivo* EPR experiments demonstrate that the switch between His/neutral residue and His/Cys coordination environments observed for the purified oxidized and reduced proteins also occurs within cells. It appears likely that the coordination environment is governed by the ambient intracellular redox potential.

The studies described here also explain the discrepancy noted by De Rosny et al.(6), i.e., that, although His/Cys ligation was observed in the crystal structure of Rev-erbβ LBD, the Soret peak was unexpectedly at 415 nm. Our results show that the fully oxidized Fe^{3+}-protein exhibits a Soret peak at 416 nm, while this band for the reduced ferric protein is observed at 424 nm, which is characteristic of His/Cys ligation (6, 33). Therefore, the crystal structure of the TCEP-incubated protein seems to have trapped one of the two

stable states of the protein, i.e., the reduced state, while the His/neutral residue liganded state is responsible for the 415 nm band.

A novel aspect of the ligand switch between the His/neutral residue and His/Cys states of the Fe^{3+}-heme is that it is regulated by the change in redox state of thiols in Rev-erbβ. This ligand switch in Rev-erbβ also can be brought about by changes in the redox state of the heme (34), a property that is commonly observed when the iron undergoes redox changes between the $Fe^{3+}$and Fe^{2+} states (20, 21, 28, 33). In Rev-erbβ, the reduced LBD binds Fe^{2+}- and Fe^{3+}-heme with similar affinity (16 nM and 23 nM, respectively). Generally the anionic thiolate ligand is replaced upon reduction of the ferric ion (40). Based on the earlier experiments (39), it is possible that Fe^{2+}-heme is ligated via His only; however, the UV-visible spectrum cannot rule out the possibility of His/Met or His/Lys ligation (22, 26). Although the physiological relevance of Fe^{2+}-heme binding is not very well established (19), it is clear that replacement of a strong ligand (like thiolate) by a weak ligand facilitates reduction of the iron and promotes binding of extrinsic axial ligands, like CO, NO or H_2S as has been described in chapter 6 (Figure 5.12).

Redox-mediated ligand switching allows adjustment of the activity of heme proteins, in response to changes in the ambient redox potential within the cell, which occur during oxidative stress or conversely, hypoxia. Oxidative stress, a factor in many important diseases (14, 51, 60, 61), is correlated with disruptions in the circadian rhythm (18, 50). Oxidative stress may also play a role in different diseases, originating from imbalance in circadian rhythm such as shift work sleep disorder (50). Because Rev-erbβ is considered to link the circadian cycle and metabolism (44), we consider that under more reducing

intracellular redox conditions, Rev-erbβ (containing the reduced thiolate form of Cys384) is in its heme-bound state, which is optimal for recruitment of nuclear corepressor and repression of target genes. When subjected to oxidative stress conditions, Cys384 of Rev-erbβ undergoes oxidation to form a disulfide bridge with Cys374. This disulfide and a conformational change upon oxidation of the protein, as observed in the limited proteolysis experiment, may trigger a ligand switch of heme from Cys/His to His/neutral residue. Due to low heme affinity of the oxidized state of the protein, as measured in the binding analysis, it might further result in release of bound heme and derepression of target genes. These redox- and ligand-dependent changes could then trigger alterations in circadian patterns and, if not reversed, result in circadian and/or metabolic disorders (Figure 5.12). The effects of heme, redox, and intrinsic ligands on RevErb would likely be complemented by those on other heme proteins with key roles in the circadian cycle, such as NPAS2 and Per2 (25, 59).

Thus, based on the results described here and with heme oxygenase-2, the redox state of the thiol groups in heme proteins may markedly influence their properties, including their affinity for heme and their Fe-coordination environment.

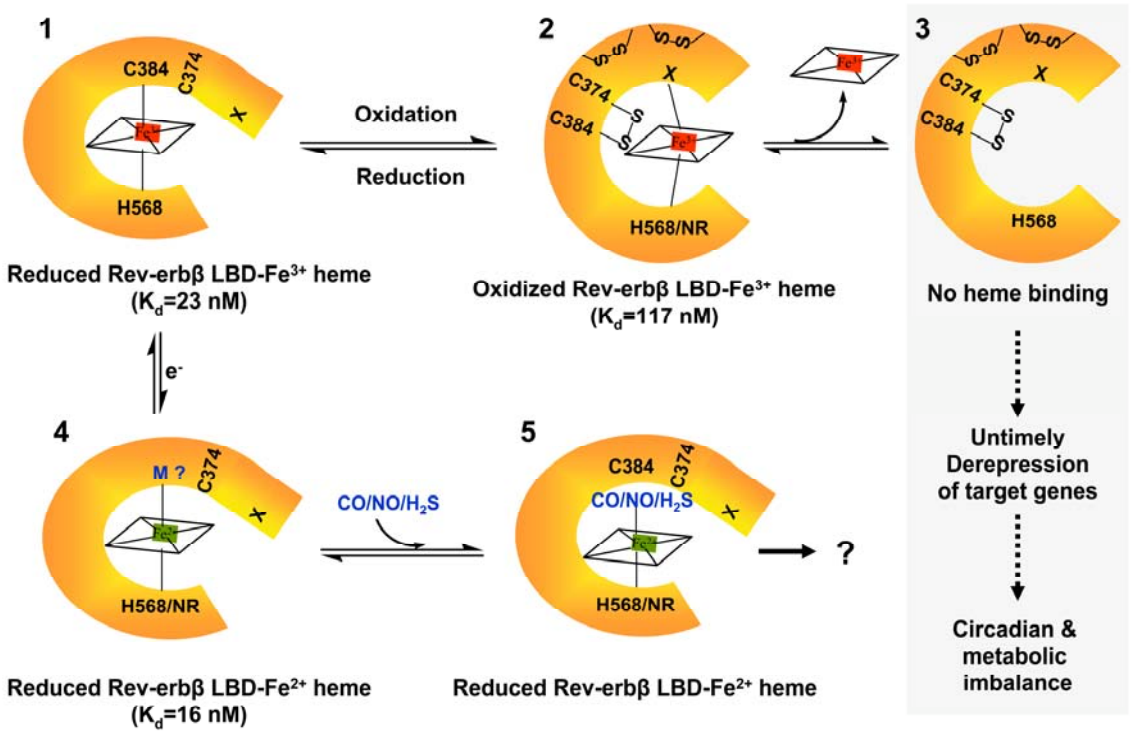

Figure 5.12: Model for redox modulation of heme binding and heme ligand switching in Rev-erbβ. Ferric heme is ligated via Cys384 and His568 in the ligand binding domain of the thiol-reduced form of Rev-erbβ (**1**). Disulfides, formed after the oxidation of the protein, change the conformation of the protein, which results in His/NR (neutral residue) ligation (His/His or His/Met or His/Lys) of the heme (**2**). Formation of the disulfide bond between Cys374 and Cys384 interferes with heme binding and lowers the heme affinity of the protein. This might cause heme release from Rev-erbβ (**3**) and ultimately may result in untimely derepression of target genes and thus circdain and/or metabolic imbalance, The LBD can bind ferrous heme with similar affinity to the ferric heme (**4**). In this state, Cys384 appears to be replaced by a neutral ligand, suggested to be Met (22, 26). This neutral ligand can replaced by any of the gaseous ligands (**5**), described in the next chapter. The effect of gas binding on the function of the protein is either not yet confirmed or has not yet been tested. Note: The part of the figure shown in gray box is based on our hypothesis and not on experimental results shown in this chapter or anywhere else.

5.6 References

1. Berry EA, Trumpower BL. 1987. Simultaneous determination of hemes a, b, and c from pyridine hemochrome spectra. *Anal Biochem* 161: 1-15

2. Boehning D, Snyder SH. 2002. Circadian rhythms. Carbon monoxide and clocks. *Science* 298: 2339-40

3. Bulaj G, Kortemme T, Goldenberg DP. 1998. Ionization-reactivity relationships for cysteine thiols in polypeptides. *Biochemistry* 37: 8965-72

4. Burris TP. 2008. Nuclear Hormone Receptors for Heme: REV-ERB{alpha} and REV-ERB{beta} Are Ligand-Regulated Components of the Mammalian Clock. *Mol Endocrinol* 22: 1509-20

5. Cheesman MR, Little PJ, Berks BC. 2001. Novel heme ligation in a c-type cytochrome involved in thiosulfate oxidation: EPR and MCD of SoxAX from Rhodovulum sulfidophilum. *Biochemistry* 40: 10562-9

6. de Rosny E, de Groot A, Jullian-Binard C, Borel F, Suarez C, et al. 2008. DHR51, the Drosophila melanogaster homologue of the human photoreceptor cell-specific nuclear receptor, is a thiolate heme-binding protein. *Biochemistry* 47: 13252-60

7. de Rosny E, de Groot A, Jullian-Binard C, Gaillard J, Borel F, et al. 2006. Drosophila nuclear receptor E75 is a thiolate hemoprotein. *Biochemistry* 45: 9727

8. Dioum EM, Rutter J, Tuckerman JR, Gonzalez G, Gilles-Gonzalez MA, McKnight SL. 2002. NPAS2: a gas-responsive transcription factor. *Science* 298: 2385-7

9. Dooley CT, Dore TM, Hanson GT, Jackson WC, Remington SJ, Tsien RY. 2004. Imaging dynamic redox changes in mammalian cells with green fluorescent protein indicators. *J Biol Chem* 279: 22284-93

10. Downes M, Burke LJ, Bailey PJ, Muscat GE. 1996. Two receptor interaction domains in the corepressor, N-CoR/RIP13, are required for an efficient interaction with Rev-erbA alpha and RVR: physical association is dependent on the E region of the orphan receptors. *Nucleic Acids Res* 24: 4379-86

11. Duez H, Staels B. 2008. Rev-erb[alpha] gives a time cue to metabolism. *FEBS Letters* 582: 19-25

12. Ellis KJ, Morrison JF. 1982. Buffers of constant ionic strength for studying pH-dependent processes. *Methods Enzymol* 87: 405-26

13. Ellman GL. 1958. A colorimetric method for determining low concentrations of mercaptans. *Arch Biochem Biophys* 74: 443-50

14. Elswaifi SF, Palmieri JR, Hockey KS, Rzigalinski BA. 2009. Antioxidant nanoparticles for control of infectious disease. *Infect Disord Drug Targets* 9: 445-52

15. Garrick MD, Scott D, Kulju D, Romano MA, Dolan KG, Garrick LM. 1999. Evidence for and consequences of chronic heme deficiency in Belgrade rat reticulocytes. *Biochim Biophys Acta* 1449: 125-36

16. Gupta N, Ragsdale SW. 2008. Dual Roles of an Essential Cysteine Residue in Activity of a Redox-regulated Bacterial Transcriptional Activator. *J. Biol. Chem.* 283: 28721-8

17. Gygi SP, Rist B, Gerber SA, Turecek F, Gelb MH, Aebersold R. 1999. Quantitative analysis of complex protein mixtures using isotope-coded affinity tags. *Nat Biotechnol* 17: 994-9

18. Hardeland R, Coto-Montes A, Poeggeler B. 2003. Circadian rhythms, oxidative stress, and antioxidative defense mechanisms. *Chronobiol Int* 20: 921-62

19. Igarashi J, Murase M, Iizuka A, Pichierri F, Martinkova M, Shimizu T. 2008. Elucidation of the heme binding site of heme-regulated eukaryotic initiation factor 2alpha kinase and the role of the regulatory motif in heme sensing by spectroscopic and catalytic studies of mutant proteins. *J Biol Chem* 283: 18782-91

20. Inagaki S, Masuda C, Akaishi T, Nakajima H, Yoshioka S, et al. 2005. Spectroscopic and redox properties of a CooA homologue from Carboxydothermus hydrogenoformans. *J Biol Chem* 280: 3269-74

21. Ishitsuka Y, Araki Y, Tanaka A, Igarashi J, Ito O, Shimizu T. 2008. Arg97 at the heme-distal side of the isolated heme-bound PAS domain of a heme-based oxygen sensor from Escherichia coli (Ec DOS) plays critical roles in autoxidation and binding to gases, particularly O2. *Biochemistry* 47: 8874-84

22. Ito S, Igarashi J, Shimizu T. 2009. The FG loop of a heme-based gas sensor enzyme, Ec DOS, functions in heme binding, autoxidation and catalysis. *J Inorg Biochem* 103: 1380-5

23. Jones DP. 2002. Redox potential of GSH/GSSG couple: assay and biological significance. *Methods Enzymol* 348: 93-112

24. Kaasik K, Lee CC. 2004. Reciprocal regulation of haem biosynthesis and the circadian clock in mammals. *Nature* 430: 467-71

25. Kitanishi K, Igarashi J, Hayasaka K, Hikage N, Saiful I, et al. 2008. Heme-binding characteristics of the isolated PAS-A domain of mouse Per2, a transcriptional regulatory factor associated with circadian rhythms. *Biochemistry* 47: 6157-68

26. Kooter IM, Moguilevsky N, Bollen A, van der Veen LA, Otto C, et al. 1999. The sulfonium ion linkage in myeloperoxidase. Direct spectroscopic detection by isotopic labeling and effect of mutation. *J Biol Chem* 274: 26794-802

27. Kovac J, Husse J, Oster H. 2009. A time to fast, a time to feast: the crosstalk between metabolism and the circadian clock. *Mol Cells* 28: 75-80

28. Kurokawa H, Lee DS, Watanabe M, Sagami I, Mikami B, et al. 2004. A redox-controlled molecular switch revealed by the crystal structure of a bacterial heme PAS sensor. *J Biol Chem* 279: 20186-93

29. Lee C, Etchegaray JP, Cagampang FR, Loudon AS, Reppert SM. 2001. Posttranslational mechanisms regulate the mammalian circadian clock. *Cell* 107: 855-67

30. Leichert LI, Gehrke F, Gudiseva HV, Blackwell T, Ilbert M, et al. 2008. Quantifying changes in the thiol redox proteome upon oxidative stress in vivo. *Proc Natl Acad Sci U S A* 105: 8197-202

31. Liu SC, Zhai S, Palek J. 1988. Detection of hemin release during hemoglobin S denaturation. *Blood* 71: 1755-8

32. Makino Y, Okamoto K, Yoshikawa N, Aoshima M, Hirota K, et al. 1996. Thioredoxin: a redox-regulating cellular cofactor for glucocorticoid hormone action. Cross talk between endocrine control of stress response and cellular antioxidant defense system. *J Clin Invest* 98: 2469-77

33. Marvin KA, Kerby RL, Youn H, Roberts GP, Burstyn JN. 2008. The transcription regulator RcoM-2 from Burkholderia xenovorans is a cysteine-ligated hemoprotein that undergoes a redox-mediated ligand switch. *Biochemistry* 47: 9016-28

34. Marvin KA, Reinking JL, Lee AJ, Pardee K, Krause HM, Burstyn JN. 2009. Nuclear receptors homo sapiens Rev-erbbeta and Drosophila melanogaster E75 are thiolate-ligated heme proteins which undergo redox-mediated ligand switching and bind CO and NO. *Biochemistry* 48: 7056-71

35. McCoubrey WK, Jr., Huang TJ, Maines MD. 1997. Heme oxygenase-2 is a hemoprotein and binds heme through heme regulatory motifs that are not involved in heme catalysis. *J Biol Chem* 272: 12568-74

36. Mense SM, Zhang L. 2006. Heme: a versatile signaling molecule controlling the activities of diverse regulators ranging from transcription factors to MAP kinases. *Cell Res* 16: 681-92

37. Ogawa K, Sun J, Taketani S, Nakajima O, Nishitani C, et al. 2001. Heme mediates derepression of Maf recognition element through direct binding to transcription repressor Bach1. *EMBO J* 20: 2835-43

38. Ostergaard H, Henriksen A, Hansen FG, Winther JR. 2001. Shedding light on disulfide bond formation: engineering a redox switch in green fluorescent protein. *EMBO J* 20: 5853-62

39. Pardee KI, Xu X, Reinking J, Schuetz A, Dong A, et al. 2009. The structural basis of gas-responsive transcription by the human nuclear hormone receptor REV-ERBbeta. *PLoS Biol* 7: e43

40. Perera R, Sono M, Sigman JA, Pfister TD, Lu Y, Dawson JH. 2003. Neutral thiol as a proximal ligand to ferrous heme iron: implications for heme proteins that lose cysteine thiolate ligation on reduction. *Proc Natl Acad Sci U S A* 100: 3641-6

41. Pop SM, Gupta N, Raza AS, Ragsdale SW. 2006. Transcriptional Activation of Dehalorespiration: IDENTIFICATION OF REDOX-ACTIVE CYSTEINES REGULATING DIMERIZATION AND DNA BINDING. *J. Biol. Chem.* 281: 26382-90

42. Preitner N, Damiola F, Lopez-Molina L, Zakany J, Duboule D, et al. 2002. The orphan nuclear receptor REV-ERBalpha controls circadian transcription within the positive limb of the mammalian circadian oscillator. *Cell* 110: 251-60

43. Raghuram S, Stayrook KR, Huang P, Rogers PM, Nosie AK, et al. 2007. Identification of heme as the ligand for the orphan nuclear receptors REV-ERBalpha and REV-ERBbeta. *Nat. Struct. Mol. Biol.* 14: 1207

44. Ramakrishnan SN, Muscat GE. 2006. The orphan Rev-erb nuclear receptors: a link between metabolism, circadian rhythm and inflammation? *Nucl Recept Signal* 4: e009

45. Reinking J, Lam MM, Pardee K, Sampson HM, Liu S, et al. 2005. The Drosophila nuclear receptor e75 contains heme and is gas responsive. *Cell* 122: 195

46. Retnakaran R, Flock G, Giguere V. 1994. Identification of RVR, a novel orphan nuclear receptor that acts as a negative transcriptional regulator. *Mol Endocrinol* 8: 1234-44

47. Rivera M, Walker FA. 1995. Biosynthetic preparation of isotopically labeled heme. *Anal Biochem* 230: 295-302

48. Rutter J, Reick M, McKnight SL. 2002. Metabolism and the control of circadian rhythms. *Annu Rev Biochem* 71: 307-31

49. Sassa S. 2006. Biological implication of heme metabolism. *J. Clin. Biochem. Nutr.* 38: 138-55

50. Sharifian A, Farahani S, Pasalar P, Gharavi M, Aminian O. 2005. Shift work as an oxidative stressor. *J Circadian Rhythms* 3: 15

51. Shi P, Gal J, Kwinter DM, Liu X, Zhu H. 2009. Mitochondrial dysfunction in amyotrophic lateral sclerosis. *Biochim Biophys Acta*

52. Shirogane T, Jin J, Ang XL, Harper JW. 2005. SCFbeta-TRCP controls clock-dependent transcription via casein kinase 1-dependent degradation of the mammalian period-1 (Per1) protein. *J Biol Chem* 280: 26863-72

53. Steiner H, Kispal G, Zollner A, Haid A, Neupert W, Lill R. 1996. Heme binding to a conserved Cys-Pro-Val motif is crucial for the catalytic function of mitochondrial heme lyases. *J Biol Chem* 271: 32605-11

54. Takahashi JS, Hong HK, Ko CH, McDearmon EL. 2008. The genetics of mammalian circadian order and disorder: implications for physiology and disease. *Nat Rev Genet* 9: 764-75

55. Tanaka H, Makino Y, Okamoto K, Iida T, Yoshikawa N, Miura T. 2000. Redox regulation of the nuclear receptor. *Oncology* 59 Suppl 1: 13-8

56. Taylor MF, Boylan MH, Edmondson DE. 1990. Azotobacter vinelandii flavodoxin: purification and properties of the recombinant, dephospho form expressed in Escherichia coli. *Biochemistry* 29: 6911-8

57. Terenzi H, Cassia RO, Zakin MM. 1996. Expression, Purification, and Functional Analysis of the DNA Binding Domain of the Nuclear Receptor Rev-Erb[beta]. *Protein Expression and Purification* 8: 313-8

58. Tsubaki M, Nakayama M, Okuyama E, Ichikawa Y, Hori H. 1997. Existence of two heme B centers in cytochrome b561 from bovine adrenal chromaffin vesicles as revealed by a new purification procedure and EPR spectroscopy. *J Biol Chem* 272: 23206-10

59. Uchida T, Sato E, Sato A, Sagami I, Shimizu T, Kitagawa T. 2005. CO-dependent activity-controlling mechanism of heme-containing CO-sensor protein, neuronal PAS domain protein 2. *J. Biol. Chem.* 280: 21358-68

60. Uttara B, Singh AV, Zamboni P, Mahajan RT. 2009. Oxidative stress and neurodegenerative diseases: a review of upstream and downstream antioxidant therapeutic options. *Curr Neuropharmacol* 7: 65-74

61. Watanabe K, Thandavarayan RA, Gurusamy N, Zhang S, Muslin AJ, et al. 2009. Role of 14-3-3 protein and oxidative stress in diabetic cardiomyopathy. *Acta Physiol Hung* 96: 277-87

62. Yang J, Ishimori K, Oâ€™Brian MR. 2005. Two heme binding sites are involved in the regulated degradation of the bacterial iron response regulator (Irr) protein. *J. Biol. Chem.* 280: 7671

63. Yang J, Kim KD, Lucas A, Drahos KE, Santos CS, et al. 2008. A novel heme-regulatory motif mediates heme-dependent degradation of the circadian factor period 2. *Mol Cell Biol* 28: 4697-711

64. Yi L, Jenkins PM, Leichert LI, Jakob U, Martens JR, Ragsdale SW. 2009. Heme regulatory motifs in heme oxygenase-2 form a thiol/disulfide redox switch that responds to the cellular redox state. *J Biol Chem* 284: 20556-61

65. Yi L, Morgan JT, Ragsdale SW. 2010. Identification of a thiol/disulfide redox switch in the human BK channel that controls its affinity for heme and CO. *J Biol Chem* 285: 20117-27

66. Yi L, Ragsdale SW. 2007. Evidence that the heme regulatory motifs in heme oxygenase-2 serve as a thiol/disulfide redox switch regulating heme binding. *J Biol Chem* 282: 21056-67

67. Yin L, Lazar MA. 2005. The orphan nuclear receptor Rev-erbalpha recruits the N-CoR/histone deacetylase 3 corepressor to regulate the circadian Bmal1 gene. *Mol Endocrinol* 19: 1452-9

68. Yin L, Wu N, Curtin JC, Qatanani M, Szwergold NR, et al. 2007. Rev-erbα, a Heme Sensor That Coordinates Metabolic and Circadian Pathways. *Science* 318: 1786

69. Zhang L, Guarente L. 1995. Heme binds to a short sequence that serves a regulatory function in diverse proteins. *EMBO J* 14: 313-20

Chapter 6

REDOX-SPECIFIC GAS BINDING TO THE LIGAND BINDING DOMAIN OF A THIOL-BASED REDOX REGULATED HEME SENSOR; Rev-erbβ

The CO binding analysis described in this chapter is published and the reference is as follows: Gupta, N., and Ragsdale, SW. 2011. Thiol-Disulfide Redox Dependence of Heme Binding and Heme Ligand Switching in the Nuclear Hormone Receptor, Rev-erbβ. *J. Biol. Chem.* 286(6):4392-403. Epub 2010 Dec 1.

6.1 Abstract

Reb-erbβ is a heme responsive nuclear receptor that is expressed in various organs and tissues, such as brain, heart, liver, spleen, lung, skeletal muscle, adipose tissues, testes, and ovaries. In these tissues, Reb-erbβ regulates multiple metabolic genes in addition to the clock genes and thus has been predicted to connect metabolism with the circadian rhythm. CO and NO are predicted to modulate the activity of Reb-erbβ by binding to its heme center. In this study, we have measured CO, NO and H_2S binding to the ligand binding domain of Reb-erbβ (Reb-erbβ LBD). We have determined that the Fe^{2+}-heme bound to the reduced protein has a high affinity for CO (K_d = 60 nM) but lower affinity for NO (K_d ~300 μM) and negligible affinity for H_2S. The reduced (dithiol) form of the Reb-erbβ LBD containing Fe^{3+}-heme, on the other hand, lacked affinity for NO, but exhibited moderate affinity for H_2S (K_d = 1 μM). Further, the oxidized (disulfide) state of the Reb-erbβ LBD containing Fe^{3+}-heme showed very low affinity for NO (K_d ~ 9 μM) and negligible affinity for H2S. The dissociation constants for the complexes between the LBD and gaseous signaling molecules are in the physiological range, except for NO, which appears to have a much lower physiological concentration (up to 5 nM).

6.2 Introduction

Heme is a prosthetic group in several hemoproteins that include gas sensors, P450 enzymes, cytochromes, catalases, peroxidases, nitric oxide synthases (NOS), guanylyl cyclases and several transcriptional factors (30). An important attribute of heme-dependent proteins is their ability to bind gaseous signaling molecules; CO, NO, and H_2S (10, 26). Diverse functions of these gaseous autocrine/paracrine messengers or gasotransmitters are critical to vertebrate physiology and probably to the physiology of all living organisms. Gasotransmitters are functionally analogous to hormones but are lipid soluble and are not constrained by cellular membranes. Because gasotransmitters are unconstrained and they diffuse down a partial pressure gradient, precise uptake or metabolizing processes are not required for signal termination. Signal termination easily occurs with the falling concentration of gasotransmitters (17).

In addition to exogenous gas uptake, CO is mainly produced in cells and tissues as an elimination product of heme degradation, catalyzed by heme oxygense (HO) (18, 29). The biosynthesis of NO, on the other hand, takes place during the conversion of L-arginine to L-citrulline, and this process is catalyzed by nitric oxide synthase (NOS) (28). At a molecular level, CO binds to ferrous heme, whilst NO can bind to both ferrous and ferric heme (13). CO has vasoregulatory, anti-inflammatory, anti-proliferative and anti-apoptotic effects that are largely mediated by guanylyl cyclase and mitogen-activated protein kinase (MAPK) signaling pathways (28). Apart from its role in normal physiology, the role of CO has also been linked to abnormalities in metabolism in a variety of diseases; including neurodegeneration, hypertension, heart failure, and inflammation (34). NO also plays a role as a neurotransmitter, vasorelaxant, and has an

additional role in immune cells during macrophage-mediated killing of microbes and tumor cells (6). Guanyl cyclase and cytochrome c-oxidase have been proposed as major physiological targets for NO (11). Furthermore, NO has been implicated in various pathophysiological states such as septic shock, hypertension, stroke, and neurodegenerative diseases (6).

While NO is the most studied gasotransmitter, H_2S is the newest addition to the family of gasotransmitters. H_2S is generated in mammalian cells by the action of cystathionine β-synthase (in liver and neuronal tissue) and cystathionine γ-lyase (in cardiovascular systems) and by 3-mercaptopyruvate sulfurtransferase (in vascular endothelium, vascular smooth muscle and brain) (14, 17, 24). Mechanisms for H_2S generation by these enzymes using different substrates (5, 14) and H_2S generation by numerous other pathways in invertebrates have been reported (14, 24). At the molecular level, H_2S binds to ferric heme and converts it to ferrous heme in *Lucina pectinata* (26). However, its preference either towards ferric or ferrous heme has not been documented yet. Similar to the functions of CO and NO, H_2S is also suggested to act as a neuroprotector, neuromodulator and smooth muscle relaxant/contractor (26). Pathophysiologies associated with malfunction of H_2S-producing enzymes have been observed and include homocytinuria, cystathioninuria and others (14).

Like some other heme-dependent transcriptional regulators, Rev-erbβ appears to bind diatomic (CO/NO) gases (25); however, the affinities have not been measured. Based on Raman and MCD studies, it has been proposed that NO/CO replaces Cys384 as an axial ligand and that a neutral ligand binds to the sixth coordination site in the (CO/NO)-bound

form of Rev-erbβ (19, 25). To ascertain the potential physiological relevance of gas binding, we have quantitatively measured the binding affinities of CO NO, and H_2S to the Reb-erbβ LBD *in vitro*. CO binding is restricted to Fe^{2+}-heme bound protein. However, both NO and H_2S show preferential binding towards specific redox states of thiols in Rev-erbβ and/or its bound heme, as described in the Results section.

6.3 Experimental procedures

6.3.1 Protein expression and purification: Expression and purification of the Rev-erbβ LBD is described in section 5.3.1.

6.3.2 Reduction and oxidation of Rev-erbβ LBD: Reduction and oxidation of the Rev-erbβ LBD is mentioned in section 5.3.3. Throughout, we refer to the disulfide and dithiol states of the Rev-erbβ LBD when we describe the "oxidized" and "reduced" protein; the redox state of the heme, i.e., Fe^{3+} or Fe^{2+}, is stated explicitly.

6.3.3 Reconstitution of the protein with heme for binding assays: For the gas binding assays, the heme-protein complex was formed first and then passed through two Bio-Gel P-6 (Bio-Rad., Hercules, CA) columns to remove any free heme. This heme-protein complex was used for gas titrations and binding was detected by UV-visible spectroscopy.

6.3.4 CO binding assay: Rev-erbβ LBD-heme complexes were prepared anaerobically as described above. For experiments with the Fe^{2+} form of the LBD, the heme-protein complex was treated with sodium dithionite (2.5 mM, final), and transferred anaerobically to the reaction cuvette. Aliquots of CO were added to the assay mixture from an anaerobic stock solution consisting of Buffer A (see section 5.3.1) that had been bubbled with a gas mixture of N_2/CO (75%/25%, providing a stock CO concentration of 0.25 mM). Gas mixes (25% CO) were purchased from Metro Welding Supply Corporation (Detroit, MI). The final concentration of CO in the CO-saturated buffer was confirmed by titration with myoglobin, whose concentration was determined based on its published extinction coefficient (121 mM^{-1} cm^{-1} at 435 nm) (15).

6.3.5 NO binding assay: Reduced and oxidized Rev-erbβ LBD-heme complexes were prepared anaerobically and were transferred anaerobically to a reaction cuvette. NO-saturated buffer was prepared by bubbling Buffer A (see section 5.3.1) with 99.9 % pure NO from NO cylinders (Metheson, Garden city, MI). An NO gas assembly set up in Dr. Mark Meyerhoff's lab was used. Aliquots of this buffer were added anaerobically to the reaction mixture and UV-visible spectra were recorded. When studying the ferrous heme complex, 2.5 mM dithionite was added to the reaction cuvette. All assays with NO, regardless of the redox-state of Rev-erbβ LBD or heme, were performed anaerobically to prevent any free radical generation via exposure to oxygen.

6.3.6 H_2S binding assay: NaHS (Sigma-Aldrich) was utilized as an H_2S donor in order to investigate H2S binding to the heme-Rev-erbβ LBD complex. NaHS dissociates into Na^+ and HS^- in solution and then HS^- re-associates with H^+ to produce H_2S. However, at pH 7, only 33.3% is present as H_2S and 66.7% exists as HS^- (8). This equilibrium was taken into account while calculating the final concentration of H_2S in the binding experiments.

6.4 Results

6.4.1 Tight CO binding to Rev-erbβ LBD

CO is an important signaling molecule and is shown to interact *in vitro* with the Fe^{2+} heme-Rev-erbβ complex, probably by replacing Cys as an axial ligand. In order to quantify the interaction between CO and the LBD, we performed CO titrations. Addition of CO to the Rev-erbβ LBD resulted in a blue-shift in the Soret band from 428 to 422 nm. The UV-visible spectra and difference spectra are shown in figure 6.1A & B respectively. The spectral features of CO bound Rev-erbβ LBD is indicative of a 6-coordinate heme. Moreover, MCD and Resonance Raman studies also support a 6-coordinate heme with neutral ligand or histidine trans to CO (19).

Data obtained from the titration were subjected to quadratic analysis (section 5.3.4), which showed very high affinity (Figure 6.1.C) of the LBD for CO (K_d = 60 ± 15 nM). Therefore, re-examination of *in vivo* CO binding is required and its strategy is discussed in section 6.5.

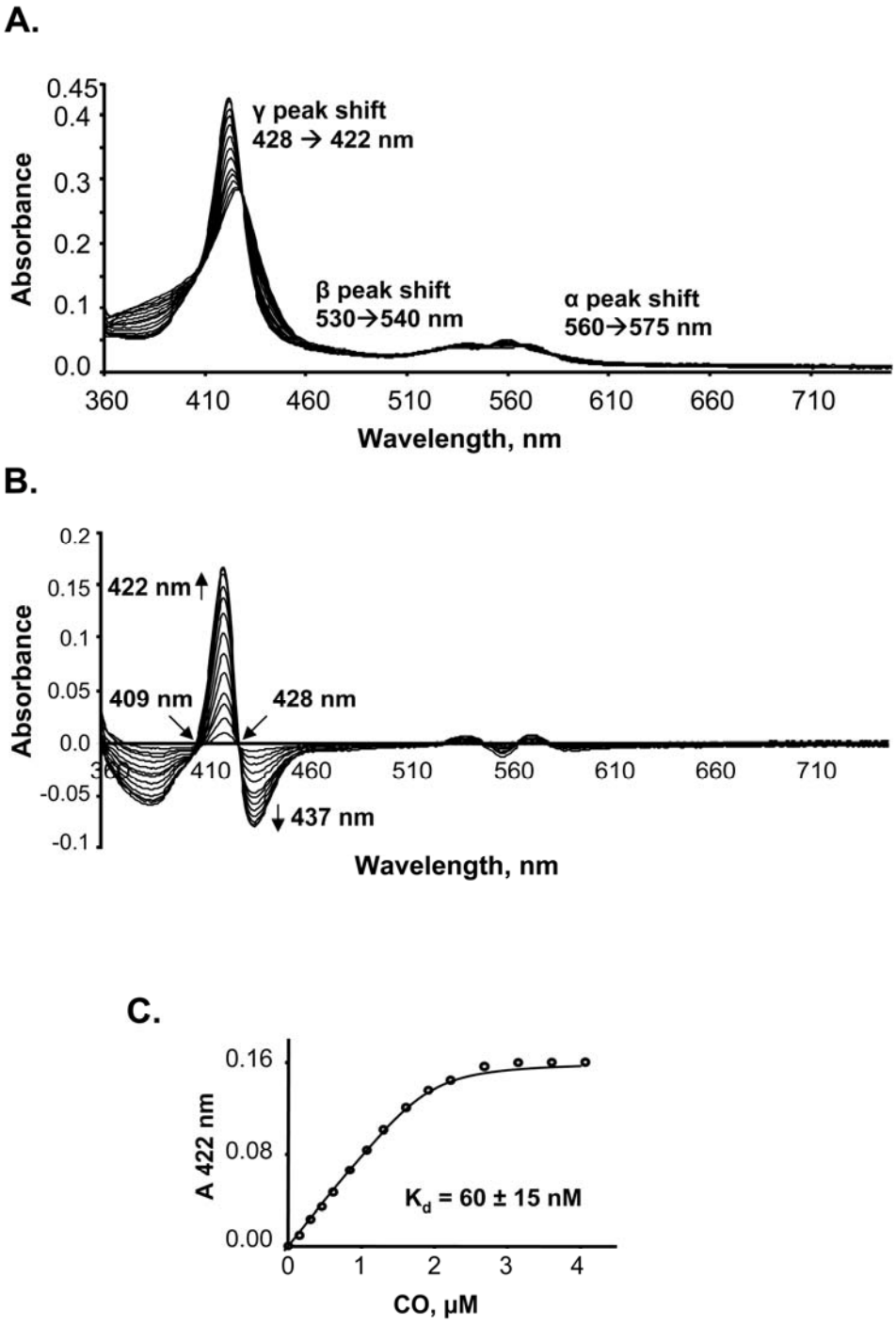

Figure 6.1: High affinity of CO towards Fe^{2+} heme-reduced Rev-erbβ LBD complex. UV-visible spectra (A) and difference spectra (B) following titration of Rev-erbβ LBD with CO. C. Fitting the binding isotherm for the CO titration yielded a K_d value of 60 ± 15 nM. The CO titration was performed anaerobically in Buffer B, in the presence of 2.5 mM dithionite with 2 µM Fe^{2+}-heme-LBD complex, as described in experimental procedures.

6.4.2 Redox-dependent NO binding to Rev-erbβ LBD

NO, as reported earlier, is capable of binding both the Fe^{2+} and Fe^{3+} forms of hemoproteins (13). Thus, NO binding was assessed with both the Fe^{2+}- and Fe^{3+}- heme-Rev-erbβ LBD complexes (Figure 6.2 and 6.3). Titration of NO with the Fe^{2+}-heme-reduced Rev-erbβ LBD complex resulted in a Soret peak shift from 427 nm to a less intense Soret band at 422 nm accompanied by a decrease in the α and β band intensities (Figure 6.2.A). Similar changes in the spectrum of the NO-bound Rev-erbβ LBD were observed by Marvin and others (19). Characteristics of the difference spectra are given in figure 6.2.B. Proteins in which one neutral endogenous ligand is retained opposite to NO, in general, exhibit sharp Soret bands between 415 nm – 425 nm (19). Moreover, EPR and Resonance Raman spectra of the NO bound Fe^{2+} heme-reduced Rev-erbβ LBD complex also confirmed a 6-coordinate NO-heme adduct (19). This binding assay gave a binding constant of ~300 nM when the data was fitted to equation 1 (see experimental procedures in chapter 5).

Titration of NO with the Fe^{3+} heme-reduced Rev-erbβ LBD complex did not show any changes in the spectrum, which reflected negligible binding. Titration of NO with Fe^{3+}-heme-oxidized Rev-erbβ LBD complex, however, did show changes in the spectrum, but exhibited no peak shift of the Soret band (Figure 6.3). Isosbestic points and peaks that shifted upon NO binding are labeled in figure 6.3A & 3B. The dissociation constant obtained from this analysis is 7 μM ± 1.4 μM (Figure 6.3C). This value is not only higher than the K_d values reported for other NO binding proteins, but is also well above the physiological concentrations of NO in the cell (up to 5 nM) (12). The high dissociation

constants ($K_{d)}$ indicates that NO binding to Rev-erbβ is not relevant *in vivo*, except, under acute conditions, for example during infections, as discussed below in section 6.5.

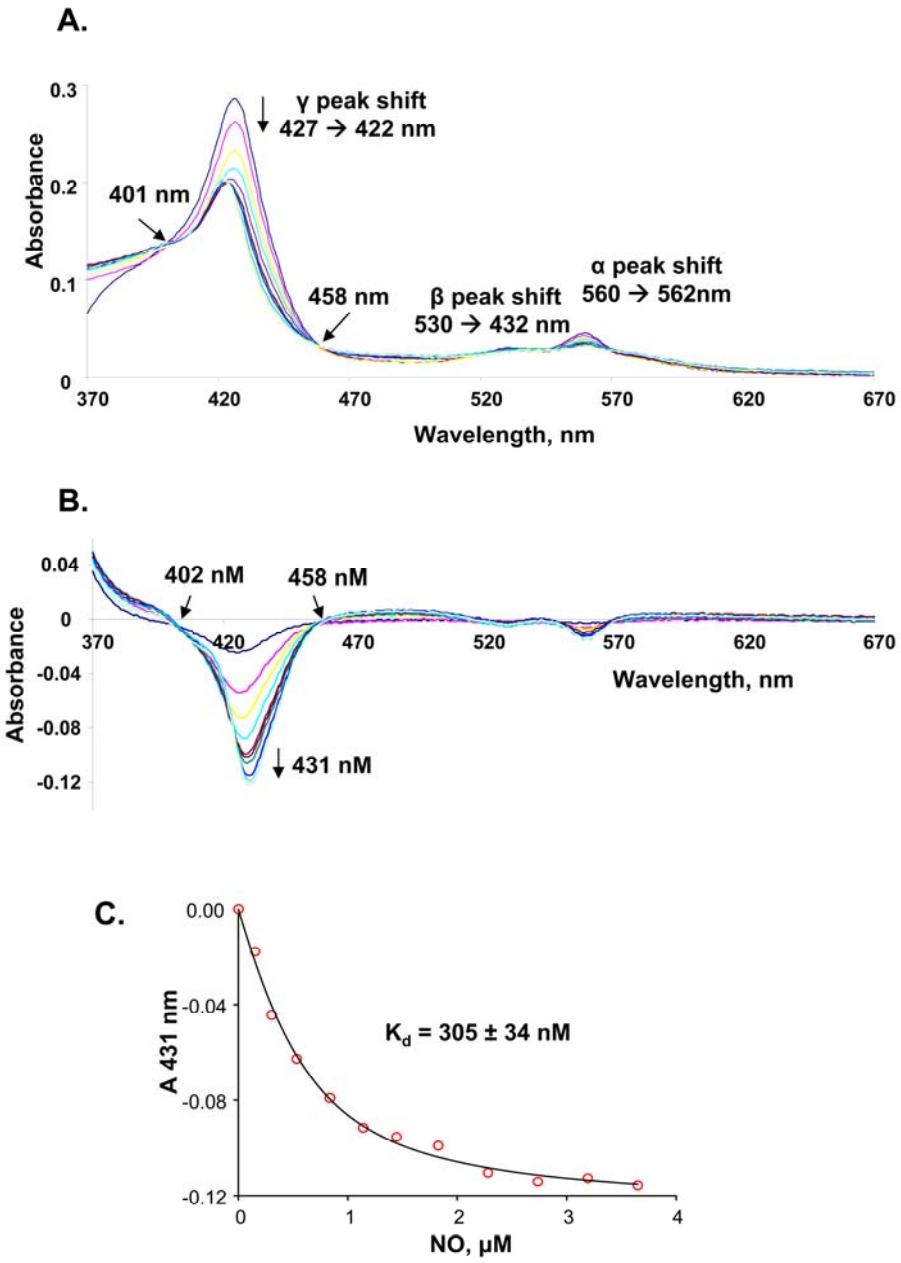

Figure 6.2: NO binding with the Fe^{2+} heme- reduced Rev-erbβ LBD complex. UV-visible spectra (A) and difference spectra (B) following titration of Fe^{2+} heme- Rev-erbβ LBD complex with NO. C. Fitting the binding isotherm for the NO titration yielded a K_d value of 305 ± 30 nM. The NO titration was performed anaerobically in Buffer B, in the presence of 2.5 mM dithionite with 2 μM Fe^{2+}-heme-LBD complex, as described in experimental procedures.

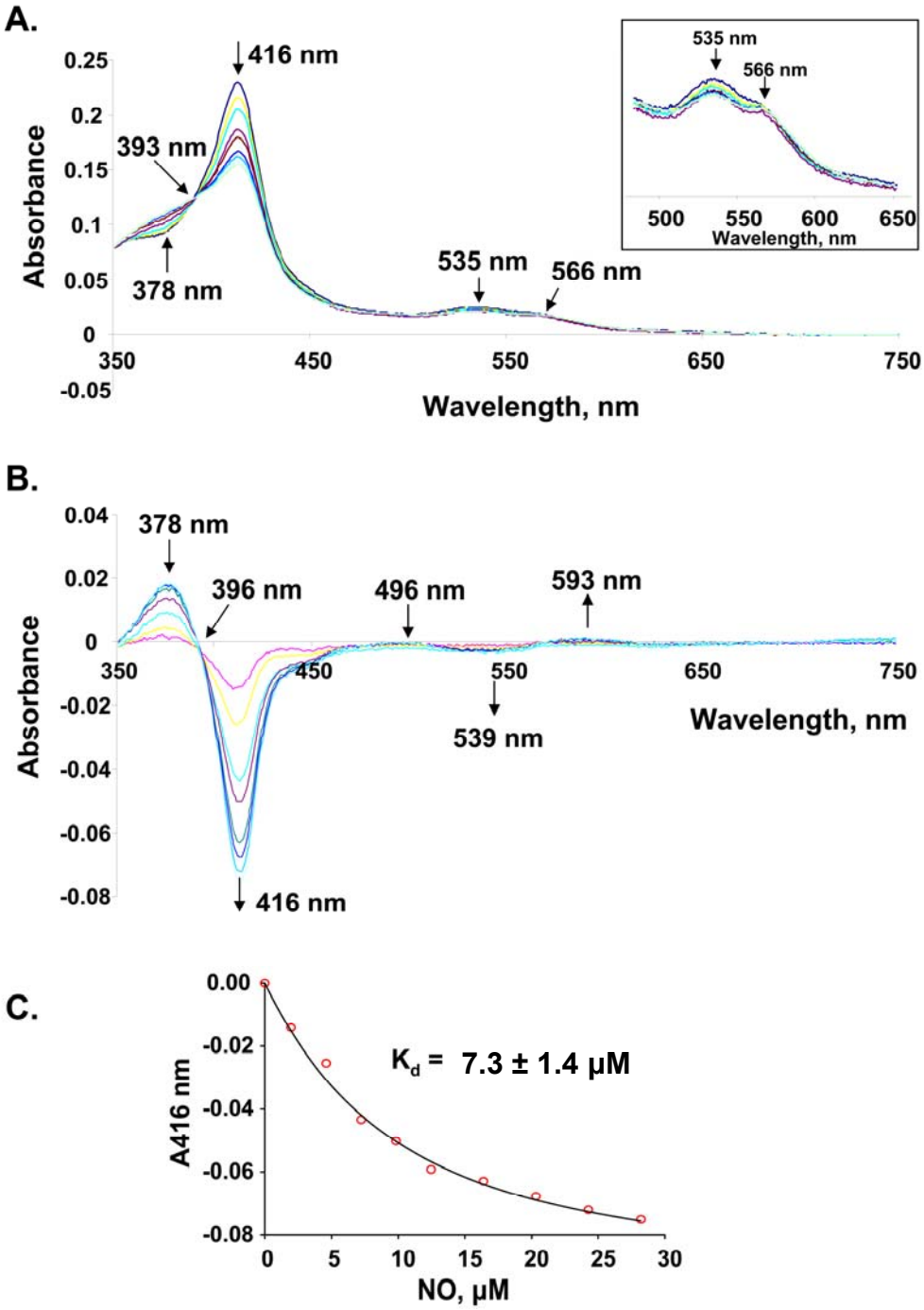

Figure 6.3: NO binding with the Fe^{3+}heme-oxidized Rev-erbβ LBD complex. UV-visible spectra (A) and difference spectra (B) following titration of Fe^{3+} heme-Rev-erbβ LBD complex with NO. C. Fitting the binding isotherm for the NO titration yielded a K_d value of 7 ± 1 µM. The NO titration was performed anaerobically in Buffer B with 3.5 µM Fe^{2+}-heme-LBD complex, as described in experimental procedures.

6.4.3 Redox-specific H_2S binding to Rev-erbβ LBD

H_2S is a newly recognized gasotransmitter and its affinities for different redox-states of Rev-erbβ LBD and its bound heme were also analyzed. Titration of NaHS with the Fe^{3+} heme-reduced Rev-erbβ LBD complex resulted in a blue-shifted Soret band from 424 to 420 nm with a reduction in peak intensity (Figure 6.4). UV-visible and difference UV-visible spectra are shown in Figures 6.4A & B, respectively. H_2S can ligate to heme either as H_2S or in HS^- form. Quadratic analysis (equation 1 in chapter 6) of NaHS titration curve yielded a binding constant of ~2 μM for HS^- (Figure 6.4C) and ~1 μM for H_2S binding to the Fe^{3+} heme-reduced Rev-erbβ LBD complex. To distinguish between HS^- and H_2S binding to Rev-erbβ EPR analysis of NaHS saturated Fe^{3+} heme-reduced Rev-erbβ LBD complex was done. EPR spectra of H_2S bound to the Fe^{3+} heme-reduced Rev-erbβ LBD complex (data not shown) was not different from the spectrum of the Fe^{3+} heme-reduced Rev-erbβ LBD complex itself (Figure 5.5 A). Therefore, H_2S might be binding to the heme center of reduced Rev-erbβ LBD complex by replacing an internal Cys ligand in HS^- form similar to thiolate of the cysteine. Moreover, features of the EPR spectrum of NaHS saturated Fe^{3+} heme-reduced Rev-erbβ LBD complex are identical to what has been observed for HS^--ligated myoglobin (2). Therefore, it is plausible to predict HS^- ligation to the heme center of Rev-erbβ. However, further confirmation via other methods is needed as discussed in section 6.5.

Titration of NaHS with the Fe^{3+} heme-oxidized Rev-erbβ LBD complex gave a saturation curve after a long lag phase. This phase could be due to reduction of oxidized Rev-erbβ LBD by NaHS. In fact, the DTNB assay (refer section 5.3.3) confirmed that NaHS is able to reduce the oxidized Rev-erbβ LBD (data not shown). Therefore, H_2S appears to only

bind to the Fe^{3+} heme center of the protein in the reduced state. No binding was observed when NaHS was titrated against the Fe^{2+} heme-reduced Rev-erbβ LBD complex.

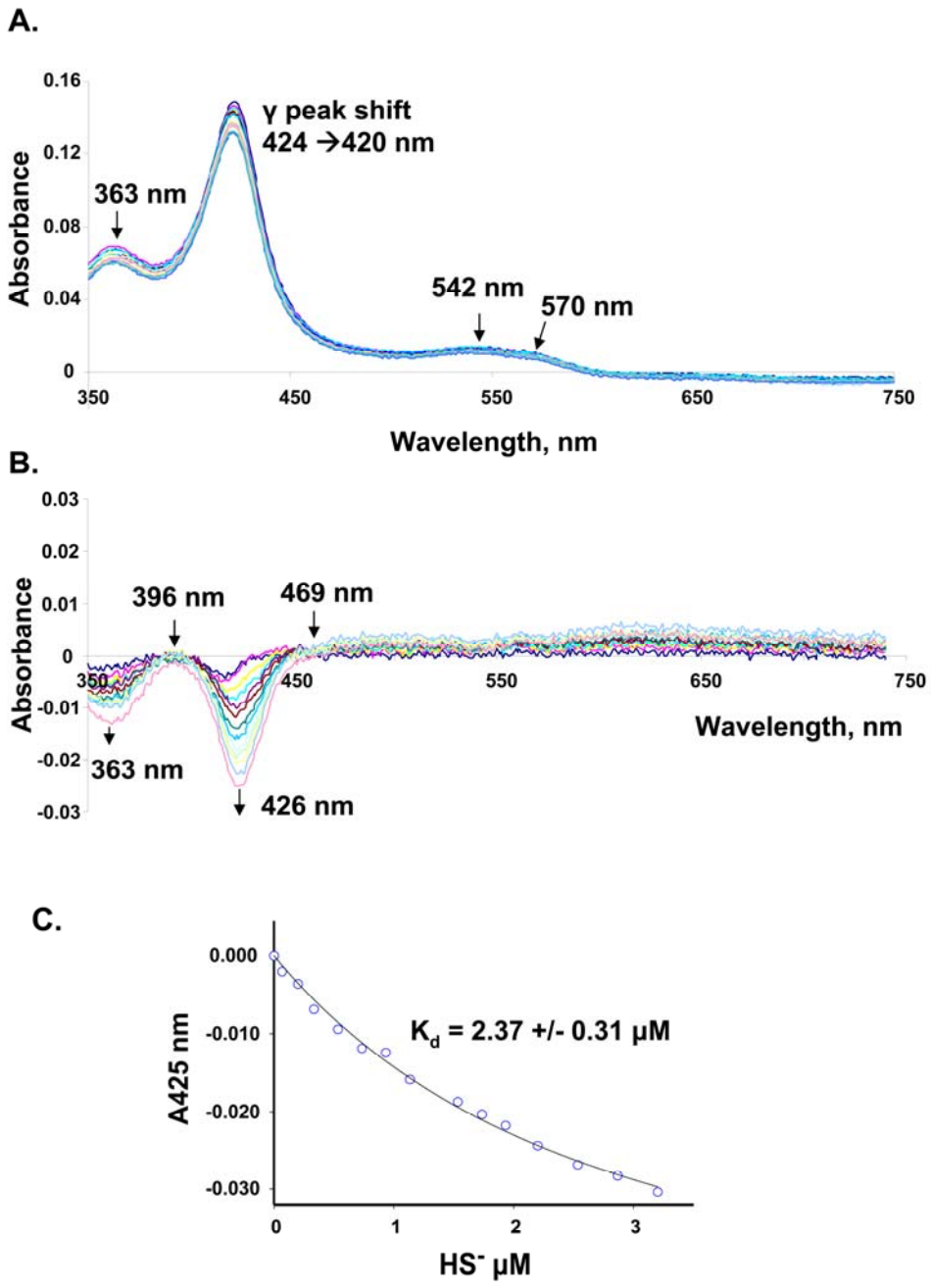

Figure 6.4: H_2S binding to the Fe^{3+}heme-reduced Rev-erbβ LBD complex. UV-visible spectra (A) and difference spectra (B) following titration of Fe^{3+} heme-Rev-erbβ LBD complex with NaHS. C. Fitting of the binding isotherm for the H_2S titration provided a K_d value of 2.37 ± 0.31 µM. The H_2S titration was performed anaerobically with 2 µM Fe^{2+}-heme-LBD complex, as described in experimental procedures.

6.5 Discussion

Gaseous signal mediators such as NO, CO and H_2S modulate cellular activity either via signaling or directly via binding to their targets (21, 23, 32, 33). The role of gasotransmitters has been established in modulation of the circadian rhythm. CO and NO both have been shown to play a role in cholinergic signaling to the suprachiasmatic nucleus (SCN) clock via binding to soluble guanylyl cyclase (sGC). In cholinergic signaling to circadian clock, NO provides tonic stimulation of a discrete sGC/cGMP pool, which is later required for CO-mediated clock resetting. Additionally, NO also shows a circadian pattern of expression (20). Moreover, H_2S mediated rhythmic expression of proteins in the rat retinal ganglion was shown in a study done by Nevalennaya and others (22).

In addition to sGC, many targets have been described for CO and NO, including proteins involved in the circadian rhythm. NPAS2, which directs transcription of the Per and Cry proteins after forming a heterodimer with Bmal1, has been found to be under regulation of CO. Dioum and colleagues have revealed that CO binds to the heme center of NPAS2 and inhibits the DNA binding capacity of NPAS2-Bmal1 heterodimer *in vitro* (7). Expression of Per1 has also been shown to be regulated by NO. Kunieda and colleagues have discovered that NO mediated S-nitrosylation of Bmal1 stabilizes the protein, which in turn stably induces Per1 expression via an E-box (16).

Similarly, Rev-erbβ LBD was shown to interact with CO and NO *in vitro*. In combination with previous studies showing that CO can interact with Rev-erbβ LBD (19, 25), the high affinity (K_d = 60 nM) suggests a potential role for CO in regulating the functional

properties of Rev-erbβ. In comparison, NPAS2 (K_d = 1 μM) and a bacterial CO sensor (CooA) (K_d = 11 μM) bind CO with significantly lower affinity (7, 35). Thus, such tight binding of CO to Rev-erbβ might indicate CO as a preferred ligand for the heme center in Rev-erbβ in the cell. Therefore, the conclusion that Rev-erbβ cannot respond to CO *in vivo* (25) needs to be reexamined carefully with a wider range of physiological assays.

Our studies indicate that NO has a poor affinity for the ferrous heme center. The dissociation constant (K_d) for NO is ~300 nM for the Fe^{2+} heme-reduced Rev-erbβ LBD complex and 7 μM for the Fe^{3+} heme-oxidized Rev-erbβ LBD complex. These K_d values are higher than the known physiological concentration of NO (100 pM - 5 nM) (12), thus casting doubt on a potential functional role for *in vivo* NO binding to Rev-erbβ under physiological conditions. However, NO has been shown to cause de-repression via Rev-erbβ on Bmal1 promoter in a luciferase assay. In this assay, cells were treated with NO producing compounds and therefore unphysiologically high NO levels might have been reached during this experiment (25). Thus, neither these nor our results confirm the physiological relevance of NO binding to Rev-erbβ.

However, NO concentrations may reach the μM range in macrophages during infection (31). Interestingly, the role of Rev-erbs has been implicated in inflammation (27). Therefore, binding of NO to the Rev-erbβ complex may become relevant in macrophages during infection and might play a role in regulating an antimicrobial inflammatory response of this key transcriptional regulator.

Interaction of H_2S with hemeoproteins has been recognized and studied for many years. H_2S-responsive proteins include hemoglobin1 from *Lucina pectinata* (26), mitochondrial

cytochrome c oxidase (3) and human neuroglobin (4). However, no circadian target of H_2S has been found so far. Identification of H_2S binding to Rev-erbβ is remarkable, because it might be the first known circadian target of H_2S. H_2S concentration in cells has been determined by different groups and results vary over a wide range from ~ 15 nM to 300 μM (9, 23). Kabil and Banerjee have discussed these variations in concentration measurements and have pointed out that most of the physiological effects of H_2S observed so far are in hundreds of μM range. Therefore, H_2S might exist in μM range in microenvironment of the cell (14). We have found that binding constant for H_2S is about 2 μM, which might be physiologically relevant. However, this needs to be confirmed in an *in vivo* set up as described below.

Studies described above have been done with the ligand binding domain of Rev-erbβ, and they all need to be extended to the full length Rev-erbβ. In fact, we have recently been successful in purifying full-length hRev-erbβ, which is described in chapter 7. We plan to do spectroscopic evaluation of gas binding by EPR, MCD and resonance Raman with full-length hRev-erbβ, which will shed further light on the importance of gas binding to the heme center of the protein. Furthermore, the physiological relevance of these gaseous interactions with Rev-erbβ needs to be assessed in detail with the full-length protein. A luciferase reporter assay system has been developed for this and has been described in chapter 7. This will help identify the effect of gas binding on the function of Rev-erbβ. Gas binding not only offers another possible layer of regulating Rev-erb activity, but might also expand our knowledge about the signaling role of gasotransmitters in the circadian clock (1) and merits testing.

6.6 References

1. Artinian LR, Ding JM, Gillette MU. 2001. Carbon monoxide and nitric oxide: interacting messengers in muscarinic signaling to the brain's circadian clock. *Exp Neurol* 171: 293-300

2. Berzofsky JA, Peisach J, Blumberg WE. 1971. Sulfheme proteins. I. Optical and magnetic properties of sulfmyoglobin and its derivatives. *J Biol Chem* 246: 3367-77

3. Blackstone E, Morrison M, Roth MB. 2005. H2S induces a suspended animation-like state in mice. *Science* 308: 518

4. Brittain T, Yosaatmadja Y, Henty K. 2008. The interaction of human neuroglobin with hydrogen sulphide. *IUBMB Life* 60: 135-8

5. Chiku T, Padovani D, Zhu W, Singh S, Vitvitsky V, Banerjee R. 2009. H2S Biogenesis by Human Cystathionine Î³-Lyase Leads to the Novel Sulfur Metabolites Lanthionine and Homolanthionine and Is Responsive to the Grade of Hyperhomocysteinemia. *Journal of Biological Chemistry* 284: 11601-12

6. Davies SA, Stewart EJ, Huesmann GR, Skaer NJ, Maddrell SH, et al. 1997. Neuropeptide stimulation of the nitric oxide signaling pathway in Drosophila melanogaster Malpighian tubules. *Am J Physiol* 273: R823-7

7. Dioum EM, Rutter J, Tuckerman JR, Gonzalez G, Gilles-Gonzalez MA, McKnight SL. 2002. NPAS2: a gas-responsive transcription factor. *Science* 298: 2385-7

8. Fiorucci S, Antonelli E, Distrutti E, Rizzo G, Mencarelli A, et al. 2005. Inhibition of hydrogen sulfide generation contributes to gastric injury caused by anti-inflammatory nonsteroidal drugs. *Gastroenterology* 129: 1210-24

9. Furne J, Saeed A, Levitt MD. 2008. Whole tissue hydrogen sulfide concentrations are orders of magnitude lower than presently accepted values. *Am J Physiol Regul Integr Comp Physiol* 295: R1479-85

10. Gilles-Gonzalez MA, Gonzalez G. 2005. Heme-based sensors: defining characteristics, recent developments, and regulatory hypotheses. *J Inorg Biochem* 99: 1-22

11. Hall CN, Attwell D. 2008. Assessing the physiological concentration and targets of nitric oxide in brain tissue. *J Physiol* 586: 3597-615

12. Hall CN, Garthwaite J. 2009. What is the real physiological NO concentration in vivo? *Nitric Oxide* 21: 92-103

13. Hartsfield CL. 2002. Cross talk between carbon monoxide and nitric oxide. *Antioxid Redox Signal* 4: 301-7

14. Kabil O, Banerjee R. 2010. Redox biochemistry of hydrogen sulfide. *J Biol Chem* 285: 21903-7

15. Kooter IM, Moguilevsky N, Bollen A, van der Veen LA, Otto C, et al. 1999. The sulfonium ion linkage in myeloperoxidase. Direct spectroscopic detection by isotopic labeling and effect of mutation. *J Biol Chem* 274: 26794-802

16. Kunieda T, Minamino T, Miura K, Katsuno T, Tateno K, et al. 2008. Reduced nitric oxide causes age-associated impairment of circadian rhythmicity. *Circ Res* 102: 607-14

17. Leffler CW, Parfenova H, Jaggar JH, Wang R. 2006. Carbon monoxide and hydrogen sulfide: gaseous messengers in cerebrovascular circulation. *J Appl Physiol* 100: 1065-76

18. Maines MD. 1997. The heme oxygenase system: a regulator of second messenger gases. *Annu Rev Pharmacol Toxicol* 37: 517-54

19. Marvin KA, Reinking JL, Lee AJ, Pardee K, Krause HM, Burstyn JN. 2009. Nuclear receptors homo sapiens Rev-erbbeta and Drosophila melanogaster E75 are thiolate-ligated heme proteins which undergo redox-mediated ligand switching and bind CO and NO. *Biochemistry* 48: 7056-71

20. Mitome M, Shirakawa T, Oshima S, Nakamura W, Oguchi H. 2001. Circadian rhythm of nitric oxide production in the dorsal region of the suprachiasmatic nucleus in rats. *Neurosci Lett* 303: 161-4

21. Naseem KM. 2005. The role of nitric oxide in cardiovascular diseases. *Mol Aspects Med* 26: 33-65

22. Nevalennaya LA, Romanov YA, Bekchanov AN. 2002. Chronobiological regularities of protein content in rat retinal ganglion cells during exposure to products of Astrakhan gas-processing plant. *Bull Exp Biol Med* 133: 617-9

23. Olson KR. 2009. Is hydrogen sulfide a circulating "gasotransmitter" in vertebrate blood? *Biochim Biophys Acta* 1787: 856-63

24. Olson KR. 2011. The Therapeutic Potential of Hydrogen Sulfide: Separating Hype from Hope. *American Journal of Physiology - Regulatory, Integrative and Comparative Physiology*

25. Pardee KI, Xu X, Reinking J, Schuetz A, Dong A, et al. 2009. The structural basis of gas-responsive transcription by the human nuclear hormone receptor REV-ERBbeta. *PLoS Biol* 7: e43

26. Pietri R, Lewis A, Leon RG, Casabona G, Kiger L, et al. 2009. Factors controlling the reactivity of hydrogen sulfide with hemeproteins. *Biochemistry* 48: 4881-94

27. Ramakrishnan SN, Muscat GE. 2006. The orphan Rev-erb nuclear receptors: a link between metabolism, circadian rhythm and inflammation? *Nucl Recept Signal* 4: e009

28. Ryter SW, Otterbein LE. 2004. Carbon monoxide in biology and medicine. *Bioessays* 26: 270-80

29. Tenhunen R, Marver HS, Schmid R. 1969. Microsomal Heme Oxygenase. *Journal of Biological Chemistry* 244: 6388-94

30. Tsiftsoglou AS, Tsamadou AI, Papadopoulou LC. 2006. Heme as key regulator of major mammalian cellular functions: Molecular, cellular, and pharmacological aspects. *Pharmacology & Therapeutics* 111: 327-45

31. Vouldoukis I, Riveros-Moreno V, Dugas B, Ouaaz F, Becherel P, et al. 1995. The killing of Leishmania major by human macrophages is mediated by nitric oxide induced after ligation of the Fc epsilon RII/CD23 surface antigen. *Proc Natl Acad Sci U S A* 92: 7804-8

32. Wallace JL. 2007. Hydrogen sulfide-releasing anti-inflammatory drugs. *Trends Pharmacol Sci* 28: 501-5

33. Wang R. 2003. The gasotransmitter role of hydrogen sulfide. *Antioxid Redox Signal* 5: 493-501

34. Wu L, Wang R. 2005. Carbon monoxide: endogenous production, physiological functions, and pharmacological applications. *Pharmacol Rev* 57: 585-630

35. Yamashita T, Hoashi Y, Watanabe K, Tomisugi Y, Ishikawa Y, Uno T. 2004. Roles of heme axial ligands in the regulation of CO binding to CooA. *J Biol Chem* 279: 21394-40

Chapter 7

ONGOING WORK AND FUTURE DIRECTIONS

7.1 Collateral redox modulation of ligand and DNA binding by Rev-erbβ

The nuclear hormone receptor Rev-erbβ was first discovered in 1994 in three parallel and independent studies. Dumas and others, while searching for nuclear receptors, isolated a Rev-erbβ clone from a cDNA library of human lymphocytes (4). Bonnelye and colleagues isolated a chicken Rev-erbβ, and reported its expression in the central and peripheral nervous system, spleen, mandibullar and maxillar processes and in blood islands during embryonic development (1). Another study, where Enmark and others searched for nuclear receptors in the adult rat brain, reported high expressions of Rev-erbβ in the cerebellum, dentate gyrus of the hippocampus and pituitary gland (5). The role of Rev-erbβ was initially proposed in neuronal differentiation (1). However, due to the presence of Rev-erbβ in a wide variety of tissues, its role in different processes of cellular physiology was postulated. Over the almost two decades since its discovery, Rev-erbβ has been identified to have several targets. These targets are mostly present in metabolically active tissues including those described above and in chapter 4.

The mRNA transcript of Rev-erbβ is robustly induced in the presence of planar aromatic antioxidants, which indicates a role for this nuclear receptor in cellular redox processes

(4). These results are likely to be related to the recent demonstration that the ligand binding domain of Rev-erbβ is subject to redox modulation (8). Rev-erbβ binds heme tightly, (2). We have shown that Rev-erbβ has similar affinities for ferrous and ferric heme. On the other hand, changes in the redox state of specific cysteines in Rev-erbβ markedly affect the affinity for heme, which might ultimately influence the function of the protein (8).

We have recently cloned and expressed full-length human Rev-erbβ (FL hRev-erbβ) in *E. coli*. Preliminary results indicate that the full-length protein shows redox-dependent heme binding and redox-dependent heme ligand switching, similar to what has been observed with Rev-erbβ LBD (8). In addition, our recent results indicate that changes in redox poise affect DNA binding ability of the full-length protein. As shown by the electrophoretic mobility gel-shift assay (EMSA), oxidation of FL hRev-erbβ by diamide results in decreased productive protein-DNA complex formation. Moreover, when heme was present along with diamide, it enhanced the loss of productive protein-DNA complex.

7.2 Experimental procedures

7.2.1 Cloning, Expression, and Purification of full length hRev-erbβ

A FL hRev-erbβ cDNA clone was purchased from the mammalian genome collection via ATCC (Manassas, Virginia); catalogue no.10435076. This construct contained the FL hRev-erbβ cDNA sequence in a pBluscriptR plasmid inserted between SalI-XhoI (5') and BamHI (3') sites. For overexpression in *E. coli*, the FL hRev-erbβ sequence was excised and cloned into a pGB1 vector, which contained an N-terminal 6XHis-GB1 tag and was a generous gift from William Clay Brown (University of Michigan, Ann Arbor). Ligase independent cloning (LIC) was performed using the following PCR primers that contain LIC regions, highlighted in gray (3): Forward primer 5′tacttccaatccaatgct gaggtgaatg caggaggtgt 3′; Reverse primer 3′ct tggcct ttaaagttca ccct taa cattggaagtggataa 5′. These LIC regions correspond to an SspI restriction site, which is also present in the pGB1 vectors thus allowing for LIC of the FL hRev-erbβ into the pGB1 vector. After the ligation reaction, plasmid (*pGB1::FL hRev-erbβ*) was transformed into Top10 competent cells (Invitrogen) and plasmid DNA from the selected colonies were sent for sequencing to the DNA sequencing core (University of Michigan, Ann Arbor).

Later, to overexpress the protein, *pGB1::FL hRev-erbβ* was transfected in BL21 cells (Invitrogen). To overexpress the 6XHis-GB1-hRev-erbβ fusion protein, *E. coli* cells were induced at OD_{600} ~ 0.8 with 1 mM IPTG and grown overnight at 25 ºC. The cell pellet was collected by centrifugation and frozen at -80 ºC. Purification of the protein was carried out at 4 ºC on a Ni-NTA column as directed by the manufacturer (Qiagen, Valencia, CA). The purified protein was dialyzed and stored in 20 mM Tris-HCl (pH 8.0), 300 mM NaCl and 10 % glycerol.

7.2.2 Reduction and oxidation of FL hRev-erbβ: Please refer to section 5.3.3.

7.2.3 Heme binding analysis: Please refer to section 5.3.4.

7.2.4 EPR spectroscopy: Please refer to section 5.3.5.

7.2.5 Whole cell EPR spectroscopy: Please refer to section 5.3.6.

7.2.6 Electrophoretic mobility gel-shift assay (EMSA)

A 25 bp double-stranded Rev-DR2 promoter sequence (7) that was labeled with 6-carboxy fluorescein (FAM) at the 3′ end of the forward oligonucleotide was used for the EMSA. The forward (labeled with FAM at 3′ end) and reverse oligonucleotides were purchased from TriLink biotechnologies (San Diego, CA) and their duplex DNA was prepared by heating the oligonucleotides at 94 ºC in a water bath and then by slow cooling to room temperature. Rev-erbβ and DNA complexes were prepared in binding buffer containing 20% glycerol, 5 mM $MgCl_2$, 2.5 mM EDTA, 250 mM NaCl, 50 mM Tris-HCl, pH 7.5 and 0.25 mg/ml poly(dI-dC)-poly(dI-dC) (final concentrations are given). Heme and diamide (Sigma–Aldrich, St. Louis, MO), when required, were also added to the assay mixture. The reaction mixture was incubated for 20 min at room temperature. Nondenaturing acrylamide gels (8%) were used to analyze the retardation of the protein-DNA complex. Gels were prepared according to a standard Promega protocol (Promega, Madison, WI). The oligonucleotide duplex was visualized in the gel using a Typhoon 7000 fluorescence gel imager (GE healthcare).

7.2.7 Mammalian cell culture and *in vivo* assay

7.2.7.1 Plasmids

For reporter assays, five plasmids were used and are as follows: **1:** The *Bmal1* promoter upstream of the luciferase gene in the *pGL3* plasmid (*pGL3Basic:P(Bmal(s))-dLuc*) was a generous gift from Dr. Vivek Kumar (University of Texas). **2:** Constitutively expressed full-length Rev-erbβ, a negative regulator of the *bmal1* promoter, in the *pEZ-M12-3XFlag::hrev-erbβ* plasmid (purchased from gene copeia). **3**: The same vector lacking *rev-erbβ* was used as a negative control as well as to make up the total tranfectant volume equal when lower amounts of the *rev-erbβ* plasmid were used. **4:** A plasmid carrying the *rorα* gene (*pCMV-SPORT6:rorα*), a positive activator of the *bmal1* promoter, was purchased from ATCC (MGC-5892). **5.** The *pCMV:lacZ* plasmid and was used later to normalize the transfection efficiency via β-galactosidase assay. This plasmid was kindly provided by Dr. Daniel Bochar (University of Michigan).

7.2.7.2 Reporter assays

HEK293 cells were maintained in DMEM medium supplemented with 2 mM glutamine, 10 % FBS and 1x penicillin/streptomycin (Invitrogen) at 37 ºC /5 % CO_2 incubator. The cells were seeded as 3 x 10^5 cells/well/ml in 12-well plates and were grown up to 70 % confluency. Co-transfection of the above described 5 plasmids was performed using the TransIT-2020 transfection reagent (Mirus Bio LLC) as directed by the manufacturer. Amounts of plasmids transfected during the experiment are given below in section 7.3.4. At 24 hrs post transfection, cells were harvested and stored as per the protocol provided by Promega. The next day, the luciferase reporter assay and the β-galactosidase assay were performed using kits as directed by the manufacturer (Promega).

7.3 Results, discussion and future directions

7.3.1 Expression and purification of FL hRev-erbβ

The 6XHis-GB1-hRev-erbβ fusion protein was overexpressed in *E. coli* as described in section 7.2.1. Overexpression of FL hRev-erbβ resulted in amber colored *E. coli* cells, an indication that the protein is able to bind heme *in vivo*, similar to what was observed during Rev-erbβ LBD expression in *E. coli* (8). Purification of the 6XHis-GB1-hRev-erbβ fusion protein was performed on a Ni-NTA column and a representative of SDS-PAGE gel with fractions of eluted protein is shown in Figure 7.1. Elution fractions from E6 to E12 were collected and concentrated for further use. The protein eluted with some other unknown contaminants and I am in the process of further purifying the protein by ion-exchange chromatography. The preliminary results shown in this section are obtained with the protein purified from the Ni-NTA column only.

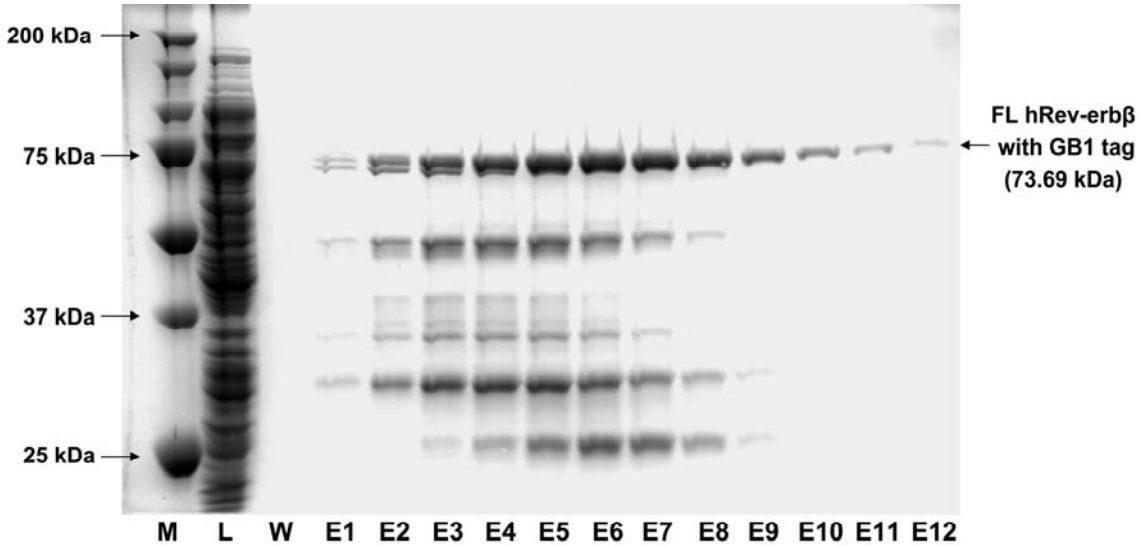

Figure 7.1: SDS-PAGE analysis of the 6XHis-GB1-hRev-erbβ fusion protein. A one –step purification of FL hRev-erbβ was performed on a Ni-NTA column and 10 µl of eluted fractions were run on a 10% SDS-PAGE. M=molecular weight marker, L= lysate, W= wash, E= eluent.

7.3.2 Redox-dependent heme binding in FL hRev-erbβ

To determine the affinity of the oxidized and reduced FL hRev-erbβ proteins for heme, a quantitative heme binding analysis was conducted by UV-visible spectroscopy. Absorption spectra and difference absorption spectra of the FL hRev-erbβ-heme complexes in different redox states are shown in figure 7.2 and figure 7.3, respectively. Throughout, we refer to the disulfide and dithiol states of FL hRev-erbβ when we describe the "oxidized" and "reduced" protein; the redox state of the heme, i.e., Fe^{3+} or Fe^{2+}, is stated explicitly. The oxidized and reduced proteins and complexes were prepared as described in section 5.3.3. When the oxidized GB1-FL hRev-erbβ fusion protein was incubated with Fe^{3+}-heme, the UV visible spectrum showed a Soret band at 416 nm, α peak at 569 nm and β peak at 539 nm. The spectrum of the complex between Fe^{3+}-heme and reduced Rev-erbβ (prepared anaerobically), showed a Soret band at 424 nm, α peak at 574 nm and β peak at 548 nm. The complex between Fe^{2+}-heme and reduced Rev-erbβ was prepared in the presence of 2.5 mM dithionite in an anaerobic chamber. The spectrum of the Fe^{2+}-heme- reduced Rev-erbβ complex exhibited a Soret band at 427 nm, α peak at 560 nm and β peak at 530 nm. The spectra of these three states of the protein are in concordance with those observed for the Rev-erbβ LBD-heme complexes (Table 7.1), suggesting that the heme coordination environments in the LBD and full-length Rev-erbβ are identical (described later in this chapter).

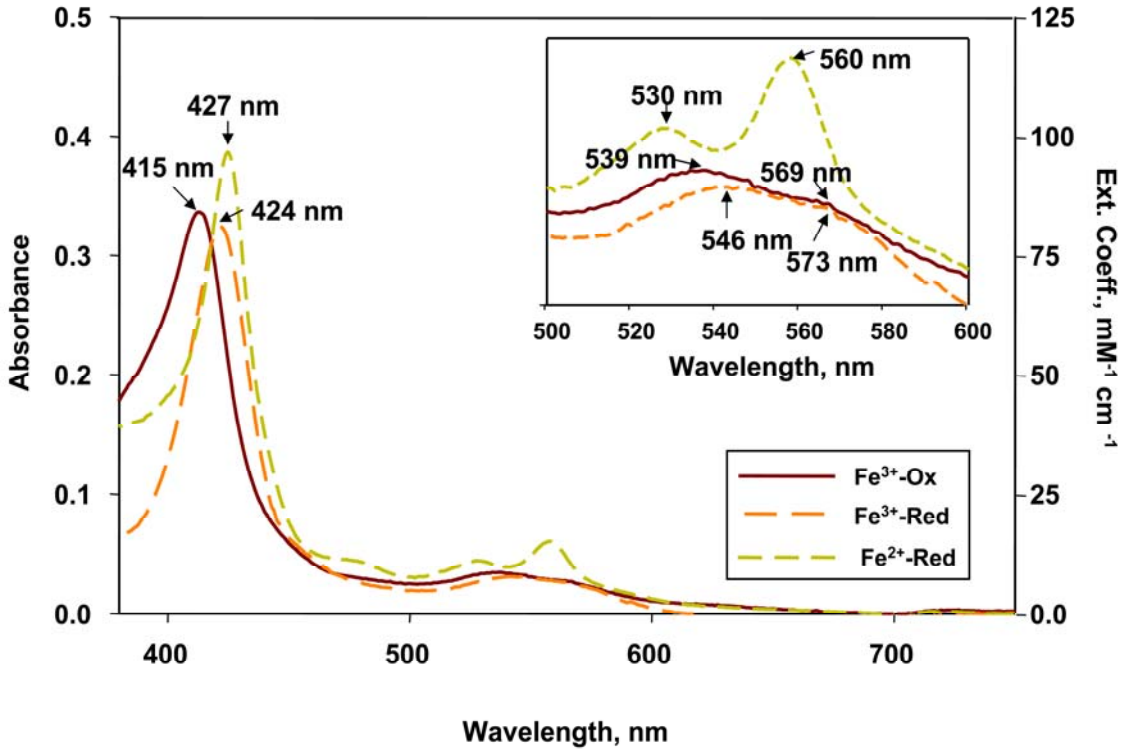

Figure 7.2: Absorption spectra of FL hRev-erbβ-heme complexes. Absorption spectra of FL hRev-erbβ-heme complexes in different redox-states are shown. FL hRev-erbβ (5 μM) and heme (4 μM) were used to record the spectra of the complexes. Dithionite (2.5 mM) was also added in the reaction in order to record the spectrum of Fe^{2+}-heme-FL hRev-erbβ complex. Spectra of the Fe^{3+}heme-reduced protein complex and the Fe^{2+}heme-reduced protein complex were recorded anaerobically.

Complex	Construct used	Soret band	β peak	α peak	K_d (nM)
Red Rev-erbβ - Fe^{2+}heme	FL	427 nm	530 nm	560 nm	226
	LBD	428 nm	530 nm	560 nm	16
Oxd Rev-erbβ - Fe^{3+}heme	FL	415 nm	539 nm	569 nm	1420
	LBD	415 nm	537 nm	567 nm	117
Red Rev-erbβ - Fe^{3+}heme	FL	424 nm	546 nm	573 nm	97
	LBD	424 nm	542 nm	570 nm	23

Table 7.1: Comparison of redox-dependent heme binding properties of FL hRev-erbβ and Rev-erbβ LBD. The spectral peaks provided here are taken from the UV-visible spectra of respective complexes for the FL hRev-erbβ (Figure 7.2 and 7.3) and Rev-erbβ LBD (Section 5.4.1). Details of the dissociation constants are provided in text and also in figure 7.2. Ox = oxidized, Red= reduced, FL= full-length protein, LBD= ligand binding domain. Note: The Rev-erbβ LBD data provided here are taken from Gupta et al. 2008 (8).

To determine the affinity of FL hRev-erbβ for heme, 0.3 μM of the fusion protein was titrated with varying concentrations of Fe^{3+}-heme and the UV-visible spectra were recorded. Because the dissociation constants obtained from hyperbolic fits were lower than the concentration of the protein used during titrations, the data obtained from the heme titration of FL hRev-erbβ (Figure 7.3) were fit to the quadratic equation 1 (see section 5.3.4). Titration of the reduced protein with Fe^{2+}-heme (Figure 7.3 A and B) gave a K_d value of 226 nM, and 97 nM with Fe^{3+}-heme. (Figure 7.3 C and D). The affinity of the oxidized FL hRev-erbβ for Fe^{3+}-heme was markedly lower (K_d ~ 1 μM) (Figure 7.3 E and F). In spite of the fact that the preliminary dissociation constants obtained for the full-length protein are higher than the values determined for Rev-erbβ LBD (Table 7.1) (8), the general characteristics are the same, i.e., the affinity of the oxidized protein for Fe^{3+}- heme is markedly lower than that of the reduced protein. Thus, binding of Fe^{3+}-heme by full-length Rev-erbβ is controlled by a redox switch, just as observed with the LBD. On the other hand, the higher dissociation constants of FL hRev-erbβ might be due to impurities present in the protein after the Ni-NTA column (Figure 7.1). Therefore, binding analysis need to be repeated after obtaining a more homogeneous protein.

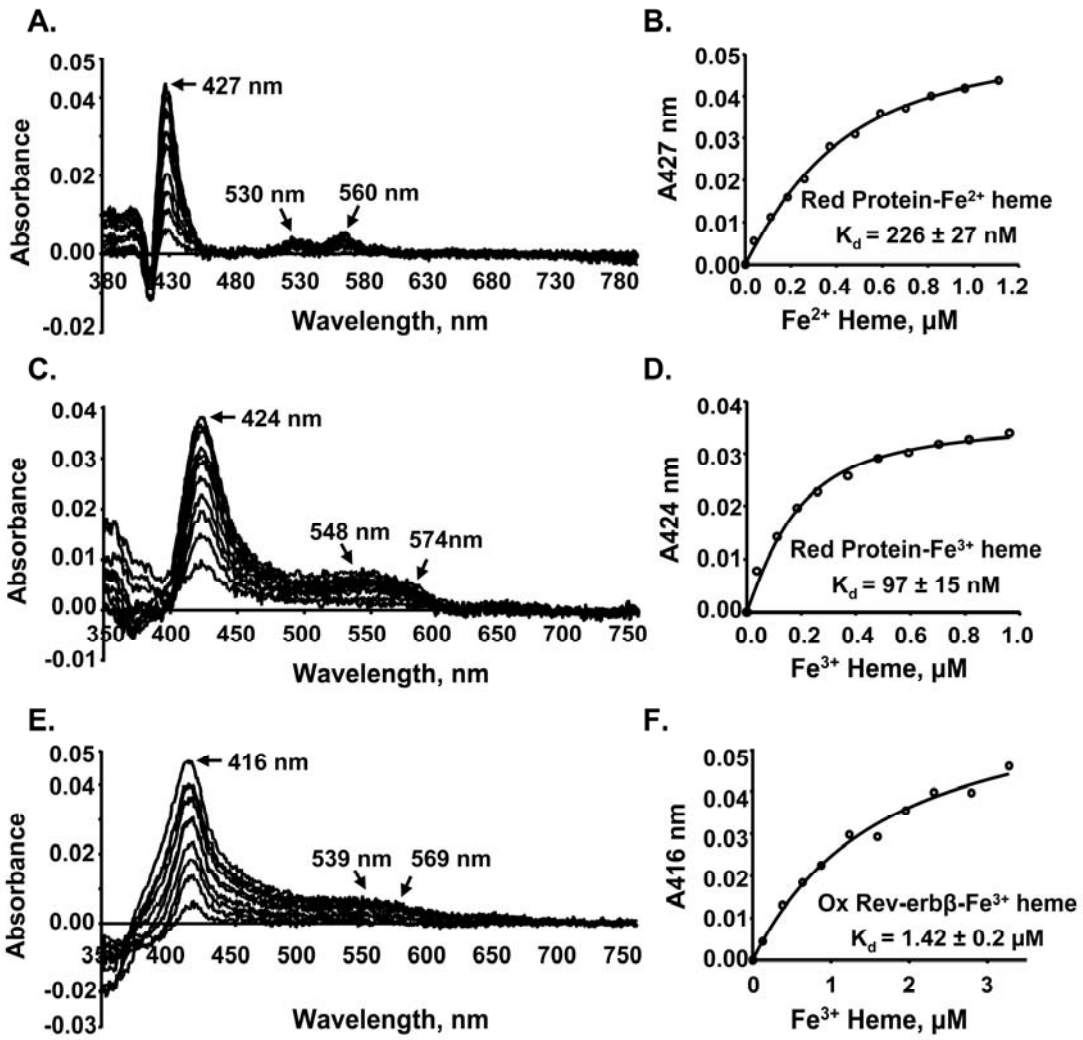

Figure 7.3: Redox dependent heme binding in FL hRev-erbβ. Difference absorption spectra and titration curves of reduced Rev-erbβ with Fe^{2+}-heme (A and B, respectively), oxidized Rev-erbβ with Fe^{3+}heme (C and D, respectively) and reduced Rev-erbβ with Fe^{3+}heme (E and F, respectively). The titrations were performed with 0.3 µM protein in Buffer B (see experimental procedure in chapter 5). Titrations of reduced Rev-erbβ with Fe^{3+}-heme or with Fe^{2+}-heme were performed anaerobically to avoid thiol and heme-oxidation during the experiment.

7.3.3 Redox-dependent heme ligand switching in FL hRev-erbβ

The marked differences in the UV-visible absorption spectra (Figure 7.2) between the oxidized versus reduced forms of heme-bound FL hRev-erbβ indicated that oxidation of FL hRev-erbβ induces a ligand switch, as observed with the isolated LBD (8). The ligand switching in the full-length protein was confirmed by EPR *in vitro* (Figure 7.4) and *in vivo* (Figure 7.5) analyses. The analyses indicated some differences in the spectra between the full-length and Rev-erbβ LBD proteins (8). A rhombic EPR spectrum was observed for the reduced FL hRev-erbβ -Fe^{3+}- heme complex (Figure 7.4, upper panel), with *g*-values of 2.49 2.27 and 1.88, which are indicative of Cys/His heme ligation. Oxidation of the protein resulted in mixed heme ligation including Cys/His (g-values 2.49, 2.27 and 1.86) and His/His (or Met or Lys) (g-values 2.94, 2.27 and 1.54), akin to Rev-erbβ LBD (8). Interestingly, the intensity of the low-spin (*g* ~2) Fe^{3+}- heme complex with the oxidized protein was much less than that observed with the reduced protein (Figure 7.4, upper panel). Moreover, the oxidized protein exhibited a new peak in the high spin region (*g* ~ 6) (Figure 7.4, red traces). Thus, we hypothesized that most of the heme in the oxidized protein was either loosely bound or free and was concentrated in the *g* ~ 6 regions in the spectrum. An estimate of the total spin number in *g*=6 peak of the oxidized protein-Fe^{3+}-heme complex by comparing its peak height with the peak height of free heme of the same concentration (Figure 7.4), lower panel indicated that almost 80 % heme was present in the high spin state. This peak (*g*~6) was most probably due to loosely bound heme with His/OH^- ligation (6) as was observed in the *in vivo* EPR spectrum of Rev-erbβ described below. Thus, oxidation of the full-length protein appears to lead to significant release of heme.

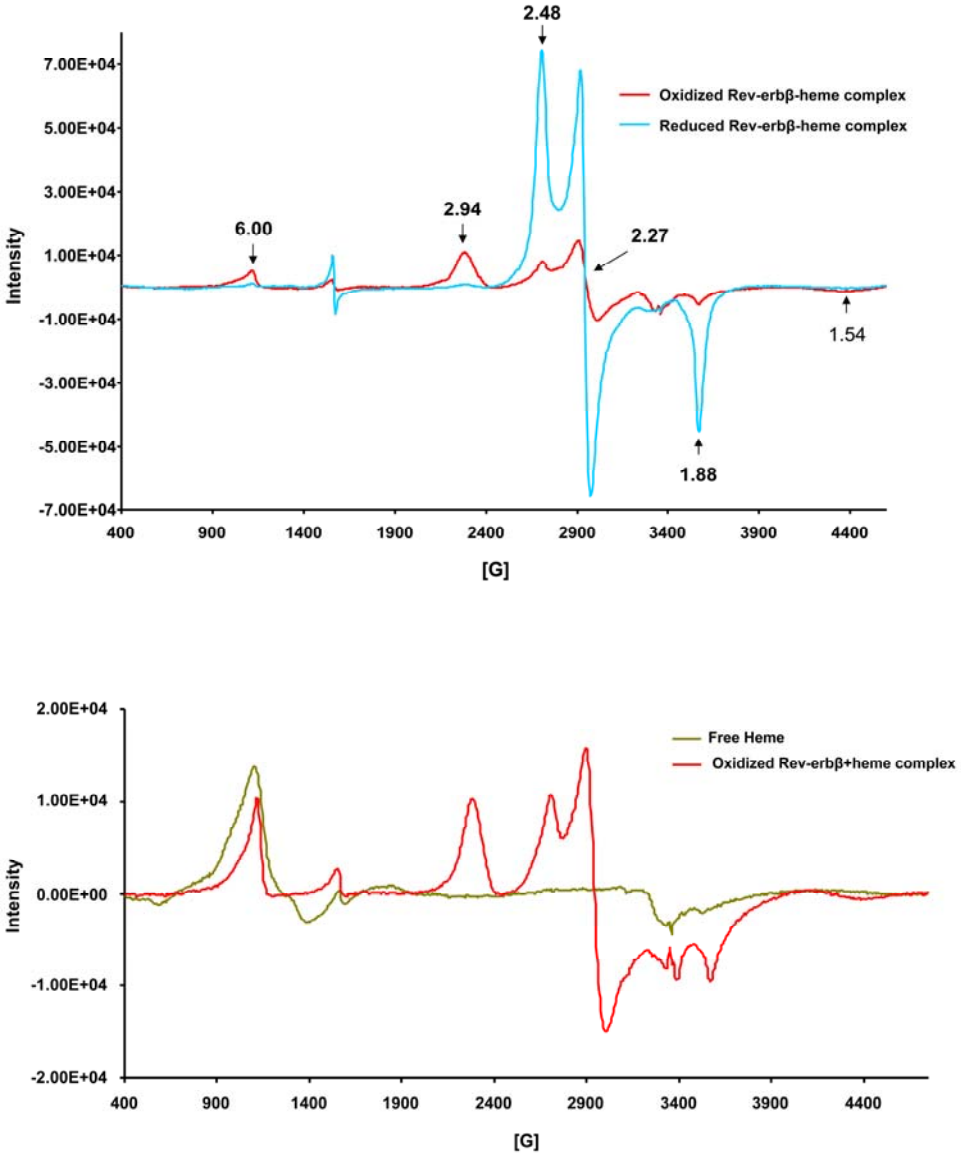

Figure 7.4: *In vitro* redox-dependent ligand switching in FL hRev-erbβ. EPR analysis of heme complexes with the full-length reduced and oxidized proteins. Complexes were prepared at a ratio of 250 μM: 300 μM of Fe^{3+}-heme: protein. Free heme spectrum in lower panel was run under similar condition to heme-protein complex (see experimental procedures) and had the same concentration as used for heme-protein complex.

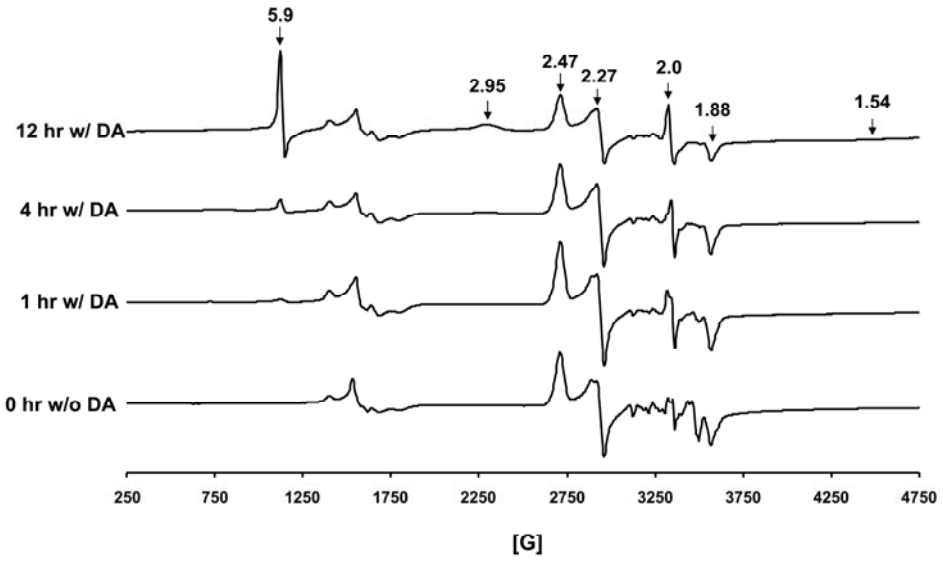

Figure 7.5: *Ex vivo* redox-dependent ligand switching in FL hRev-erbβ. EPR analysis of *E. coli* cells over-expressing Rev-erbβ and exposed to none or 30 mM diamide (DA) for 1, 4 and 12 hours

Ex vivo whole-cell EPR analysis of *E. coli* overexpressing FL hRev-erbβ depicted a rhombic spectrum with *g*-values of 2.49, 2.27 and 1.88 (Figure 7.5), which is similar to the EPR spectrum obtained for the purified protein-heme complex, as described above. Diamide treatment of growing *E. coli* cells resulted in a mixed ligation state of the bound Fe^{3+}-heme (Figure 7.5). The mixed ligation state included a low-spin component with *g*-values of 2.49, 2.27 and 1.88 (as observed for the reduced protein- Fe^{3+}heme complex) and a high-spin component with *g* values of 5.9 and 2 indicating His and water as heme ligands (6). As observed with the purified protein, the low-spin component is assigned to a His/Cys ligated heme, while the high-spin component appears to derive from His/water ligation. A third but minor species with *g*-values of 2.95, 2.27 and 1.54, indicative of His/neutral residue ligation was also observed (Figure 7.5). This ligation state was also observed in the EPR spectrum of the oxidized Rev-erbβ LBD-heme complex that represented almost 50 % of the ligation state of heme in the Rev-erbβ LBD (8). Thus, the

other domains of the full-length protein appear to affect heme binding to the LBD and might be causing the differential ligand switching between the FL hRev-erbβ (i.e. Cys/His to His/Water) and Rev-erbβ LBD (Cys/His to His/neutral residue), upon oxidation of proteins.

7.3.4 Redox and heme dependent binding of FL hRev-erbβ to DNA

To analyze the effect of oxidative stress on DNA binding activity of FL hRev-erbβ, a gel-shift assay was performed (Figure 7.6). No shift in DNA mobility was observed in the absence of the protein (lane 1). When reduced with 5 mM TCEP, the protein formed a Rev-erbβ dimer-DNA complex that resulted in retarded DNA mobility in the gel (lane 3). However, results with the air-oxidized protein are difficult to interpret. As shown in lane 2, free DNA was not observed in the absence of the Rev-erbβ dimer-DNA complex. However, a faint band was observed on top of the lane, which indicated that some of the DNA, remained in the well and didn't enter the gel. When TCEP was used either below 5 mM (i.e., 3 mM, lane 4) or in the presence of 0.5 to 2.5 mM diamide (lanes 5 -7), similar results were observed. Very faint and smeared bands appeared at the expected place of Rev-erbβ dimer-DNA complex and no free DNA was observed (lanes 4-7). Similar to lane 2, a band was observed on top of each lane (lanes 4-7), which is indicative of DNA in the well that didn't enter in the gel. When higher concentrations of diamide (5 and 10 mM) were used in the presence of 5 mM TCEP (lanes 8 & 9), the Rev-erbβ dimer-DNA complex was not observed at all. Some of the free DNA appeared at the bottom of lanes 8 & 9 this time, with the rest of the DNA remaining in the well as before. The oxidation of Rev-erbβ seems to abrogate the protein dimer-DNA complex formation; however, because of the absence of the free DNA, these results are ambiguous at present.

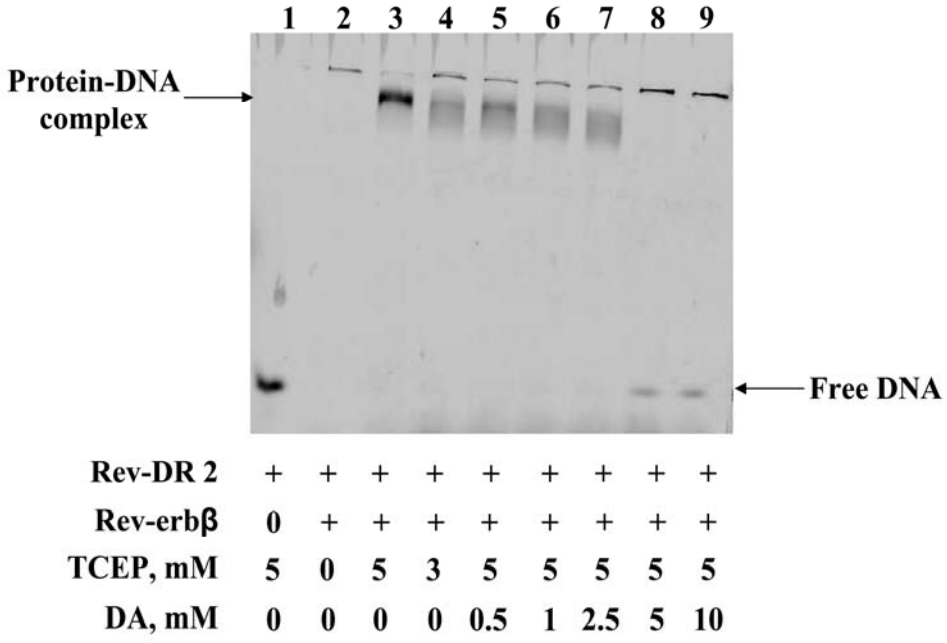

Figure 7.6: Decreased Rev-erbβ dimer-DNA complex formation upon oxidation of the protein. For binding reactions 22 μM of FL hRev-erbβ was incubated with 60 nM Rev-DR2 duplex (lanes 2-9) in the presence of absence of TCEP or diamide (DA). Lane 1 is a control where no protein was used.

It might be possible that the oxidation causes aggregation of protein that is still bound to DNA, causing this complex to remain in the well. Moreover, 22 μM protein was used to achieve an complete shift with 60 nM DNA for the EMSA. This protein concentration is more then 300 times the DNA concentration and indicates that the protein is not fully active, nor it is very pure. It could be due to some non-specific DNA which may remain bound to the protein during purification of FL hRev-erbβ. This is common when DNA binding proteins are expressed in heterologous organisms. . Therefore, we are working to obtain more active and homogeneous full-length protein from *E. coli* and to understand the modulation of DNA binding properties of the protein upon oxidation.

Rev-erbβ is constitutively bound to its promoter in cells. Suppression of the target genes occurs when heme binds to the LBD of the protein. We have earlier shown that oxidation

of FL hRev-erbβ not only results in lower heme binding affinity (Figure 7.3), but also interferes with the proper DNA binding of the protein (Figure 7.6) similar to what has been proposed for glucocorticoid receptor (10). To assess whether these two phenomena, are linked or independent, EMSA in the presence of heme and diamide was performed (Figure 7.7).

Binding reactions were performed in the presence of 0.3 mM diamide (lower concentration of diamide was used in order to be able to see some protein-DNA complex) and varying concentrations of heme (Figure 7.7; lanes 6-9). As a control experiment, varying concentrations of heme in the absence of diamide were also used (Figure 7.7; lanes 2-5). Sample without protein reveals mobility of free DNA (lane 1), while in the presence of TCEP, FL hRev-erbβ showed a band-shift due the formation of Rev-erbβ dimer-DNA complex (lane 2). This protein-DNA complex moved faster in the presence of 1X heme (equivalent heme and Rev-erbβ) (lane3), whereas it is lost in the presence of higher concentration of heme lane 4 & 5). As expected, the presence of low concentrations of diamide did not have a significant effect on protein binding to DNA (compare lane 6 to 2) However, a synergistic effect of heme and diamide on the loss of DNA binding was observed, which was dependent on the concentration of heme (lane 7-9). It is unclear if the excess heme interfered with the protein-DNA complex formation via binding to the protein or to the DNA. Flurescence anisotropy experiments are being planned in order to quantitatively analyze the affinity of FL hRev-erbβ towards its promoter DNA in the presence of diamide and/or heme and, to validate the above findings.

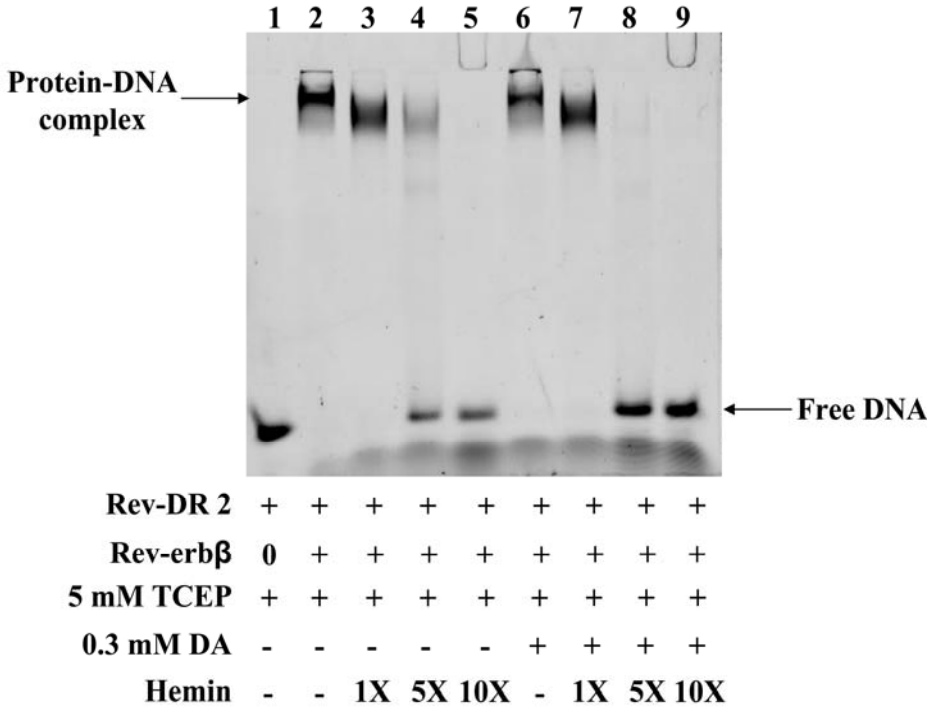

Figure 7.7: **Decreased Rev-erbβ dimer-DNA complex formations in the presence of excessive heme and diamide**. For binding reactions 22 μM of FL hRev-erbβ was incubated with 60 nM Rev-DR2 duplex (lanes 2-9) in the presence or absence of TCEP, diamide (DA) or hemin as indicated in the figure. Lane 1 is a control where no protein was used.

The results described in this section are controversial because heme is a ligand for Rev-erbβ and should not cause its dissociation from the promoter. However, ligand dependent degradation of Rev-erbα has been proposed during adipogenesis, where overproduction of heme was associated with decreased protein levels of Rev-erbα with no change in mRNA levels. Further, proteosome-mediated degradation of Rev-erbα was observed and no role of heme in the degradation was identified (9). Intriguingly, combining our results with theirs, it is possible that the overproduction of heme in the cell may cause the protein to dissociate from the promoter, which may then be targeted for proteosomal degradation. Nonetheless, this hypothesis needs to be tested and its experimental design has been described later in this chapter.

In addition to *in vitro* studies, it is imperative to study the effect of redox-status on transcriptional activity of Rev-erbβ in the cell. To examine this, a luciferase based reporter assay has been set up in HEK293 cells. Constitutively expressed full-length 3XFlag::hRev-erbβ gene under CMV promoter in one plasmid and Bmal1 promoter in front of luciferase gene in pGL3 plasmid were co-transfected in HEK293 cells. Co-transfection of these two plasmids should result in repression of the Bmal1 promoter via Rev-erbβ and thus decreased expression of luciferase, as observed in Figure 7.8.

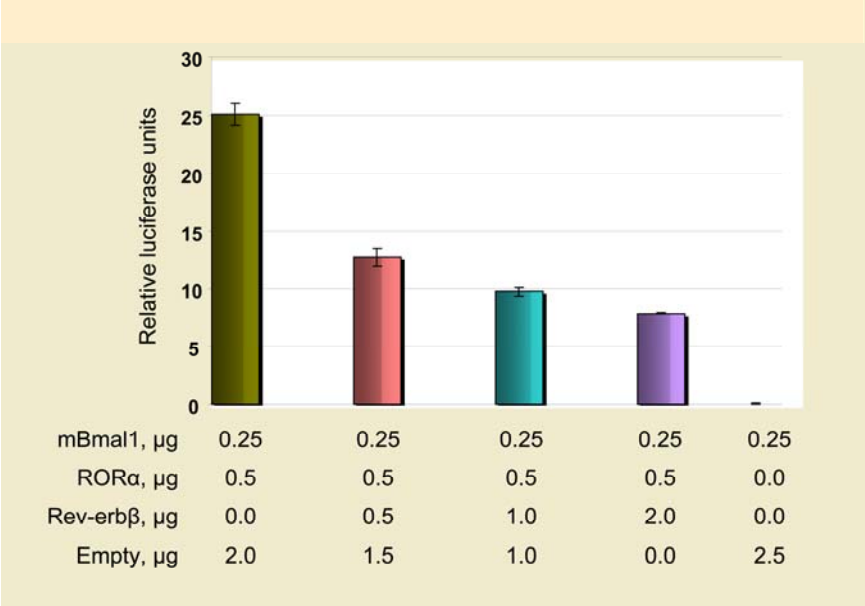

Figure 7.8: hRev-erbβ mediated repression of Bmal1 promoter activity in HEK293 cells. Transfection of RORα resulted in upregulation on Bmal1 promoter- mediated higher expression of luciferase gene. Overexpression of hRev-erbβ exerted repression on Bmal1 promoter in a dose dependent manner. The concentration of plasmid used for the transfection as given below the graph. A control plasmid carrying the *lacZ* gene was also co-transfected, which was used as efficiency of transfection control.

To elucidate the redox-regulation of Rev-erbβ function, cells will be treated with diamide and hydrogen peroxide to generate oxidative stress and then the transcriptional activity of

Rev-erbβ will be observed via luciferase assay. Simultaneously, cells can be treated with succinyl acetone and δ-ALA which will down-regulate and upregulate the heme-biosynthesis, respectively. The effect of altered cellular heme concentrations on DNA binding by Rev-erbβ will also be examined by the luciferase assay in HEK293 cells. Furthermore, the cells can be treated by both diamide and δ-ALA to observe their combined effect on the transcriptional activity of Rev-erbβ via the luciferase assay. In addition to the luciferase assay, ChIP can also be performed under the conditions described above, to further confirm the results obtained from the luciferase assay.

After confirmation of redox-modulation of FL hRev-erbβ, the cellular redox-partner needs to be identified. To identify the redox-partner of Rev-erbβ in cells, thioredoxin will be overexpressed or cells will be treated with glutathione mono ethyl ester. If either of these redox-protein/molecules is a redox partner of Rev-erbβ in cells, then their overproduction should reverse the function of oxidized Rev-erbβ and can be analyzed by the luciferase and ChIP assays.

Furthermore, crystallization of Rev-erbβ in presence of heme, DNA or both will shed additional light on its structure and function. Additionally, crystallization of oxidized and reduced Rev-erbβ with heme would enable us to identify the structural changes responsible for reduced heme binding upon oxidation of Rev-erbβ. Adding DNA during crystallization will also enhance our understanding of effects of oxidation on the DNA binding activity of Rev-erbβ.

7.4 References

1. Bonnelye E, Vanacker JM, Desbiens X, Begue A, Stehelin D, Laudet V. 1994. Rev-erb beta, a new member of the nuclear receptor superfamily, is expressed in the nervous system during chicken development. *Cell Growth Differ* 5: 1357-65

2. Cho HY, Cho HJ, Kim YM, Oh JI, Kang BS. 2009. Structural insight into the heme-based redox sensing by DosS from Mycobacterium tuberculosis. *J Biol Chem* 284: 13057-67

3. Donnelly MI, Zhou M, Millard CS, Clancy S, Stols L, et al. 2006. An expression vector tailored for large-scale, high-throughput purification of recombinant proteins. *Protein Expr Purif* 47: 446-54

4. Dumas B, Harding HP, Choi HS, Lehmann KA, Chung M, et al. 1994. A new orphan member of the nuclear hormone receptor superfamily closely related to Rev-Erb. *Mol Endocrinol* 8: 996-1005

5. Enmark E, Kainu T, Pelto-Huikko M, Gustafsson JA. 1994. Identification of a novel member of the nuclear receptor superfamily which is closely related to Rev-ErbA. *Biochem Biophys Res Commun* 204: 49-56

6. Fiege R, Schreiber U, Renger G, Lubitz W, Shuvalov VA. 1995. Study of heme Fe(III) ligated by OH- in cytochrome b-559 and its low temperature photochemistry in intact chloroplasts. *FEBS Lett* 377: 325-9

7. Gervois P, Torra IP, Chinetti G, Grotzinger T, Dubois G, et al. 1999. A truncated human peroxisome proliferator-activated receptor alpha splice variant with dominant negative activity. *Mol Endocrinol* 13: 1535-49

8. Gupta N, Ragsdale SW. 2010. Thiol-disulfide redox dependence of heme binding and heme ligand switching in nuclear hormone receptor rev-erb{beta}. *J Biol Chem* 286: 4392-403

9. Kumar N, Solt LA, Wang Y, Rogers PM, Bhattacharyya G, et al. 2010. Regulation of adipogenesis by natural and synthetic REV-ERB ligands. *Endocrinology* 151: 3015-25

10. Makino Y, Okamoto K, Yoshikawa N, Aoshima M, Hirota K, et al. 1996. Thioredoxin: a redox-regulating cellular cofactor for glucocorticoid hormone action. Cross talk between endocrine control of stress response and cellular antioxidant defense system. *J Clin Invest* 98: 2469-77